INSTITUTO SUPERIOR TÉCNICO
Universidade Técnica de Lisboa

Establishment of mouse Embryonic Stem cell lines with a reporter of *Dll1* activity

Rúben Duarte Magalhães Alves Pereira

Dissertação para obtenção do Grau de Mestre em

Engenharia Biomédica

Júri:

Presidente:	Prof. Joaquim M. S. Cabral
Orientador:	Prof. Domingos Henrique
Co-orientador:	Dr.ª Evguenia Beckman
Vogal IST:	Dr.ª Margarida Diogo
Vogal FML:	Dr.ª Elsa Abranches

Novembro de 2009

Acknowledgements

I would like to thank all the people from the Developmental Biology Unit lab, especially Evguenia Beckman, Elsa Abranches and Filipe Vilas-Boas for their help and guidance in each step of my work and Domingos Henrique for the opportunity I was given to work in the lab.

Also to my family, and particularly to my girlfriend, for the support through all the difficult moments (and through the good ones too) that always helped me “getting there”.

Thank you very much.

"It is not birth, marriage, or death, but gastrulation, which is truly the most important time in your life."

Lewis Wolpert (1986)

Resumo

O trabalho em seguida descrito procura contribuir para a compreensão do mecanismo Notch, mais particularmente para esclarecer a correlação possível entre o gene *Notch* e o ciclo celular durante a neurogénese. Especificamente, este trabalho tem como objectivo gerar uma linha celular transgénica de células estaminais embrionárias de ratinho contendo um repórter fluorescente com o intuito de visualizar a actividade do gene *Dll1* nas células estaminais embrionárias através de BAC recombineering. Assim, o trabalho desenvolvido foi dividido em duas partes de considerável importância para este projecto.

Na primeira parte procurou-se contribuir para a geração da linha celular transgénica de células estaminais embrionárias de ratinho, nomeadamente através da instituição de um protocolo de extracção do BAC, assim como um para a sua visualização. Este objectivo foi alcançado através do estudo dos vários passos de extracção de DNA utilizando um kit comercial e um método de extracção "tradicional", protocolos que foram posteriormente comparados. Esta parte do estudo revelou vários pontos fracos na utilização do kit commercial e levou à instituição de um protocolo de extracção baseado num outro descrito por Bill Richardson e Nicoletta Kessaris, em 2006.

Na segunda parte do trabalho, o intuito era o de contribuir para a validação do modelo utilizado no laboratório, mais especificamente atendendo à relação entre a expressão do gene *Dll1*, o "movimento nuclear inter-cinético" e o ciclo celular nas rosetas. Para isso, realizaram-se ensaios imunocitoquímicos em células estaminais embrionárias de ratinho contendo um repórter fluorescente para monitorizar a actividade do gene *Dll1*, amplificadas e diferenciadas *in vitro*, e concluiu-se que o seu comportamento podia ser considerado análogo ao observado em células do tubo neural (*in vivo*).

Palavras-chave: Extracção de BAC, PFGE, *Delta-like1* (*Dll1*), repórter fluorescente, células estaminais embrionárias.

Abstract

The work described here aims to contribute to the understanding of Notch pathway, particularly to enlighten the possible correlation between *Notch* and the cell cycle during neurogenesis. Specifically, this work aims to generate a transgenic mouse ES cell lines containing a fluorescent reporter for the purpose of visualizing the activity of *Dll1* in ES cells using BAC recombineering. Therefore, the work performed was divided in two important parts for this project.

The first part of the work aimed to contribute to the generation of the transgenic mouse ES cells line, namely by establishing a reproducible and consistent BAC extraction, as well as a visualization protocol. This objective was achieved by studying the several steps of DNA extraction using a commercial kit and a "traditional extraction" protocol that were compared a posteriori. This study revealed several weaknesses of the commercial kit and led to the establishment of an extraction protocol based on one described by Bill Richardson and Nicoletta Kessaris, in 2006.

In the second part, the aim was to contribute to the validation of the model used in the lab, namely concerning the relation between *Dll1* expression, INM and cell cycle in the rosettes. For this, we did immunocytochemistry assays in mouse ES cells with a fluorescent reporter for *Dll1* activity, amplified and differentiated *in vitro*, and concluded that their behavior might be considered analogous to that observed in cells from the neural tube (*in vivo*).

Key-words: BAC extraction, PFGE, *Delta-like1* (*Dll1*), fluorescent reporter, ES cells.

Index

Introduction ... 1
- Nervous system development ... 2
- Neural tube ... 3
- Cell cycle and interkinetic nuclear migration ... 4
- Molecular mechanisms regulating the cell cycle ... 5
- Notch signaling and the nervous system development ... 6
- Notch signaling pathway ... 8
- Notch pathway, cell cycle INM and neurogenesis ... 11
- Two Notch pathway reporters in the mouse: Dll1 and Hes5 ... 12
- Stem cells ... 12
- Stem cells culture and differentiation towards neural lineage ... 14
- Model ... 15

Objectives and experimental strategy ... 17

Experimental procedures ... 19

1st part – BAC extraction, digestion and visualization ... 19
- Generation of the *Dll1*:*mCherry*:*NLS* BAC construct ... 19
- Establishment of the final extraction and visualization protocols ... 22
- Initial BAC extraction protocol ... 22
- Initial BAC visualization protocol ... 29
- Protocol studies using the “PSI Ψ Clone Big BAC – DNA isolation kit” ... 32
- The Pulsed Field Gel-Electrophoresis (PFGE) ... 38
- Defining PFGE conditions ... 40
- Traditional extraction protocol studies ... 44
- Final extraction protocol ... 48

2nd part – Contributing to validation of the in vitro model ... 50
- Mouse ES cells line ... 50
- Culture of undifferentiated ES cells and monolayer differentiation ... 50
- Immunocytochemistry on cover-slips ... 54

Results and Discussion ... 56

Conclusion ... 63

Future work ... 65

Future perspectives for stem cells therapies ... 66

References ... 67

Figures index

Figure 1. Wild type *Drosophila melanogaster* wing (left) **and *Notch* mutant's wing** (right). This is the notching wing phenotype, associated with the haploinsufficiency of the *Notch* locus. 1

Figure 2. Schematic view of neurulation. The notochord induces the neural fate of cells from the ectoderm forming the neural plate. Later, the neural plate folds and forms the neural groove that after closure will give rise to the neural tube (image adapted from *www.thebrain.mcgill.ca*). 3

Figure 3. Schematic (left) **and Sox2 stained (transcription factor)** (right) **cut view from the neural tube** (image adapted from *www.betacell.org*). 3

Figure 4. Scheme of the interkinetic nuclear migration observed in vertebrate neuroepithelia. Neuroepithelial cells displace their nuclei as they progress through the cell cycle. During G1, nuclei are displaced to the basal surface, where they undergo DNA replication (S-phase). Once S-phase is finished, nuclei move back to the apical portion of the neuroepithelium as they go through G2, and then they divide to give rise to two daughter cells (M) (*Latasa, 2008*). 4

Figure 5. Schematic diagram of cell cycle and its main regulators. Progression through the cell cycle is regulated by cyclin/CDK complexes and their inhibitors (INK4 family and Kip/Cip family). Two main restriction points have been described, that control whether cells enter a new round of DNA replication (G1/S check point), and whether DNA replication has been correctly performed before the cell divide (G2/M check point) (*Latasa, 2008*). 5

Figure 6. *Drosophila melanogaster* embryos stained with an antibody against horseradish peroxidase that recognizes neural tissue. Wild-type and Notch null mutant *D. melanogaster* embryos, showing the hypertrophy of both the central nervous system (CNS) and peripheral nervous system (PNS) that occurs in the absence of Notch (adapted from *Louvi and Artavanis-Tsakonas, 2006*). 6

Figure 7. A schematic summarizing of the effects of Notch signal activation on cell fate decisions in the vertebrate nervous system. The self-renewing stem cells can give rise to neuronal progenitors and glial progenitors. The firsts are inhibited to progress to neurons by Notch signal activation, in contrast to the glial progenitors that differentiate into astrocytes with the help of Notch signals. Finally, oligodendrocyte precursors derived from glial progenitors fail to differentiate into mature oligodendrocytes in the presence of active Notch signals (adapted from *Louvi and Artavanis-Tsakonas, 2006*). 7

Figure 8. Domain Organization of Notch Pathway Receptors, Ligands, and Coligands. (A) Notch receptors are large type I proteins that contain multiple extracellular EGF-like repeats.

EGF repeats 11–12 (red) and 24–29 (green) mediate ligand interactions. These repeats may contain consensus motifs for fucosylation by O-Fut1 and glycosylation by Rumi; the putative distribution of fucosylation sites (common, green; unique, light blue) and glycosylation sites (common, dark blue; unique, magenta) are shown for mNotch1 and mNotch2. EGF repeats are followed by the negative regulatory region (NRR), which is composed of three cysteine-rich Lin12-Notch repeats (LNR-A, -B, and -C) and a heterodimerization domain (HD). Notch also contains a transmembrane domain (TMD), a RAM (RBPjκ association module) domain, nuclear localization sequences (NLSs), a seven ankyrin repeats (ANK) domain, and a transactivation domain (TAD) that harbors conserved proline/glutamic acid/serine/threonine-rich motifs (PEST). The transactivation domain in *Drosophila* Notch also has a glutamine-rich repeat (OPA). (B) Known ligands and putative ligands of Notch receptors can be divided into several groups on the basis of their domain composition. Classical DSL ligands (DSL/DOS/EGF ligands) contain the DSL (Delta/Serrate/LAG-2), DOS (Delta and OSM-11-like proteins), and EGF (epidermal growth factor) motifs and are not found in *C. elegans*. *C. elegans* and mammalian DSL-only ligands lacking the DOS motif (DSL/EGF ligands) are a subtype of DSL ligands that may act alone or in combination with DOS coligands (for example, cDSL-1 and possibly Dll3). This subfamily includes soluble/diffusible ligands (adapted from *Kopan and Ilagan, 2009*)..... 9

Figure 9. Schematic view of the Notch signaling pathway. The proneural genes *Mash1* and *Ngn2* induce expression of Notch ligands such as Dll1, which activate Notch signaling in neighboring cells. Upon activation, the NICD is released from the transmembrane region and transferred to the nucleus, where it forms a complex with RBPjκ and induces *Hes1* and *Hes5* expression. Hes1 and Hes5 repress proneural gene expression (*Kageyama, 2008*). 10

Figure 10. Schematic view of ES cells in context of mouse embryogenesis (top) **and their isolation from the ICM** (bottom); **lineage diagram of mouse development** (middle)**.** ES cells derived from the ICM (*top, in yellow*) can give rise to all lineages along mouse development (*middle, in blue*) except trophectoderm. However, they can produce hypoblast derivatives *in vitro* but rarely do so *in vivo* (adapted from *Austin Smith, 2003*). 13

Figure 11. Cooperative Lineage Restriction by BMP/Id and LIF/STAT3. ES cell self-renewal requires suppression of lineage commitment. *Id* genes induced by BMP or other signals blockade entry into neural lineages, which is otherwise only partially prevented by LIF/STAT3. In parallel, the capacity of BMP to induce mesodermal and endodermal differentiation is constrained by STAT3, probably involving direct as well as indirect mechanisms (*Qi-Long Ying and Austin Smith, 2003*). 15

Figure 12. Rosette of neural progenitors depicting cells organization analogous to the neural tube. Cells are stained for the apical junction marker PAR-3 (green) ,evidencing cell polarity and apical -basal organization, and for the cell cycle exit marker Tuj1 (red), depicting an external zone analogous to the mantle zone of the neural tube. The cells' nuclei are stained with bromodeoxyuridine – BrdU (blue), a synthetic thymidine analog that gets incorporated into a

cell's DNA when the cell is dividing (during the S-phase of the cell cycle) (image from *Abranches et al., 2009*). 16

Figure 13. Classic recombinant DNA technology versus recombineering. Recombineering steps to generate a BAC recombinant include: Amplifying a cassette by PCR with flanking regions of homology; Introducing phage recombination functions into a BAC containing bacterial strain, or introducing a BAC into a strain that carries recombination functions; Transforming the cassette into cells that contain a BAC and recombination functions; Generating a recombinant *in vivo*; Detecting a recombinant by selection, counter-selection or by direct screening (colony hybridization) (image adapted from *Copeland et al., 2001*). 20

Figure 14. Schematic representation of the BAC with the inserted cassette. The inserted cassette substituted the coding region of the *Dll1* gene inside the BAC. The promoter maintenance ensures the expression of the reporter under the same conditions and levels of expression as the endogenous *Dll1*. The *FRT* sites allow the removal of the resistance cassette. 21

Figure 15. Schematic representation of the recombination step between the plasmid with the resistance cassette and the BAC. The inserted cassette substitutes the coding region of the *Dll1* gene inside the BAC due to recombination between the regions of homology (5' and 3' arms). The promoter maintenance ensures the expression of the reporter under the same conditions and levels of expression as the endogenous *Dll1*. 21

Figure 16. Procedure Guide for PSI Ψ Clone Big BAC DNA isolation kit (1st page). This kit is designed for BAC DNA extraction from up to 50 mL culture per column. The separation process is based on a highly efficient, hydrophilic non-silica anion exchanger resin (*Princeton Separations – prinsep.com*). 23

Figure 17. Procedure Guide for PSI Ψ Clone Big BAC DNA isolation kit (2nd page). (*Princeton Separations – prinsep.com*). 24

Figure 18. Restriction profile of the *Dll1* BAC DNA regarding single (PmeI) and double (AscI, NotI and RsrII) restriction enzymes. The figure shows the recognition sites for each enzyme. (*tools.neb.com*). 25

Figure 19. Restriction profile of XhoI for the *Dll1* BAC DNA. The restriction enzyme XhoI was used on the studies to improve the protocols and is mentioned furtherer in this thesis (*tools.neb.com*). 26

Figure 20. The CHEF-DR III system: chamber (upper left), power module (upper middle), variable speed Pump (lower left), Cooling Module (lower middle), and casting lid and comb (upper right) (*Chef-DR III instructions manual*). 29

Figure 21. λ-DNA Mono cut mix fragments' sizes (left) **and PFGE photo** (right). Here, the first set of parameters for PFGE was used and the samples were extracted from previously frozen pellets. 31

Figure 22. λ-DNA Mono cut mix fragments' sizes (left) **and PFGE photo** (right). Here, the first set of parameters was used for PFGE and the samples were extracted freshly prepared pellets. In lane 3, AscI digested sample, only a smear is observed..... 32

Figure 23. λ-DNA Mono cut mix fragments' sizes (left) **and PFGE photo** (right) **(First conditions).** The lysis samples (lanes 2, 3, 4 and 5) do not show any unexpected result and no significant amount of DNA is present. 33

Figure 24. 1 kb plus ladder fragments' sizes (left) **and electrophoresis gel photo for AscI testing** (right)**.** Lane 2 shows both super-coiled (lower band) and relaxed form (upper band) of the plasmid. In lane 3 the partial digestion is observed. Lane 4 shows complete digestion with new AscI enzyme. 34

Figure 25. λ-DNA Mono cut mix fragments' sizes (left) **and PFGE photo** (right). The DNA samples (lanes 2 and 3) only show a smear. The first set of conditions for the PFGE run was used. 35

Figure 26. λ-DNA Mono cut mix fragments' sizes (left) **and PFGE photo** (right). The DNA samples (lanes 2, 3 and 4) all show a visible band. The first set of parameters for the PFGE run was used. 36

Figure 27. λ-ladder fragments' sizes (left)**, λ-DNA Mono cut mix fragments' sizes** (middle) **and PFGE photo** (right). The Hes5 DNA samples (lane 7, 8, 9 and 10) all show a visible band. The λ-ladder is compacted in the middle of the gel..... 38

Figure 28. Voltage clamping by the *CHEF-DR III system*. A. Relative electrode potentials when the + 60° field vector is activated. B. Relative electrode potentials when the - 60° field vector is activated (*Chef-DR III instructions manual*). 39

Figure 29. 1 kb plus ladder, λ-DNA Mono cut mix and λ-ladder fragments' sizes (left, in order)**, and PFGE photo** (right). Lanes 7, 8 and 9 all show slight visible bands. The 1 kb plus ladder is not visible in the gel. 43

Figure 30. λ-DNA Mono cut mix fragments' sizes (left)**, 1 kb plus ladder fragments' sizes** (middle)**, and photo of the gel** (right). Lanes in the bottom row show bright bands. The λ-DNA Mono cut mix is compacted in the top of the lane as well as the rest of the high molecular DNA samples. ("ph:chloro" stands for phenol:chloroform step)..... 45

Figure 31. MidRange II PFG marker fragments' sizes (left)**, λ-DNA Mono cut mix fragments' sizes** (middle)**, and PFGE photo** (right). All DNA samples are visible, although XhoI digestion is a bit blurred. The small sized bands are also visible if we adjust the brightness. 46

Figure 32. MidRange II PFG marker fragments' sizes (left)**, λ-DNA Mono cut mix fragments' sizes** (middle)**, and PFGE photo** (right). All DNA samples obtained using Nicoletta's protocol are visible. Using the kit we can only see the Hes5 BAC bands, with a visible smear though. The samples from the protocol described by Nicoletta show much less smear..... 47

Figure 33. Immunocytochemistry: Geminin/GFP/DAPI (top)**, Geminin** (left) **and GFP** (right)**.** (Bar: 20 μm). 57

Figure 34. Immunocytochemistry: P57^{Kip2}/GFP/DAPI (top)**, P57^{Kip2}** (left) **and GFP** (right)**.** All cells expressing P57^{Kip2} also express GFP. (Bar: 20 μm)..... 59

Figure 35. Immunocytochemistry: HuC/D/GFP/DAPI (top)**, HuC/D** (left) **and GFP** (right)**.** (Bar: 20 μm). 61

Figure 36. Immunocytochemistry: Tuj1/GFP/DAPI (top right)**, Tuj1** (bottom left) **and GFP** (bottom right)**. Neuron** 62

Figure 37. Scheme of the model proposed to represent the functional organization of the neuroepithelium in terms of neurogenesis. The orthogonal arrangement of the cells moving their nuclei up and down as they progress through the cell cycle is translated into the segregation of the neuroepithelium into two zones, each made up of precursors that are transiently involved in distinct functions. In the apical (or ventricular) region (neurogenic zone), proliferating cells are able to express Notch1, Delta1, and the proneural determination gene Ngn2 (dark gray), thus being subjected to lateral inhibition. In the basal epithelium (pre-neurogenic zone), precursors either cannot express these genes or express them at low levels. Postmitotic neurons in G0 still expressing Delta1, Ngn1, and Ngn2 pass through the pre-neurogenic zone as they migrate out from the neuroepithelium. T1 and T2 represent the time points corresponding to the moment in G1 at which the cells lose their neurogenic capacity and the beginning of G2, respectively (image adapted from *Murciano et al, 2002*). 64

Graphics index

Graphic 1. Geminin (red)**, GFP** (green)**, and Geminin plus GFP** (yellow) **expression along the several levels of the apical-basal axis rosette and in the outbound**. Geminin is expressed mainly in the medial and basal zones of the rosette while GFP increases its activity towards the basal side of the rosette. 57

Graphic 2. P57^{Kip2} (red)**, GFP** (green)**, and P57^{Kip2} plus GFP** (yellow) **expression along the several levels of the apical-basal axis rosette and in the outbound**. P57^{Kip2} is expressed only in cells expressing GFP. Inside the rosettes, as the levels of P57^{Kip2} increase the expression of both P57^{Kip2} and GFP increases too. Outside the rosettes, the majority of cells express both markers and not only GFP..... 60

Tables index

Table I. Notch pathway components in different species (adapted from *Louvi and Artavanis-Tsakonas, 2006*). 8

Table III. Drug concentration for low copy BACs (adapted from *"Molecular Cloning: A Laboratory Manual"*). 22

Table IV. Bands produced upon digestion of Dll1 and Hes5 BACs with several restriction enzymes. AscI, NotI and XhoI were the enzymes used to run all the tests described in this work. Hes5 BAC is another BAC construct that was used on the studies to improve the protocols and is mentioned furtherer in this thesis, as well as the restriction enzymes XhoI and NotI. 26

Table V. Mixture for AscI digestion. AscI activity is 0,13 U/µg for 16 hours (*tools.neb.com*). 28

Table VI. Mixture for NotI digestion. NotI activity is 0,25 U/µg for 16 hours (*tools.neb.com*). 28

Table VII. Mixture for XhoI digestion. XhoI activity is 0,13 U/µg for 16 hours (*tools.neb.com*). 28

Table VIII. Suggested parameters for several DNA size ranges. (*Chef-DR III instructions manual*)..... 40

Table IX. PFGE running conditions established after the study. 42

Abbreviations list

A – Agar gel concentration
Ank – Seven Ankyrin Repeats
APC – Anaphase Promoting Complex
Asc – Achaete-Scute
Ato – Atonal
Ath – Atonal homologues
BAC – Bacterial Artificial Chromosome
BGHpA – Bovine Growth Hormone poly-Adenylation signal
bhlh – Basic Helix–Loop–Helix
BMP – Bone Morphogenetic Protein
CDK – Cyclin-Dependent Kinase
CNS – Central Nervous System
DAPI – Diamidino-2-phenylindole
Dll1 – Delta-like1
DOS proteins – Delta and OSM-11-like proteins
DSL – Delta/Serrate/LAG-2
EC cells – Embryonic Carcinoma cells
EGF – Epidermal Growth Factor
ELAV – Embryonic Lethal Abnormal Vision
EM7 – Prokaryotic Promoter
ES cells – Embryonic Stem cells
FACS – Fluorescence-Activated Cell Sorting
FBS – Fetal Bovine Serum
FGF – Fibroblast Growth Factor
bFGF – bovine Fibroblast Growth Factor
Flp – Flipase Protein
G1 – First Gap
G2 – Second Gap
GFP – Green Fluorescent Protein
GMEM – Glasgow Modified Eagles Medium
HD – Heterodimerization Domain
HES – Hairy and enhancer of split
hPSCs – human Pluripotent Stem Cells
ICM – Inner Cell Mass
Id – Inhibitor of differentiation
INM – Interkinetic Nuclear Migration
LB – Luria-Bertani
LIF – Leukemia Inhibitory Factor

M – Mitosis

NICD – Notch Intracellular Domain

Ngn – Neurogenin

NLS – Nuclear Localization Signal Sequences

NRR – Negative Regulatory Region

OPA – Glutamine-rich repeat

ORF – Open Reading Frame

PACAP – Pituitary Adenylate Cyclase-Activating Polypeptide

PEST – Proline/glutamic acid/serine/threonine-rich motif

PFA – Para-formaldehyde

PFGE – Pulsed-Field Gel Electrophoresis

PGK – Eukaryotic Promoter

PNS – Peripheral Nervous System

PBS – Phosphate Buffered Saline

RFP – Red Fluorescent Protein

RT-PCR – Real-Time Polimerase Chain Reaction

S-phase – Synthesis Phase

Su(H) – Suppressor of Hairless

T – Temperature

TAD – Transactivation Domain

TBE – Tris/Borate/EDTA buffer

TBST – Tris/Sodium chloride/Tween-20 Buffer

TE – Tris/EDTA buffer

TGF-β – Transforming Growth Factor - β

TMD – Transmembrane Domain

V – Voltage

θ – Reorientation angle

Introduction

In early metazoan development signaling-regulated gene expression relies almost entirely on five pathways, namely:

- Notch;
- Transforming Growth Factor-β (TGF-β);
- Wingless/WNT;
- Receptor Tyrosine Kinase;
- and Hedgehog;

Regarding the complexity of the metazoan development, governed by so few fundamental signaling pathways, it is not surprising that each of them presents an extraordinary action pleiotropy (reviewed in *Louvi and Artavanis-Tsakonas, 2006*). Indeed, since the *Notch* gene was first noticed in 1917 by Thomas Hunt Morgan in a strain of the fruit fly *Drosophila melanogaster* (with notches apparent in their wingblades – **Figure 1.**), the Notch signaling pathway has been subject of intense research and its involvement in numerous aspects of metazoan development is increasingly evident.

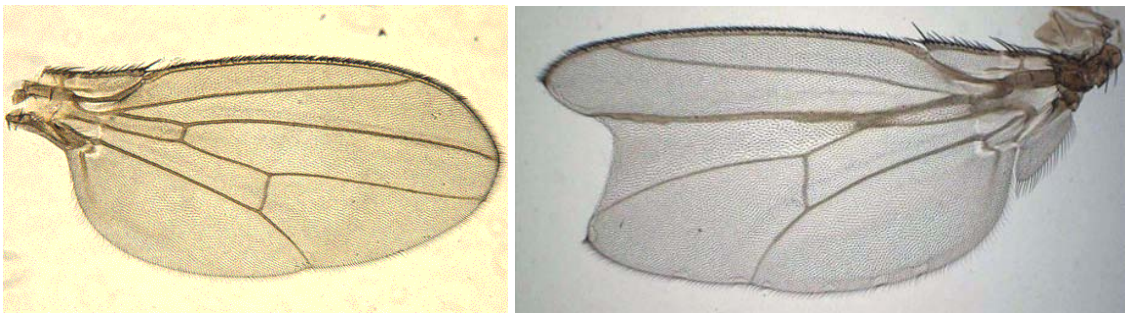

Figure 1. Wild type *Drosophila melanogaster* wing (left) **and *Notch* mutant's wing** (right)**.** This is the notching wing phenotype, associated with the haploinsufficiency of the *Notch* locus.

The Notch signaling pathway is important for cell-cell communication, and involves gene regulation mechanisms that control multiple cell differentiation processes during embryonic and adult life. It has been associated to:

- Neuronal function and development;
- Stabilization of arterial endothelial fate and angiogenesis;
- Regulation of crucial cell communication events between endocardium and myocardium during both the formation of the valve primordial and ventricular development and differentiation;
- Cardiac valve homeostasis, as well as implications in other human disorders involving the cardiovascular system;
- Timely cell lineage specification of both endocrine and exocrine pancreas;
- Influencing of binary fate decisions of cells that must choose between the secretory and absorptive lineages in the gut;

- Expansion of the hematopoietic stem cell compartment during bone development and participation in commitment to the osteoblastic lineage, suggesting a potential therapeutic role for Notch in bone regeneration and osteoporosis;
- Regulation of cell-fate decision in mammary glands at several distinct development stages;
- And possibly some non-nuclear mechanisms, such as control of the actin cytoskeleton through the tyrosine kinase Abl;

It was also shown to be deregulated in many cancers and disease states.

Besides, if we consider the action of Notch signals and keep in mind the quantitative aspects of the signal and how it integrates its action with other signaling events, we can say that Notch signaling can affect practically all cell stages (differentiation, apoptosis, proliferation and cell migration).

Nervous system development

The vertebrates nervous system starts to form fairly early in embryonic development, after the gastrulation stage, in a process referred to as neurulation.

At the end of the gastrulation stage the dorsal cord, or notochord, is formed. This cylinder of cells in the mesoderm is an important structure that defines the rostral-caudal axis of the embryo, extending along its entire length. To trigger neurulation the notochord sends molecular signals that cause the cells of the ectoderm just above it to thicken into an individualized epithelial column, the neural plate, which is found along the dorsal surface of the embryo. After this “neural induction”, the neural plate gradually folds in on itself to generate the neural groove, which then rises from the surface of the embryo and closes to form the neural tube (**Figure 2.**).

On the dorsal side of the neural tube, another special population of cells is distinguished where the neural tube protrudes, whence its name, the neural crest. Both epidermis and neural plate are capable of giving rise to neural crest cells. These cells will eventually migrate along specific pathways that will expose them once again to various inductive molecules. Ultimately, they will differentiate to form structures such as melanocytes (in the skin), neurons (in dorsal root sensory ganglia and glia), glia, autonomic neurons and chromaffin cells (reviewed in *nature reviews, neuroscience*).

On either side of the neural tube, the mesoderm thickens and divides into structures called somites. These are the precursors of the axial musculature and the skeleton. The neural tube flanking the somites will form the future spinal cord. The rostral end of the neural tube will close and continue to grow to form the various structures of the brain.

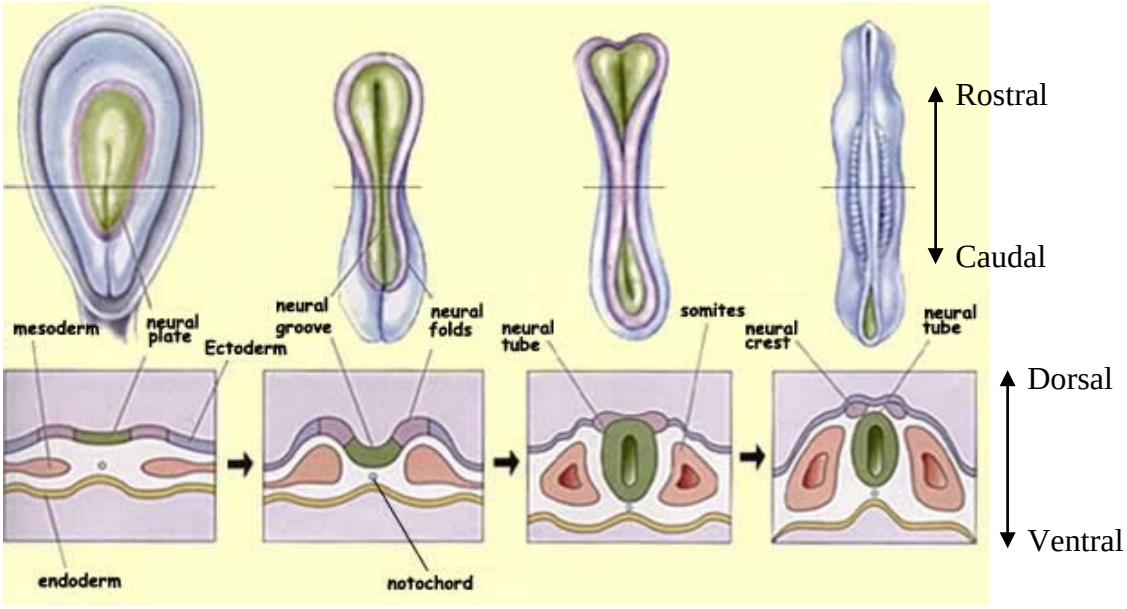

Figure 2. Schematic view of neurulation. The notochord induces the neural fate of cells from the ectoderm forming the neural plate. Later, the neural plate folds and forms the neural groove that after closure will give rise to the neural tube (image adapted from *www.thebrain.mcgill.ca*).

Neural tube

The neural tube is initially a monostratified epithelium with its apical side forming the lumenal surface of the tube. As development proceeds neuroepithelial cells divide vigorously in an unsynchronized manner, increasing dramatically its cellular density and acquiring a highly packed, pseudostratified disposition characterized by the presence of cells nuclei at different levels depending on the cell cycle stage they are (reviewd in *Latasa, 2008*).

This structure is essentially composed by the central canal, the ependymal layer (high cell proliferation zone – comprises cells within the cell cycle) and the mantle layer (cell differentiation zone) (**Figure 3.**).

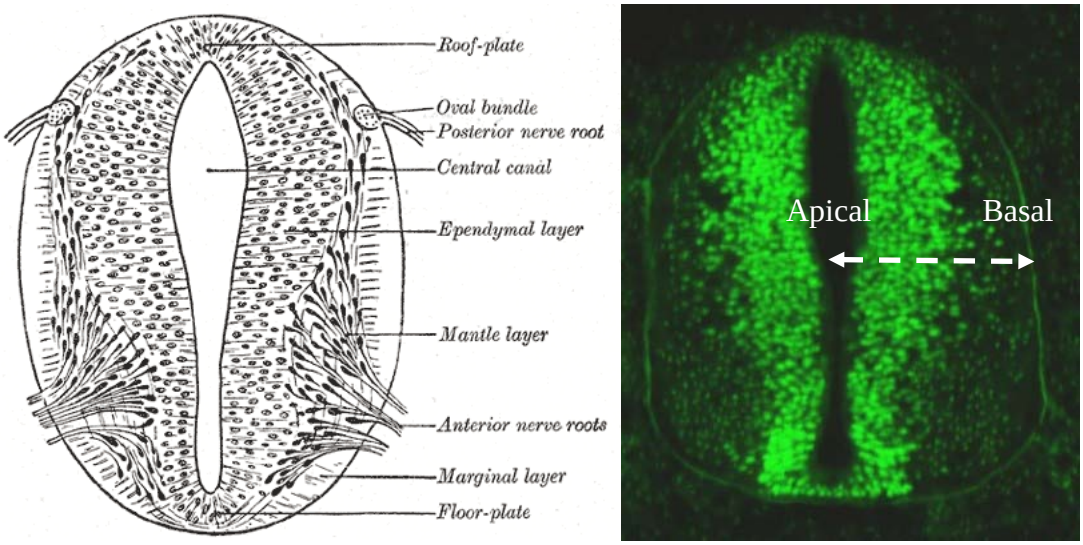

Figure 3. Schematic (left) **and Sox2 stained (transcription factor)** (right) **cut view from the neural tube** (image adapted from *www.betacell.org*).

Neurons are generated in embryonic life from multipotent progenitors close to the ventricle and, after their final mitotic division, migrate away to their ultimate destinations, where they terminally differentiate. By contrast, glial cells are generated in the proliferating subventricular zone at late embryonic and early postnatal stages (reviewed in *Louvi and Artavanis-Tsakonas, 2006*).

Cell cycle and interkinetic nuclear migration

As said before, cells nuclei in the subventricular zone are disposed at different levels along the apical-basal axis according to the cell cycle stage they are. This curious characteristic of the neuroepithelial cells suggests an apical-basal displacement of the nucleus during the cell cycle, a process termed interkinetic nuclear migration (INM).

This nuclear movement spans the entire apical-basal axis of the cell, with the nucleus migrating to the basal side during the first gap (G1) phase of the cell cycle, staying at the basal side during the DNA synthesis phase (S-phase), migrating back to the apical side during the second gap (G2) phase, and undergoing mitosis (M) at the apical side. It is so conserved throughout evolution that it can also be observed in some invertebrates, such as the eye imaginal disc of *Drosophila* (**Figure 4.**).

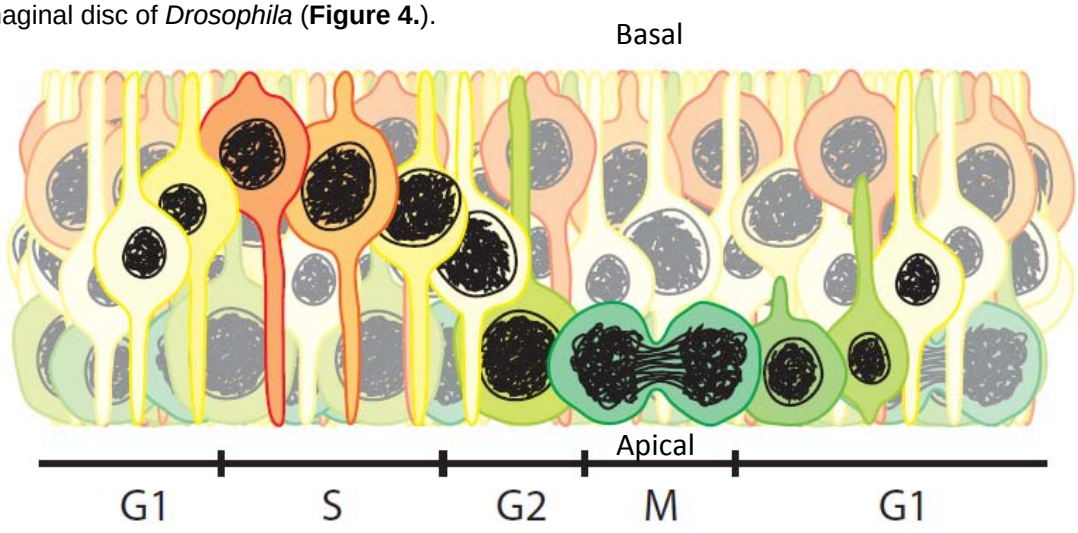

Figure 4. Scheme of the interkinetic nuclear migration observed in vertebrate neuroepithelia. Neuroepithelial cells displace their nuclei as they progress through the cell cycle. During G1, nuclei are displaced to the basal surface, where they undergo DNA replication (S-phase). Once S-phase is finished, nuclei move back to the apical portion of the neuroepithelium as they go through G2, and then they divide to give rise to two daughter cells (M) (*Latasa, 2008*).

This cellular behavior is probably due to the epithelial nature of this tissue, characterized by the attachment of neuroepithelial cells to each other by apically-located adherent junctions, which are belt-like junctions composed of cadherins linked to a ring-like cytoskeleton of actin microfilaments just above the centrosome. This tight interaction among neuroepithelial cells forces them to displace their nuclei to the apical side in order to acquire a round morphology during M, and to the basal side during interphase in order to make space for other progenitors disposed to undergo M (reviewed in *Latasa, 2008*).

Nuclear positioning in eukaryotic cells depends on active mechanisms which move nuclei within the cytoplasm and maintain them in the correct cellular location. In the vertebrate neuroepithelium, it was shown by a number of pharmacological studies that INM in this tissue is dependent on the microtubule (and microtubule-associated proteins) and actin cytoskeleton, as well as on a tightly association of the nucleus with the microtubule organizing center, the centrosome. Unlike other examples where nuclei follow the centrosome during migration, in neuroepithelial cells the centrosome remains apically located, what requires a dynamically regulated length of the microtubule network coupling the nucleus with the centrosome, and, consequently, a great dependence on molecular motors and cytoskeletal components regulators (for example the minus end-directed motor dynein, which has a “glued” phenotype associated upon truncating mutation in the dynein-regulating protein Lis1) (reviewed in *Latasa, 2008*).

Molecular mechanisms regulating the cell cycle

The G1, S, and G2 stages are globally referred to as interphase, in contrast with M, the phase when the cell generates two daughter cells with equal DNA content and chromosome number. Cell cycling exit usually happens after M completion and cells remain in a quiescent G0 state. Progression through these phases is regulated by the sequential expression, activation, and inhibition of cyclin-dependent kinase (CDK) complexes and their activating partners, the cyclins, as well as CDK inhibitors (**Figure 5.**).

The study of some of these molecular regulators has provided information that suggests a model of cell cycle progression by checkpoints, ensuring the completion of critical events in one phase before entering the next phase, and thereby coordinating cell growth with cell proliferation. There are two major check points:

- The G1/S check point, that allows a cell to initiate replication of its DNA;
- And the G2/M check point, that controls whether DNA replication has been correctly performed before the cell divide;

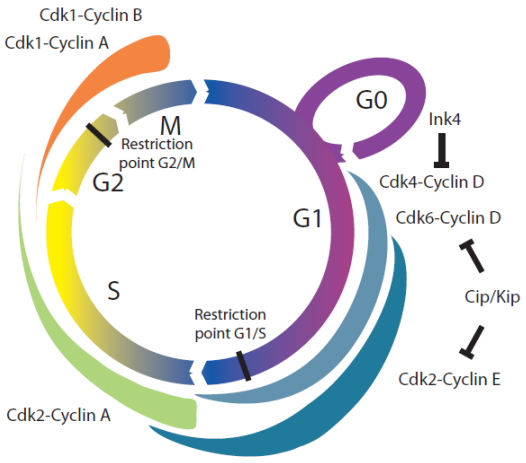

Figure 5. Schematic diagram of cell cycle and its main regulators. Progression through the cell cycle is regulated by cyclin/CDK complexes and their inhibitors (INK4 family and Kip/Cip family). Two main restriction points have been described, that control whether cells enter a new round of DNA replication (G1/S check point), and whether DNA replication has been correctly performed before the cell divide (G2/M check point) (*Latasa, 2008*).

Pharmacological studies have shown that the disruption of some molecular mechanisms regulating the cell cycle, such as inhibition of progression in S-phase with hydroxyurea, do not affect INM, and vice-versa, suggesting that both processes can be dissociated. However, such coordination is crucial for the process of neurogenesis in vertebrates as its deregulation has a dramatic influence on the size of the neural progenitor pool as well as the rate of neuronal production. This is due to lack of cell interaction cues at the right time and at the right place, such as Notch signaling (reviewd in *Latasa, 2008*).

Notch signaling and the nervous system development

The embryonic lethal phenotype linked to the homozygous, loss-of-function state of *Notch* was perhaps the first mutation associated with a clear embryonic phenotype in metazoans. The complete inactivation of *Notch* results in failure of the early neurogenic ectoderm to segregate neural and epidermal cell lineages. Instead, all cells become neuroblasts, what leads to a hypertrophy of the neural tissue at the expense of epidermal structures, giving rise to a "neurogenic" phenotype (**Figure 6.**). Studies of this phenotype carried out by Poulson (reviewed in *Louvi and Artavanis-Tsakonas, 2006*) linked *Notch* gene activity with a cell fate choice between epidermal versus neural lineage in the early embryo, relation that had not been established at the time.

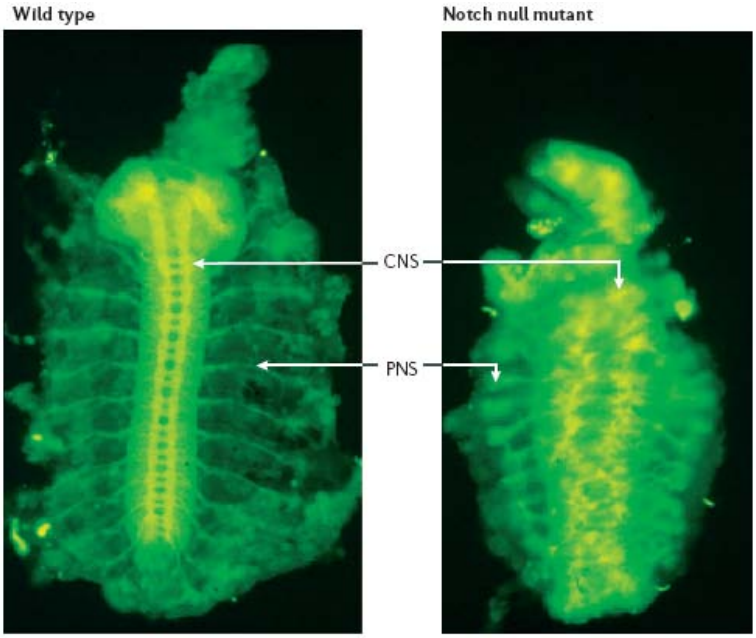

Figure 6. ***Drosophila melanogaster*** **embryos stained with an antibody against horseradish peroxidase that recognizes neural tissue.** Wild-type and Notch null mutant *D. melanogaster* embryos, showing the hypertrophy of both the central nervous system (CNS) and peripheral nervous system (PNS) that occurs in the absence of Notch (adapted from *Louvi and Artavanis-Tsakonas, 2006*).

Notch signals link the fate decisions of one cell to those of its neighbors and have been shown to be involved in neuronal progenitor maintenance, to govern the decision between the neuronal and glial lineages and to influence aspects of the behavior of terminally differentiated

neurons (elaboration of neurites in postmitotic neurons). They also contribute to aspects of brain morphogenesis, by patterning cellular fields, and might even affect neuronal migration. In fact, in the vertebrate central nervous system (CNS), neurons and glia are the two main lineages generated from the neuroepithelium which reinforces the idea that *Notch* plays an important role in neurogenesis (reviewed in *Louvi and Artavanis-Tsakonas, 2006*).

Notch activation correlates well with the inhibition of the normal differentiation pattern in the developing nervous system and the same is observed between expression of Notch pathway elements and uncommitted cells. This supports the idea that Notch signals in this context are not instructive but permissive and are responsible for maintaining a precursor cell in a pluripotent state until the correct differentiation cue is available.

Even though, the expression of a Notch pathway element does not necessarily imply Notch signaling.

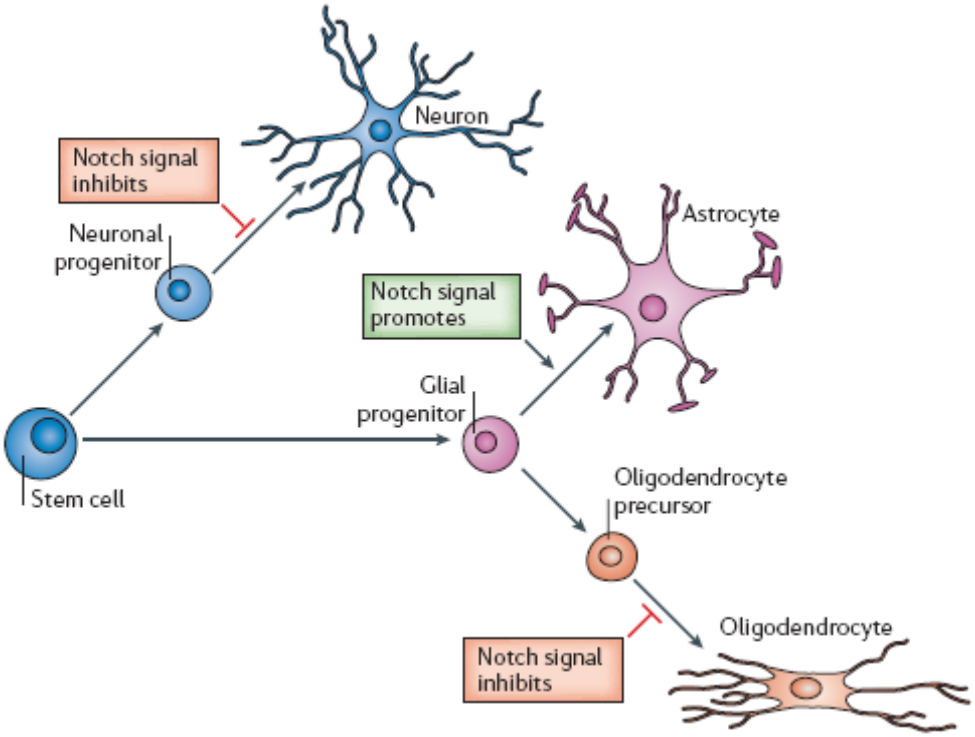

Figure 7. A schematic summarizing of the effects of Notch signal activation on cell fate decisions in the vertebrate nervous system. The self-renewing stem cells can give rise to neuronal progenitors and glial progenitors. The firsts are inhibited to progress to neurons by Notch signal activation, in contrast to the glial progenitors that differentiate into astrocytes with the help of Notch signals. Finally, oligodendrocyte precursors derived from glial progenitors fail to differentiate into mature oligodendrocytes in the presence of active Notch signals (adapted from *Louvi and Artavanis-Tsakonas, 2006*).

The molecular analysis and sequencing of Notch was undertaken in the 1980s and defined it as a 300 kDa single-pass transmembrane receptor which indicated a role for it in cell interactions, as said before. In addition, this result was compatible with the findings of Doe and Goodman and, together, they help explain the neurogenic phenotype of embryos lacking Notch function. Their laser ablation studies indicated that the commitment to a neural fate by one cell, in the early neural ectoderm, had the consequence of inhibiting its neighbors to follow the same

fate. So, this suggests that the disruption of Notch-dependent cellular communications can cause all of the neighboring cells to develop into neuroblasts leading to a hypertrophy of neural tissue (reviewed in *Louvi and Artavanis-Tsakonas, 2006*). This reveals a mechanism of action for Notch in neural development, called “lateral inhibition”.

Notch signaling pathway

The Notch signaling pathway is a highly conserved cell signaling system present in most multicellular organisms. Some species even comprise paralogues (genes at different chromosomal locations in the same organism that have functional and structural similarities) of *Notch* and\or genes encoding its ligands in their genome. Some studies suggest they retain qualitatively interchangeable biochemical activities, yet differ in their tissue-specific expression (**Table I**).

Table I. Notch pathway components in different species (adapted from *Louvi and Artavanis-Tsakonas, 2006*).

	Chick	***Drosophila melanogaster***	***Caenorhabditis elegans***	**Mammals**
Receptor	Notch1 Notch2	Notch	lin12 glp1	Notch1 Notch2 Notch3 Notch4
Ligand	Delta1 Delta2 Jagged1 Jagged2	Delta Serrate	lag2 apx1 arg2 f16b12.2	Dll1 (Delta-like 1) Dll3 Dll4 Jagged1 Jagged2
CSL	CBF1/RBPjκ	Su(H)	Lag1	CBF1/RBPjκ

The Notch receptor is a transmembrane, heterodimeric molecule composed of a large extracellular portion, which associates in a calcium-dependent, non-covalent interaction with a smaller piece of the Notch protein composed of a short extracellular region, a single transmembrane-pass, and a small intracellular region. The extracellular domain is primarily composed of small cysteine knots called EGF repeats, common to the majority of Notch ligands, which are also single-pass transmembrane molecules. The Notch intracellular domain (NICD) consists of a RAM (RBPjκ association module) domain, seven ankyrin (Ank) repeats, a C-terminal PEST domain and nuclear localization signal sequences (NLS) (**Figure 8.**) (adapted from *Kopan and Ilagan, 2009*).

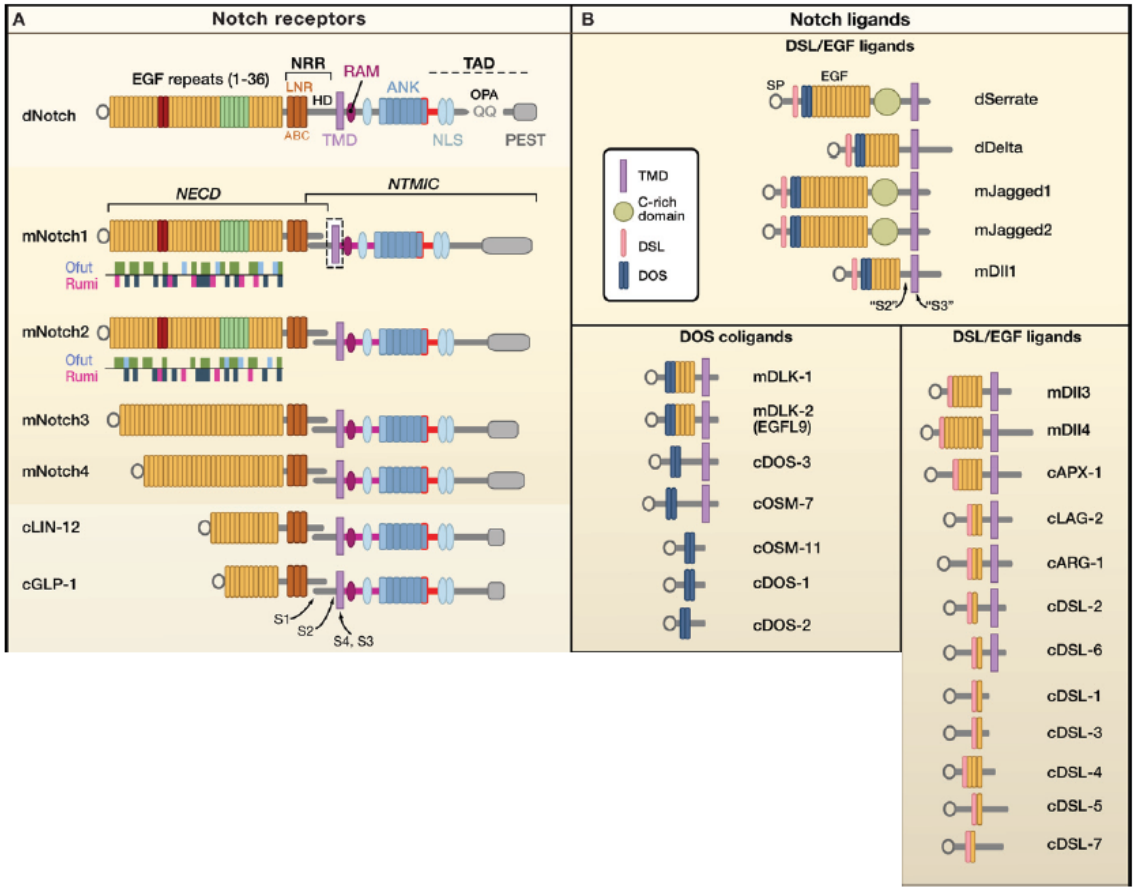

Figure 8. Domain Organization of Notch Pathway Receptors, Ligands, and Coligands. (A) Notch receptors are large type I proteins that contain multiple extracellular EGF-like repeats. EGF repeats 11–12 (red) and 24–29 (green) mediate ligand interactions. These repeats may contain consensus motifs for fucosylation by O-Fut1 and glycosylation by Rumi; the putative distribution of fucosylation sites (common, green; unique, light blue) and glycosylation sites (common, dark blue; unique, magenta) are shown for mNotch1 and mNotch2. EGF repeats are followed by the negative regulatory region (NRR), which is composed of three cysteine-rich Lin12-Notch repeats (LNR-A, -B, and -C) and a heterodimerization domain (HD). Notch also contains a transmembrane domain (TMD), a RAM (RBPjκ association module) domain, nuclear localization sequences (NLSs), a seven ankyrin repeats (ANK) domain, and a transactivation domain (TAD) that harbors conserved proline/glutamic acid/serine/threonine-rich motifs (PEST). The transactivation domain in *Drosophila* Notch also has a glutamine-rich repeat (OPA). (B) Known ligands and putative ligands of Notch receptors can be divided into several groups on the basis of their domain composition. Classical DSL ligands (DSL/DOS/EGF ligands) contain the DSL (Delta/Serrate/LAG-2), DOS (Delta and OSM-11-like proteins), and EGF (epidermal growth factor) motifs and are not found in *C. elegans*. *C. elegans* and mammalian DSL-only ligands lacking the DOS motif (DSL/EGF ligands) are a subtype of DSL ligands that may act alone or in combination with DOS coligands (for example, cDSL-1 and possibly Dll3). This subfamily includes soluble/diffusible ligands (adapted from *Kopan and Ilagan, 2009*).

There are genes codifying for transcription factors, which belong to the basic helix-loop-helix (bHLH) family, known as proneural genes. These are necessary and sufficient to promote the generation of precursors cells determined to neural differentiation, and can be divided into two families according to their homology to *achaete-scute* (*asc*) complex and *atonal* (*ato*) in *Drosophila*. In mouse, there are *Mash1* and *Mash2*, from the *asc* family (only *Mash1* was shown to be implicated in nervous system development), and the *ato* family can be divided in three

subfamilies attending to differences in their basic domain: *Neurogenin* (*Ngn*), *ato homologues* (*ath*) and *NeuroD*. These three *ato* subfamilies can be found in all vertebrates.

The proneural genes *Mash1* and *Ngn2* regulate the expression of Notch ligands, such as Delta-like1 (Dll1). When the extracellular domain of the Notch receptor interacts with one of its ligand (interaction regulated by post-translational events such as glycosylation and other modifications) a series of proteolytic events is triggered. The Notch receptor is cleaved under the presenilin-γ-secretase complex recruitment and the NICD, carrying nuclear localization signals, is released from the membrane and translocates into the cell nucleus. There, NICD acts as an activation and recruitment element, forming a complex with suppressor of hairless (Su(H)), CBF1/RBPjκ in mammals (a DNA-binding protein interacting with a co-repressor until then), and mastermind (a nuclear protein). This complex, in turn, directs the assembly of transcriptional complexes that drive target-gene expression, such as of basic helix–loop–helix (bHLH) transcriptional repressors (for example, the *hairy* and *enhancer of split* (*HES*) and *HES related* (*HESR*/*HEY*) family genes in vertebrates) (reviewed in *Louvi and Artavanis-Tsakonas, 2006*). These Notch target genes products are then responsible for inhibiting the expression of proneural genes, acting as transcriptional repressors when bound to DNA, although it is also possible that they act by interfering in the formation of proneural proteins and E proteins complexes (a type of bHLH proteins expressed ubiquitously) (**Figure 9.**).

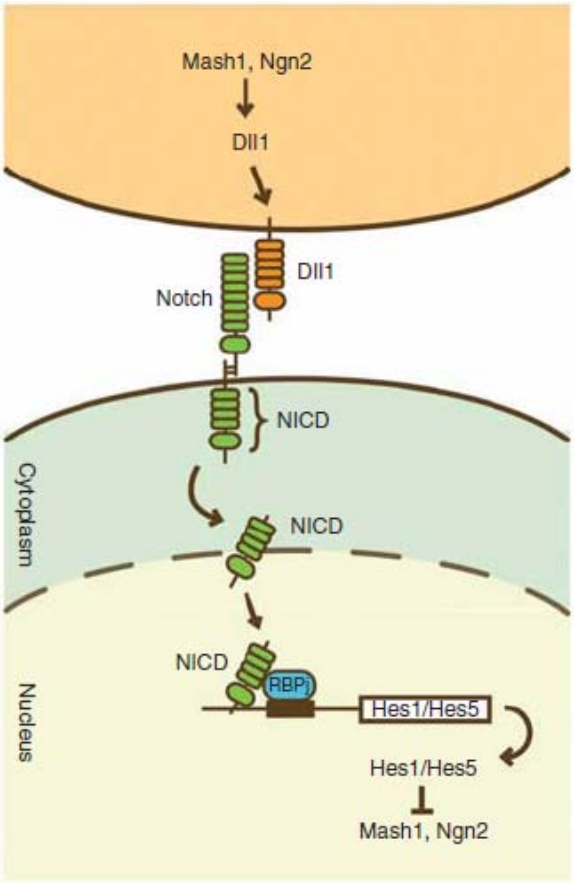

Figure 9. Schematic view of the Notch signaling pathway. The proneural genes *Mash1* and *Ngn2* induce expression of Notch ligands such as Dll1, which activate Notch signaling in neighboring cells. Upon activation, the NICD is released from the transmembrane region and transferred to the nucleus, where it forms a complex with RBPjκ and induces *Hes1* and *Hes5* expression. Hes1 and Hes5 repress proneural gene expression (*Kageyama, 2008*).

Notch pathway, cell cycle INM and neurogenesis

Lateral inhibition is an essential action mechanism by which proneural genes inhibit their own expression in adjacent cells, restricting their own activity to single progenitor cells. This is done by stabilization or amplification of differences between neighbors caused by stochastic events (reviewed in *Artavanis-Tsakonas et al., 1999*).

The process must be reiterated, because Notch activity is transient, whereas the expression of proneural genes persists in the neuroectoderm throughout the period of neurogenesis. At first, proneural genes are expressed or activated at low levels and a reversible selection of precursors takes place due to inhibitory waves of Notch signaling. At some point, it starts to act as an amplifier of those levels and progenitors undergo an irreversible commitment to the neural fate (reviewed in *Latasa, 2008*).

To better understand the mechanism one can think about a group of cells inhibiting each other through Notch signaling. This causes oscillations in each cell, whereas it is inhibited or inhibiting. However, if one cell escapes from some of its neighbors' inhibiting bursts it starts to amplify its proneural genes activity and at some point its inhibitory potential will be so high that none of its neighbors will be able to reverse its commitment any more.

Moreover, the expression levels of neurogenic and proneural genes have been shown to oscillate as the neural precursors proceed through the cell cycle. During vertebrate development, Notch1 expression increases at the neuroepithelium apical region, where neural precursors going through M are located and the newly generated neurons are born. Also, Dll1 begins to be expressed by the newly born neurons as they initiate their migration through the apical aspect of the neuroepithelium. In this manner, neural precursors basally located within the neuroepithelium, where cells in S-phase are found, show low levels of Notch1, Delta1, Ngn1 and Ngn2, while expression of these genes in proliferating precursors undergoing G2/M/early G1 phases, and situated close to the apical surface, is higher. This means that no inhibitory signals seem to be regulating the previously mentioned proneural and neurogenic genes during S-phase, which indicates the absence of neurogenic capacity during this phase (*Murciano et al., 2002*). The mechanism that prevents *Dll1*, *Ngn1* and *Ngn2* expression during S-phase is unknown at present.

Several lines of evidence suggest that, during S-phase, progenitor cells are plastic and capable of modifying their fate in response to environmental signals but that in G2/mitosis, they become committed to a particular phenotype (reviewed in *Latasa, 2008*).

At present, little is known about the molecular basis underlying this cell cycle-dependent loss of plasticity, but one hypothesis is that this phenomenon further reflects the relationship between the cell cycle and the expression of molecules that are directly involved in the process of neurogenesis (*Murciano et al., 2002*).

Two Notch pathway reporters in the mouse: Dll1 and Hes5

Since Dll1 is susceptible to regulation by the transcription factors codified by the proneural genes, Delta1 expression can be a measurement of the neurogenic capacity of neural precursors (reviewed in *Latasa, 2008*).

However, co-localization of Notch1 receptor, Delta1 ligand and several known regulators of their interaction is not enough to prove activation of Notch signaling cascade in the apical region of the neuroepithelium.

On the other side *Hes5* is downstream effector of Notch activation and its expression levels may reflect the activation of the Notch signaling pathway.

Hes1 expression is also affected by Notch1 expression, although at a lesser degree when compared to *Hes5-1* expression (reviewed in *Latasa, 2008*).

Stem cells

The promise of stem cells for therapeutic applications, together with the intrinsic scientific appeal associated with a developmentally multipotent cell, has made this elusive cell population the focus of considerable interest.

In 1970, two researchers' teams (Solter et al. and Stevens) reported that early mouse embryos grafted into adult mice produced teratocarcinomas, which are malignant multidifferentiated tumors containing a significant population of undifferentiated cells, named embryonic carcinoma (EC) cells. It had already been shown that these cells can be propagated in culture, and later this was proved to be also true for embryo-derived teratocarcinomas cells. Not only could EC cells be expanded continuously but could also differentiate either *in vitro* or via teratocarcinoma formation, retaining the capacity for differentiation and the potential to give rise to derivatives of all three primary germ layers: ectoderm, mesoderm, and endoderm. Therefore, individual EC cells are self-renewing, pluripotent stem cells (reviewed in *Austin Smith, 2001*).

The ultimate test to this capacity was performed in 1974, by Brinster, who found that some EC cell lines could participate in embryogenesis and contribute with derivatives to a variety of tissues in resultant chimaeric fetuses and live-born mice. However, most EC cell lines showed poor differentiation potential *in vitro* and *in vivo* and poor contribution to chimeras and/or production of embryonic tumors. Moreover, EC cells are almost always aneuploid and cannot consequently proceed through meiosis to produce mature gametes (the cell needs a balanced chromosome complement to go through meiosis).

Due to these findings, the concept of stem cells as cells with potential to be isolated and continuously cultured while retaining full developmental potency and identity remained open to question for some years (reviewed in *Austin Smith, 2001*).

In 1981, Evans and Kaufman, and Martin, reported the derivation of pluripotent cell lines directly from mouse, embryonic stem (ES) cells. The protocols for ES cell derivation are relatively simple and consist on plating embryos at the expanded blastocyst stage (remove the

embryos from the mouse and maintain them by *in vitro* culture), either intact or following immune-surgical isolation of the inner cell mass (ICM) (**Figure 10.**).

In contrast to EC cells, ES cells behave relatively consistently in their ability to integrate into the embryo and produce viable chimeras, producing functional differentiated progeny in all tissues and organs. Moreover, ES cells maintain a diploid karyotype, crucial for meiosis. Thus, unlike EC cells, ES cells are capable of generating functional gametes as long as they can colonize the germ cell lineage in a chimera, which depends absolutely on adherence to a rigorous tissue culture regime.

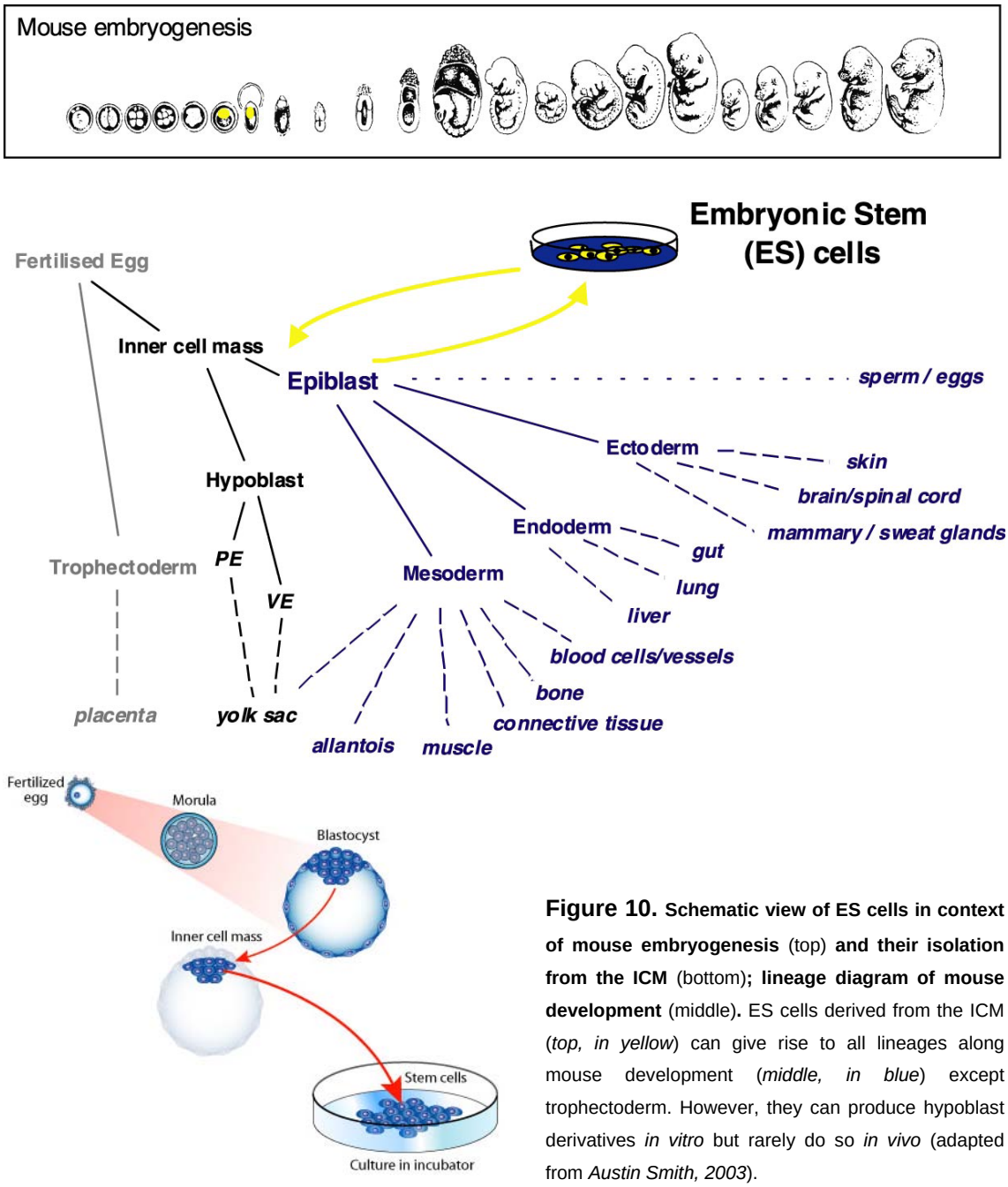

Figure 10. Schematic view of ES cells in context of mouse embryogenesis (top) **and their isolation from the ICM** (bottom)**; lineage diagram of mouse development** (middle)**.** ES cells derived from the ICM (*top, in yellow*) can give rise to all lineages along mouse development (*middle, in blue*) except trophectoderm. However, they can produce hypoblast derivatives *in vitro* but rarely do so *in vivo* (adapted from *Austin Smith, 2003*).

ES cells are most accurately described as pluripotent, reserving the term totipotent for the fertilized egg and blastomeres of the cleavage stage embryo that actually do have total developmental potency. This refers to the fact that they can give rise to germ cells except trophectoderm (**Figure 10.**). Hence, they cannot generate a blastocyst de novo and are not therefore sufficient to produce an embryo.

Although pluripotency is an essential feature of an ES cell, it does not follow that all pluripotent stem cells are equivalent to ES cells. The defining properties functionally important and/or unique to mouse ES cells are:

- Origin from the ICM/epiblast;
- Derivation without transformation or immortalization;
- Stable diploid karyotype;
- **Unlimited self-renewal capacity**;
- **Pluripotency**: can generate all fetal and adult cell types *in vitro* and in teratoma;
- Incorporation into embryonic development and **contribution to all germ layers** in chimera;
- And germ line colonization and transmission (gametogenesis contribution).

In the case of human pluripotent stem cells, the last two properties cannot be determined for obvious ethical reasons (reviewed in *Austin Smith, 2001*).

Stem cells culture and differentiation towards neural lineage

Pluripotent mouse ES cells can be expanded in culture indefinitely while retaining the capacity to produce virtually every type of fetal and adult cell. Since they were first described, they have been derived and maintained by using various empirical combinations of feeder cells, conditioned media, cytokines, growth factors, hormones, fetal calf serum, and serum extracts.

One way is to use a combination of the cytokine leukemia inhibitory factor (LIF) to activate the transcription factor STAT3 and either serum or bone morphogenetic protein (BMP) to induce expression of *inhibitor of differentiation* (*Id*) genes via the Smad pathway (**Figure 11.**) (*Qi-Long Ying and Austin Smith, 2003*).

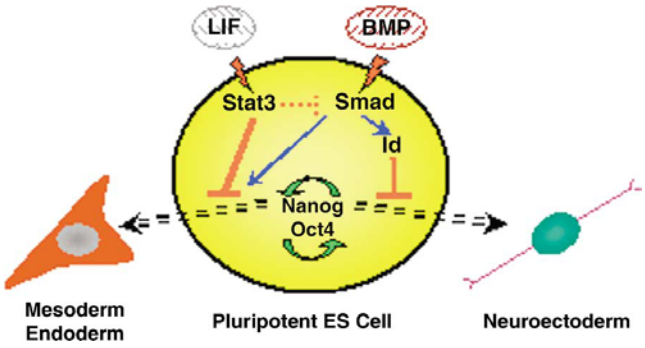

Figure 11. Cooperative Lineage Restriction by BMP/Id and LIF/STAT3. ES cell self-renewal requires suppression of lineage commitment. *Id* genes induced by BMP or other signals blockade entry into neural lineages, which is otherwise only partially prevented by LIF/STAT3. In parallel, the capacity of BMP to induce mesodermal and endodermal differentiation is constrained by STAT3, probably involving direct as well as indirect mechanisms (*Qi-Long Ying and Austin Smith, 2003*).

The specification of primary lineages has been subject of intense research. However, it still is not completely understood and consequently the differentiation protocols are empirical, yielding variable and heterogeneous outcomes, and often poorly reproducible. Some of these protocols, specifically the ones regarding ES cells commitment to neural fate, are based for example in multicellular aggregation in suspension culture – embryoid bodies (followed by treatment with retinoic acid), or co-culture on a feeder layer of mitotically inactivated mouse embryo fibroblasts.

Though, in 2003, Qi-Long Ying and Austin Smith described a protocol capable of converting ES cells into neuroectodermal precursors in adherent monoculture by eliminating inductive signals for alternative fates. In that work, they postulated that the process by which the culture components affect cells commitment to neural fate is not a default pathway, but requires the presence of autocrine fibroblast growth factor (FGF) (*Qi-Long Ying and Austin Smith, 2003*).

The monitoring of the successive steps along the differentiation pathway is usually done by sampling and subsequent analysis of gene expression, using RT-PCR (Real-time polimerase chain reaction) and immunocytochemistry. However, ES cell lines that contain fluorescent reporters under the control of genes expressed at specific differentiation states have recently become available, allowing live and precise monitoring of specific cell states and, in addition, the final purification of these cells by FACS (Fluorescence-activated cell sorting).

Model

The model used in the work described below is based on a protocol for the differentiation of mouse ES cells into neural precursors, modified from that described by Qi-Long Ying and Austin Smith (see section: *Culture of undifferentiated ES cells and monolayer differentiation*).

This *in vitro* model allows the expansion and differentiation of mouse ES cells in adherent monolayer culture and the rate of neural differentiation reaches up to 90% of the total cell population. During the process, neural progenitors organize in rosette structures that were

shown to mimic some of the neural tube cells' behavior *in vivo*. Namely, these rosettes present proper apical-basal polarity, Notch pathway activation and cells within them undergo INM and have both neurogenic and gliogenic potential (**Figure 12.**) (*Abranches et al., 2009*).

In this work, we also carried out some work contributing for the validation of this ES cell neural differentiation model, namely regarding *Dll1* activity in the rosette structures.

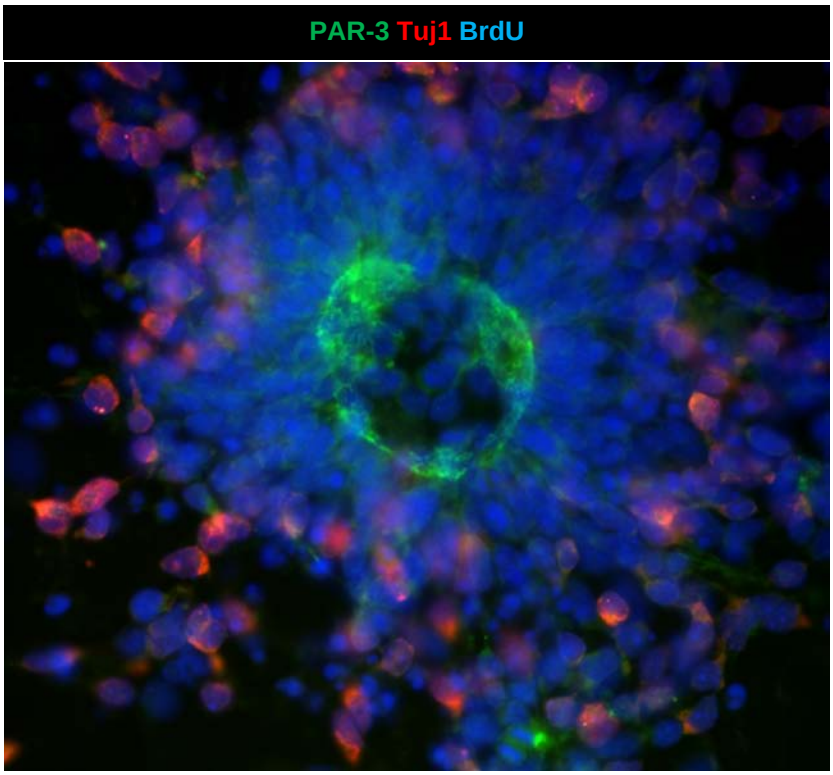

Figure 12. Rosette of neural progenitors depicting cells organization analogous to the neural tube. Cells are stained for the apical junction marker PAR-3 (green) ,evidencing cell polarity and apical -basal organization, and for the cell cycle exit marker Tuj1 (red), depicting an external zone analogous to the mantle zone of the neural tube. The cells' nuclei are stained with bromodeoxyuridine – BrdU (blue), a synthetic thymidine analog that gets incorporated into a cell's DNA when the cell is dividing (during the S-phase of the cell cycle) (image from *Abranches et al., 2009*).

Objectives and experimental strategy

The work described here aims to contribute to the understanding of Notch pathway, particularly to enlighten the possible correlation between Notch and the cell cycle during neurogenesis. To achieve this, our efforts were directed specifically towards:

- The generation of transgenic mouse ES cell lines containing a fluorescent reporter for the purpose of visualizing the activity of *Dll1* in ES cells using BAC (Bacterial Artificial Chromosome) recombineering;
- The validation of the model used in the lab, namely concerning the relation between *Dll1* expression, INM and cell cycle in the rosettes;

This work was divided in two parts, as shown above. For the first part, the objective was to continue the work already performed in the lab[1], namely by establishing a reproducible and consistent BAC extraction and visualization protocol. The schematic view of the strategy to perform this part is shown below:

1. Generation of the reporter ES cell lines:

    a. Generate the *Dll1*:*mCherry*:*NLS*[2] BAC construct:
        i. Bioinformatics search and selection of a BAC containing the gene *Dll1* (www.ensembl.org);
        ii. Construct the recombineering cassette;
        iii. Induce homologous recombination in *Escherichia coli* to generate engineered BAC for the gene;

    b. **Extract the BAC, digest it and run in pulsed-field electrophoresis gel (PFGE) to assess its integrity**[3];

    c. Transfect the engineered BAC into mouse ES cells (*E14tg2a* line) and establish clones;

    d. Excision of the drug-selectable marker;

    e. Characterize the transgenic ES clones and verify the reporter expression (*Dll1*:*mCherry*:*NLS*) during ES cells self-renewal and differentiation;

[1] The PhD student Filipe Vilas-Boas was responsible for generating the BAC construct.
[2] *mCherry* encodes a red fluorescent protein (RFP) that after electroporation will allow the monitoring of the *Dll1* promoter activity in ES cells.
[3] The work described focuses on this part of the project.

To perform the second part, ES cell culture knowledge was needed. Therefore, the experimental strategy for the second part was:

2. Validation of the *in vitro* model:

    a. **Learn ES cell culture:** expansion and neural differentiation protocols as well as quantification (FACS) and culture monitoring methods (e.g. *mycoplasma* testing);

    b. Differentiate ES cells containing the reporter *in vitro* and fixate them in immunocytochemistry cover-slips[4];

    c. Visualize cells using fluorescent microscopy (*Leyca DM 5000B* fluorescent microscope);

[4] The results shown for the second part of the work are from cell cultures performed by the post-Doctoral student Elsa Abranches.

Experimental procedures

1st part – BAC extraction, digestion and visualization

Generation of the *Dll1*:*mCherry*:*NLS*[5] BAC construct

The first step for generating the construct was to choose a BAC clone with 150-250 Kbp (kilo-base pairs) of DNA centered on the gene of interest and order it (*bacpac.chori.org*). The large size of the construct assures, in principle, that all the regulatory elements of the gene plus large pieces of the flanking DNA are present. This avoids transgene silencing or ectopic expression due to interference of elements located in the genome surrounding the place of transgene integration (chromosomal position effect) (*Carlos Rodrigues, 2007*). Also, it avoids concatemerization[6] and, thereby, the transgenic alleles with high copy number that can result in non-physiological levels of expression in the transgenic mice.

However, such large fragments of genomic DNA are difficult to manipulate (clone and modify) and approaches other than classical genetic engineering are required.

In 2001, Copeland et al. described a technique termed recombineering, based on highly efficient phage-based *E. coli* homologous recombination systems, that allows DNA manipulation without the need for restriction enzymes or DNA ligases, leading to easier and more efficient BAC manipulation (**Figure 13.**) (*Copeland et al., 2001*).

[5] *mCherry* encodes a red fluorescent protein (RFP) specifically designed to work on mouse. After electroporation it will allow the monitoring of the *Dll1* promoter activity in ES cells.

[6] A concatemer is a long continuous DNA molecule that contains multiple copies of the same DNA sequence linked in series.

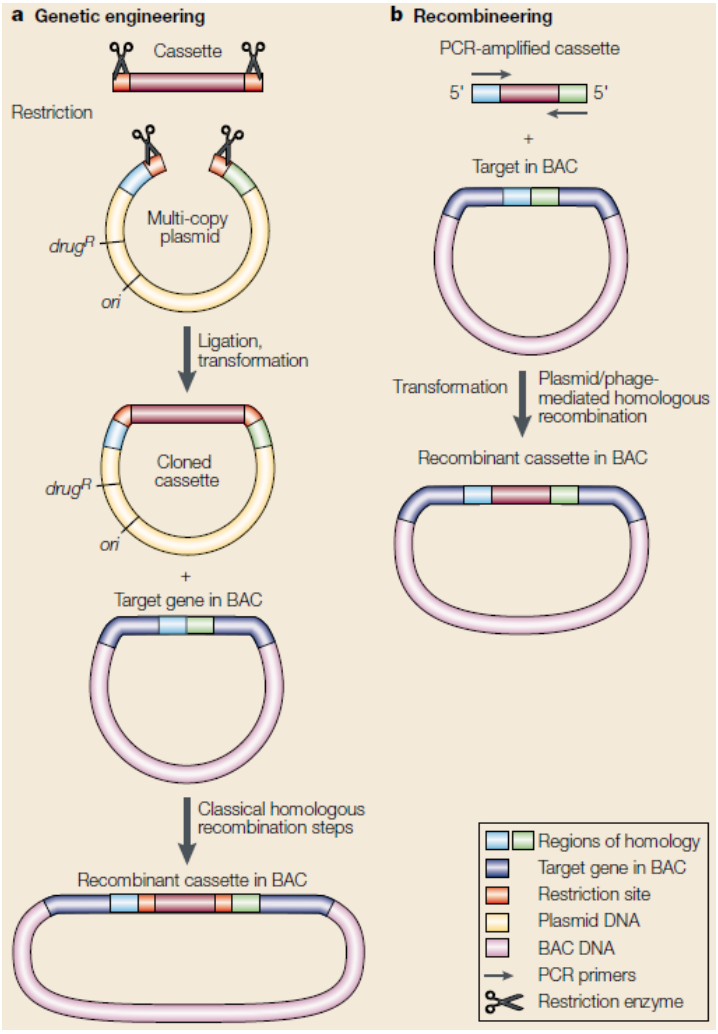

Figure 13. Classic recombinant DNA technology versus recombineering. Recombineering steps to generate a BAC recombinant include: Amplifying a cassette by PCR with flanking regions of homology; Introducing phage recombination functions into a BAC containing bacterial strain, or introducing a BAC into a strain that carries recombination functions; Transforming the cassette into cells that contain a BAC and recombination functions; Generating a recombinant *in vivo*; Detecting a recombinant by selection, counter-selection or by direct screening (colony hybridization) (image adapted from *Copeland et al., 2001*).

In this case, the system Red from the defective λ-prophage was used to carry out the BAC modifications due to its non-requirement for drug resistance to maintain it in the cells. Also, the possibility to use other plasmids disregarding incompatibility and leaky expression of recombination functions were major advantages taken in account for choosing this recombinant system. The system Red can be activated simply by exposing cells to temperatures around 37ºC.

After construction, the cassette with the fluorescent reporter was inserted in a plasmid, flanked by two regions of homology (approximately 500 bp each) for the upstream and downstream sides of *Dll1*'s coding region so that recombination can occur. The cassette was constructed by gathering several fragments using PCR and the adequate primers. It has a resistance fragment containing the *neo* (neomycin and kanamycin resistance) gene, which can be expressed both under control of a prokaryotic promoter (*EM7*) or an eukaryotic promoter

(*PGK*). It also contains a *BGHpA* region (Bovine Growth Hormone poly-Adenylation signal) that instructs the addition of an adenine tail to the mRNA, which consequently increases the RNA stability. Moreover, this resistance cassette fragment is flanked by *Flp* (Flipase protein) recombinase recognition sites (*FRT*) and this allows the excision of the cassette after the validation of the clones (**Figure 14.**).

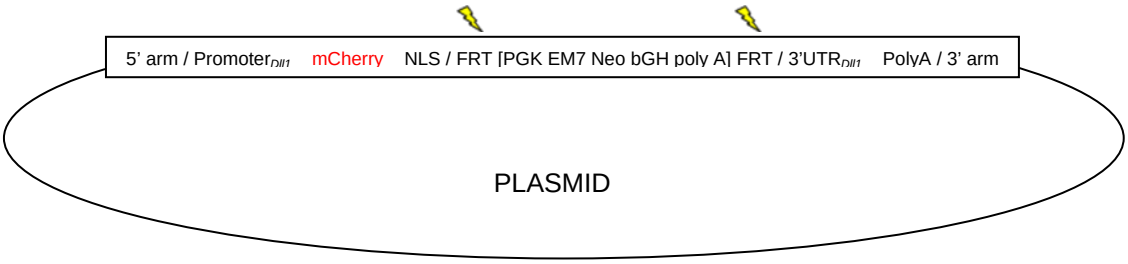

Figure 14. Schematic representation of the BAC with the inserted cassette. The inserted cassette substituted the coding region of the *Dll1* gene inside the BAC. The promoter maintenance ensures the expression of the reporter under the same conditions and levels of expression as the endogenous *Dll1*. The *FRT* sites allow the removal of the resistance cassette.

Therefore, the ordered BAC (RP23-64I11 – BAC 64I11 from the library RP23, available in *E. coli* DH10B[7] cells) was transformed into SW105 strain cells, containing the chosen recombination functions and the recombination step between the cassette and the BAC was induced. The recombination step consisted in replacing the endogenous coding sequence of *Dll1* in the BAC with the fluorescent reporter, starting at the initial ATG codon, together with the drug-selectable marker (**Figure 15.**).

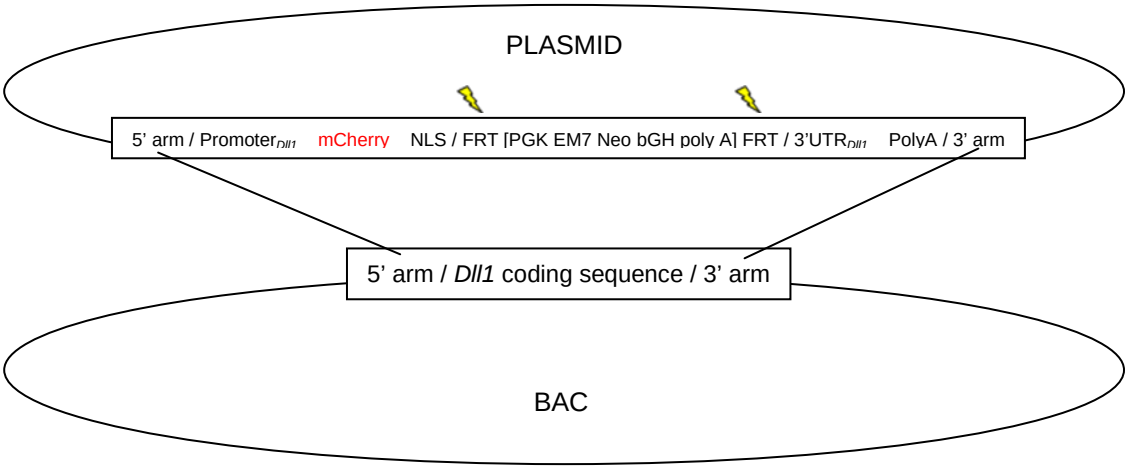

Figure 15. Schematic representation of the recombination step between the plasmid with the resistance cassette and the BAC. The inserted cassette substitutes the coding region of the *Dll1* gene inside the BAC due to recombination between the regions of homology (5' and 3' arms). The promoter maintenance ensures the expression of the reporter under the same conditions and levels of expression as the endogenous *Dll1*.

[7] *E. coli* DH10B strain is designed for the propagation of large insert DNA library clones, and is derived from the strain DH5α, which has several features that make it useful for recombinant DNA methods.

Establishment of the final extraction and visualization protocols

This part of the present thesis describes all the procedures/steps taken to get from the initial extraction and visualization protocols to the establishment of the final protocols for the same purposes. Specifically, it will focus on the most relevant problems encountered along the work in the lab and in the solutions proposed to overcome them.

Initial BAC extraction protocol

The following protocol was the one used in the lab before the establishment of the new protocols for extracting and visualizing the BAC. It is described as the first time it was performed in order to explicit all the procedures and considerations made in each step.

First, grow bacteria to amplify the number of the BAC. This procedure is initiated in the day before the BAC extraction.

In the 1st day:

Streak bacteria containing the BAC in a plate coated with LB (Luria-Bertani) medium plus agarose (LB + agar) and the selecting antibiotic[8], at a suitable concentration for a low copy BAC. (**Table II.**).

Let grow overnight at 32ºC (not to activate the recombination system).

In the 2nd day (after approximately 16 hours):

Grow bacteria overnight at 32ºC in LB using the same selecting antibiotic[9], and concentration, as before in a recipient with a volume of about 10× the volume of the culture.

Table II. Drug concentration for low copy BACs (adapted from *"Molecular Cloning: A Laboratory Manual"*).

	Ampicillin	Cloranphenicol	Kanamycin	Tetracycline
Concentration (µg/mL)	20	12,5	10	12,5

When the cell culture reaches a suitable density (OD_{600} ≈ 1.0) the BAC extract the BAC from the cells. This is the BAC extraction step.

Pellet 50 mL culture aliquots by centrifugation at 4000 rpm for 30 minutes.

Use the "PSI Ψ Clone Big BAC – DNA isolation kit" from *Princeton Separations* to extract the BAC DNA from the cells (**Figure 16.**).

[8] The cells containing the BAC not only contain resistance to neomycin/kanamycin (from the BAC, after recombineering) but also to cloranphenicol (encoded by the BAC's vector), to ampicillin (inserted along with an auxiliary vector to add an extra restriction site, previously to the recombineering step) and tetracycline (due to transfer of genomic material from the λ-phage when transfecting the recombination system Red). However, this last resistance was never used because this transference of genomic material depends on the cell strain and may not have occurred in this particular case.

[9] Using the same selecting antibiotic for streaking and growing the cells prevents their need for re-adaptation and consequent alterations in growth.

PSI Ψ Clone

Big BAC

DNA isolation kit

Catalog Number PP-121

The **PSI Ψ Clone Big BAC** DNA isolation kit accomodates culture volumes of 25 to 250mL. Any volume within this range may be processed by scaling the reagents to the culture media at a 1:10 ratio. The BAC DNA is captured in batch mode using a highly efficient, hydrophylic non-silica anion exchanger. The BAC DNA/resin complex is poured into a fritted column for washing and recovery of the DNA. The gravity based wash steps remove RNA and protein contaminants. Elution is easily achieved in a small volume of elution buffer by inserting the column into a 50mL centrifuge tube and centrifuging at low g force. Typical yields are 5-10μg BAC DNA from 25-30mL of culture.

Required but not Supplied

Ice bath
High speed centrifuge (Sorvall RC5 or equivalent)
50mL conical centrifuge tubes

Product Description	Catalog Number
PSI Ψ Clone Big BAC DNA isolation kit, reagents for processing 250mL of culture media	PP-121
PSI Ψ Clone BAC DNA isolation kit reagents and columns to process 25, 3-5mL BAC cultures	PP-120

Tel: 800.223.0902
info@prinsep.com
www.prinsep.com

79-100612D

Helpful Hints

Excessive chromosomal DNA can result from poor lysis or from high culture density. Dilute heavy cultures to an OD_{600} of 4.0 to 6.0.

Do not vortex sample at lysis step. Gentle inversion of sample is sufficient.

Do not shorten the incubation times or chromosomal DNA may not pellet.

If your centrifuge generates less than 20,000 x g, extend the spin time to achieve approximately the same g x time value.

At Step 7, be certain to spin out the remaining wash buffer as directed. In Step 8, allow the elution buffer to incubate on the matrix for at least 2 minutes before recovering the eluant.

DNA loss often occurs at the precipitation step. The pellet is barely visible due to the small amount of DNA present. Orient the microfuge tubes in the rotor in a consistent manner so that the relative position of the pellet is known. Use care when pipetting supernatants to not dislodge the pellet.

Very low yield from a clone that has previously produced higher yields, is often due to recombination resulting in insert loss. Restriction digestion and electrophoresis should be used to confirm the insert size. Since BAC's have a fixed copy number, recombination will result in a smaller insert and a lower yield.

DNA isolated from some E.coli strains (e.g., HB101 and derivatives) does not sequence well. Our recommendation is to use DH10B host strains.

Figure 16. Procedure Guide for PSI Ψ Clone Big BAC DNA isolation kit (1st page). This kit is designed for BAC DNA extraction from up to 50 mL culture per column. The separation process is based on a highly efficient, hydrophilic non-silica anion exchanger resin (*Princeton Separations – prinsep.com*).

Figure 17. Procedure Guide for PSI Ψ Clone Big BAC DNA isolation kit (2nd page). (*Princeton Separations – prinsep.com*).

Kit Components

Resuspension Buffer (Buffer #1)	25mL
Lysis Buffer (Buffer #2)	25mL
Neutralization Buffer (Buffer #3)	25mL
BAC DNA Binding Resin (Buffer #4)	25mL
Wash Buffer (Buffer #5)-2 bottles	80mL
Elution Buffer (Buffer #6)	10mL
RNase A	5.0mg (2 x 2.5mg vial)
Elution columns	5

All components except the combined Resuspension Buffer and RNAse may be stored at room temperature. After adding RNase to Resuspension buffer, store the combination at 4C.

Scaling Factors

This **PSI Ψ Clone Big BAC** DNA isolation protocol may be easily adjusted to process any volume from 25-250mL of culture. A scaling factor of 1:10 is used for all reagents except the Elution Buffer. An elution volume of 750μL is suitable for all processing volumes when the columns supplied are used. It is recommended that volumes be processed in units of 25 or 50mL. Although 250mL can be processed in one lot using appropriately sized glassware, centrifuge tubes and elution columns, 50mL is the largest volume of culture that can be processed in readily available glass or plastic ware (typically plastic screwtop centrifuge tubes). If culture volumes <50mL are processed the fritted column tubes may be washed out and reused.

The protocol on the following page uses a 30mL culture as an example. For other culture volumes, substitute the appropriate reagent volume (i.e., for 50mL cultures use 5mL of reagents).

Protocol for 25-250mL culture media

using **PSI Ψ Clone Big BAC DNA** kit (Cat# PP-121)

This protocol is designed to isolate template quality BAC DNA from cultures of 30mL LB (containing 12.5 ug/mL chloramphenicol) with a culture density as measured by OD_{600} between 4.0 to 6.0. Typical yields are between 5 to 7 ug DNA per prep.

1. Add 1mL Resuspension Buffer to each RNase A vial to dissolve the RNase A. Add contents of both RNase A vials back to the Resuspension Buffer and mix. Store unused portion of this combination at 4C.
2. Add 3mL Resuspension Buffer to the cell pellet and resuspend by gentle pipetting.
3. Add 3mL Lysis Buffer and mix by **gentle** inversion. Allow the lysis to continue for **20 minutes** at room temperature.
4. Add 3mL Neutralization Buffer and mix by **gentle** inversion until a thick white precipitate forms and incubate on ice for **20 minutes.**
5. Centrifuge the precipitate at 25,000 x g (using an SS-34 rotor or equivalent) for 20 minutes to clarify the lysate. Pour off the lysate into a clean tube; if lysate is not clear, invert to mix and centrifuge again.
6. Add 3mL BAC Binding Resin to the clarified lysate and invert several times. Incubate at room temp for 10 min (inverting every 2 minutes to mix). Then pour the solution into the column barrel provided and allow it to drain by gravity.
7. Add 3 x 3mL Wash Buffer allowing to drain by gravity, then place the column in an empty 50 mL conical tube (Falcon Tube or equivalent) and remove excess wash buffer by centrifugation at 750 x g for 2 minutes in a bench top centrifuge. Discard the wash.
8. Add 750μL Elution Buffer to the column and incubate for 2 minutes. Centrifuge as above using a clean centrifuge tube.
9. Precipitate the DNA by adding 1 volume isopropanol and mixing. Centrifuge at 20,000 x g for 30 minutes. Remove supernatant. Wash the DNA by adding 200μL 70% ethanol and mixing. Centrifuge at 20,000 x g for 5 minutes. Remove the excess 70% ethanol and allow the pellet to air dry for about 5 minutes.
10. Dissolve pellet in a suitable volume of TE or other low salt buffer of choice.

After extracting the BAC, resuspend each pellet in 50 µL of *MiliQ* water using 200 µL cut tips not to damage the BAC.

Quantify the DNA using *NanoDrop* (from *Thermo Scientific*) and, optionally, gather both final samples in only one tube.

Before transfection into the ES cells the BAC has to be digested in order to be linearized. This digestion step is important because after electroporation the cells linearize the BAC stochastically before integration in the genome and that could lead to the disruption of the cassette. Hence, the vector is cut to linearize the BAC, maintaining the whole genomic portion plus the cassette intact. The procedures and criteria used to select the restriction enzyme to linearize the BAC are described next.

Run the *Dll1* BAC DNA sequence in the *NEBcutter* (*tools.neb.com*) software from *New England BioLabs* to assess the restriction sites and respective enzymes for the BAC (**Figures 18.**, and **19.** and **Table III.**).

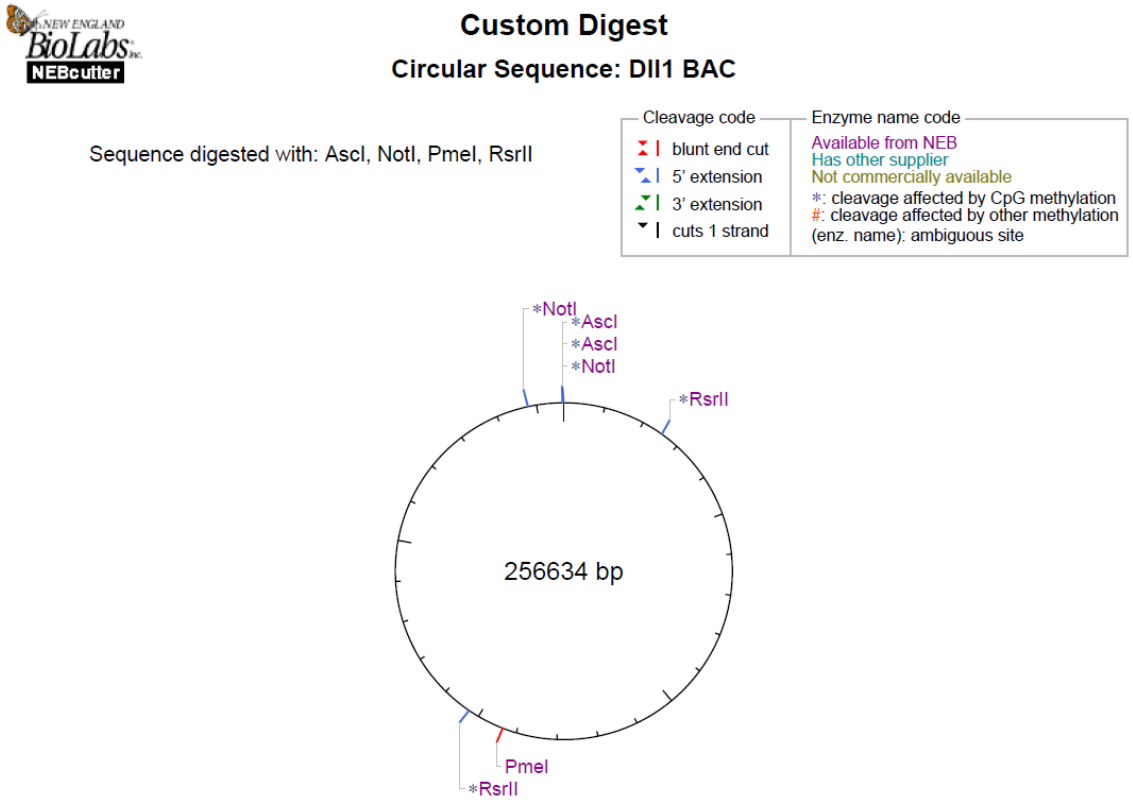

Figure 18. Restriction profile of the *Dll1* BAC DNA regarding single (PmeI) and double (AscI, NotI and RsrII) restriction enzymes. The figure shows the recognition sites for each enzyme. (*tools.neb.com*).

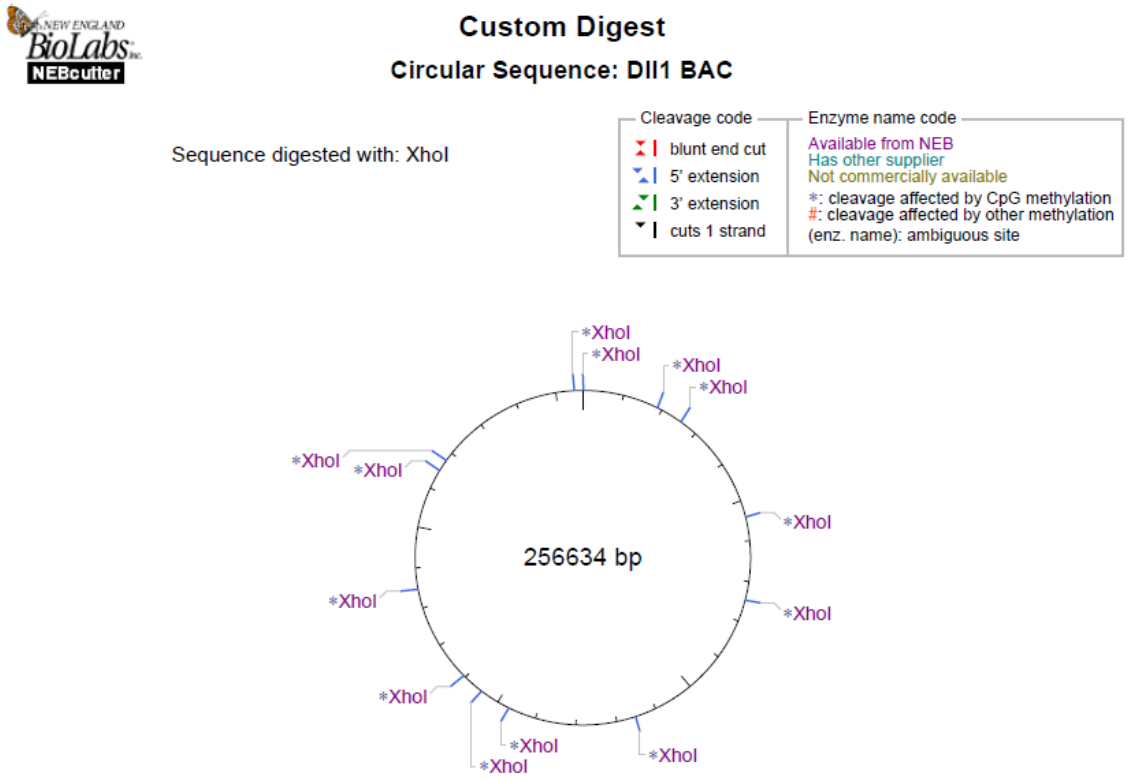

Figure 19. Restriction profile of XhoI for the *Dll1* BAC DNA. The restriction enzyme XhoI was used on the studies to improve the protocols and is mentioned furtherer in this thesis (*tools.neb.com*).

Table III. Bands produced upon digestion of Dll1 and Hes5 BACs with several restriction enzymes. AscI, NotI and XhoI were the enzymes used to run all the tests described in this work. Hes5 BAC is another BAC construct that was used on the studies to improve the protocols and is mentioned furtherer in this thesis, as well as the restriction enzymes XhoI and NotI.

	Non-digested	AscI (bp)	NotI (bp)	XhoI (bp)
Dll1	256 634	256 445 189	247 900 8 734	40 593 36 749 31 742 30 130 28 626 24 172 20 507 18 677 7 832 6 660 5 754 2 957 2 235
Hes5	153 419	153 220 189	90 718 52 106 10 585	49 180 41 826 14 219 10 208 10 142 9 288 7 841 6 064 4 213 428

The most suitable enzyme for linearizing the BAC is one that has only one restriction site. Regarding **Figure 18.** the only single restriction enzyme for the *Dll1* BAC sequence is PmeI. Although PmeI has only one restriction site, this is in the middle of the BAC's genomic region, which is not the intent. Therefore, the chosen enzyme must be a double restriction enzyme. Observing the same figure, the best option to linearize the BAC seems to be AscI, which has two restriction sites inside the vector, not affecting the genomic portion, and has the smallest resulting fragment. NotI could also be a hypothesis because it also has two restriction sites inside the vector. However, the excised fragment in NotI restriction is much bigger than in AscI restriction, which might affect the viability of the electroporated ES cells.

To confirm the positioning of the restriction sites for AscI one can search the RP23 BAC library and know that the vector region contains two restriction sites for this enzyme, which is suitable to linearize the BAC.

After selecting the restriction enzyme to use, proceed with the digestion step.

Before digesting the sample, take 5 µg of the extracted DNA sample to run as non-digested sample in the PFGE.

Prepare the digestion mixture according to the following criteria:

- The quantity of DNA to digest is the total amount minus the non-digested sample;
- The amount of enzyme needed to digest the DNA in the mix can be calculated based on its activity and concentration (**Equation 1.**). (e.g. the activity of the enzyme AscI is 0,13 U[10]/µg for 16 hours);

$$Q_{enzyme} = \frac{Q_{DNA} \times A_{enzyme}}{[enzyme]} \times 3$$

Equation 1. Enzyme amount needed to digeste a certain DNA quantity. *Q* is the amount of the molecule (µL), *A* is the enzyme's activity (U/µg) and [ ] is the enzyme's concentration (U/ µl). The total amount is multiplied by 3 to ensure the total digestion of the BACs.

- Add the optimal buffer specific for the enzyme at working concentration (1×) (e.g. dilute a 10× stock solution 1:10 in the total volume of the mixture);
- Add BSA (required to stabilize some enzymes during digestion and to prevent their adhesion to the reaction tubes) at working concentration (1×) (e.g. dilute a 100× stock solution 1:100 in the total volume of the mixture);
- Reach the total volume of the mixture by adding *MiliQ* water to the mixture;

[10] U: The amount of enzyme necessary to digest 1 µg of substrate in 1 hour.

Table IV. Mixture for AscI digestion. AscI activity is 0,13 U/µg for 16 hours (*tools.neb.com*).

Quantity (µL)	
x	DNA
((*x*0,13)/10)*3*	AscI (10 U/ µL)
40	Buffer 4 10× (enzyme's optimal buffer)
0	BSA 100× (AscI doesn't require it)
(rest)	*MiliQ* water
400[11]	Total

Table V. Mixture for NotI digestion. NotI activity is 0,25 U/µg for 16 hours (*tools.neb.com*).

Quantity (µL)	
x	DNA
((*x*0,25)/10)*3*	NotI (10 U/ µL)
40	Buffer 3 10× (enzyme's optimal buffer)
0,4	BSA 100×
(rest)	*MiliQ* water
400	Total

Table VI. Mixture for XhoI digestion. XhoI activity is 0,13 U/µg for 16 hours (*tools.neb.com*).

Quantity (µL)	
x	DNA
((*x*0,13)/10)*3*	NotI (10 U/ µL)
40	Buffer 2 10× (enzyme's optimal buffer)
0,4	BSA 100×
(rest)	*MiliQ* water
400	Total

NOTE: The two last mixture profiles for digestion are mentioned furtherer in this thesis, in the *Protocols Studies* chapter.

After preparing the mixture (**Table IV.**), let digestion occur overnight (about 16 hours) at optimal temperature for the enzyme to work (37ºC for AscI, *tools.neb.com*).

After digestion, the DNA must be purified before the electroporation step, and this is done by precipitating the DNA. Once again, take 5 µg of the sample to run as digested sample in the PFGE before precipitating the whole sample. This sample, along with the one taken after the extraction step, constitutes a standard monitoring of the whole process. Also, in case the experiment fails this monitoring can be of great importance to understand in which step to focus in order to improve. Therefore, prepare the precipitation mixture:

[11] The digestion volume was optimized by Evguenia Beckman and Filipe Vilas-Boas in order to avoid high enzymatic concentrations that could lead to unspecific cutting and at the same time that is not too low, so that digestion occurs.

- Add 1/10 of the remaining volume of digested DNA of precipitation salt (in this case sodium acetate – CH_3COONa, at 3 M and pH=7, is used) to the digested DNA to be precipitated;
- Add 2× the total volume of the mixture, after addition of the precipitation salt, of ethanol 100%;

And let precipitation occur for several hours (2-3 hours minimum) at -20ºC.

After precipitation the DNA must be stored until electroporation. The time that the PFGE results take to be available, which is necessary before proceeding to the electroporation step, is more than the DNA can stand at room temperature without degrading. For that, centrifuge at 4000 rpm for 30 minutes.

Remove the supernatant (by pouring it off), add 1,5 mL ethanol 70% to the remaining pellet and store at -20ºC.

Initial BAC visualization protocol

Assess the BAC DNA integrity using *Chef-DR® III PFGE systems*, from *Bio-Rad* (**Figure 20.**).

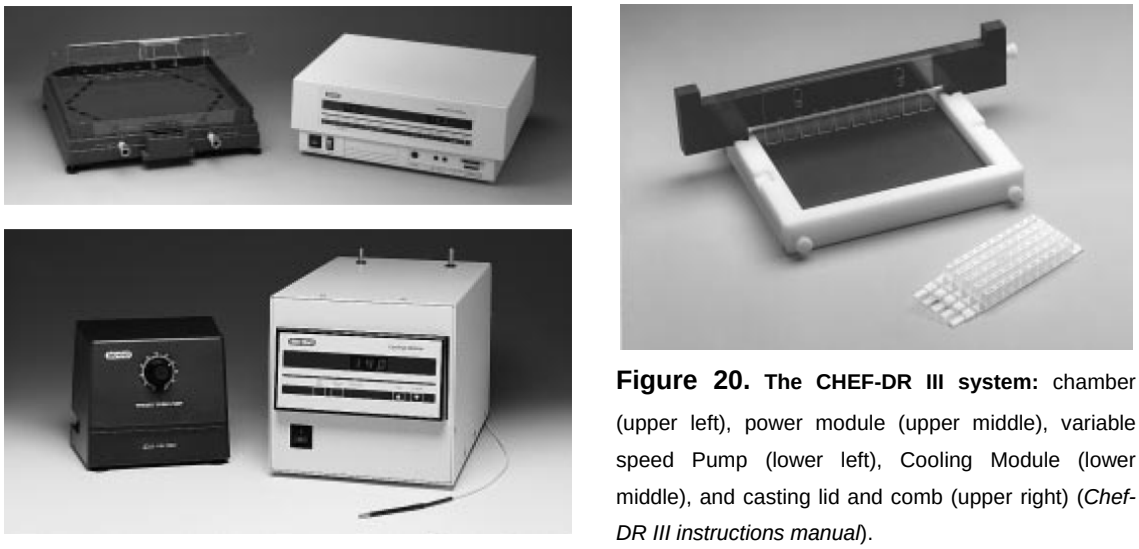

Figure 20. The CHEF-DR III system: chamber (upper left), power module (upper middle), variable speed Pump (lower left), Cooling Module (lower middle), and casting lid and comb (upper right) (*Chef-DR III instructions manual*).

Wash the machine with 3 L of distilled water with the pumping system ON and the cooling system OFF for at least 1 hour.

Meanwhile, wash the casting lid and the comb with distilled water and ethanol an prepare 3 L of TBE 0,5× (Tris/Borate/EDTA – buffer solution):

- 3 × (50 mL TBE 10×[12] : 950 mL distilled water);

Take 300 mL of the prepared TBE 0,5× to prepare the electrophoresis gel (1%):

- 3 g Agar : 300 mL TBE 0,5×;

Heat the solution in an Erlenmeyer to enhance the dissolution of the agar and let it solidify at room temperature inside the casting lid with the comb in place;

After washing the PFGE chamber for one hour, turn the pumping system OFF, remove the distilled water and refill the chamber with the TBE buffer 0,5×.

Turn the pumping system back ON as well as the cooling system (programmed to 14ºC).

Remove the solid gel from the casting lid and place it inside the chamber.

Let the buffer solution reach the programmed temperature.

After that, turn the cooling and the pumping systems OFF and load the samples and the ladder in the wells, mixed with loading buffer solution.

Program the system with the chosen PFGE run parameters (*Carlos Rodrigues, 2007*). This was the first set of parameters for PFGE run used. The conditions are specified for each PFGE image along this thesis. Turn the current ON and after 30 minutes turn the cooling and the pumping systems ON.

Let the machine operating during the chosen run time.

After the run, take the gel out of the chamber. The next step is to visualize the DNA inside the gel. To do this, Ethidium bromide is used due to its capacity to intercalate double stranded DNA and to emit radiation upon excitation with ultraviolet wavelength radiation.

Wash the chamber of the PFGE machine with 3 L distilled water for at least 1 hour.

Meanwhile, stain the gel with Ethidium bromide:

- 200 mL distilled water : 20 µL Ethidium bromide;

After staining, visualize the result under an ultraviolet emitting environment and acquire the specific emission wavelength of the Ethidium bromide (**Figure 21.**).

[12] TBE 10× stock solution (1 L):

- 54 g Tris base;
- 27,5 g Boric acid;
- 20 mL EDTA 0,5 M, pH 8,0;

Add about 500 mL distilled water and correct the solution's pH to 8,3 with a concentrated acid (e.g. HCl) or a concentrated basic solution (e.g. NaOH), depending on if the pH is higher or lower than pretended, respectively. Fill up the rest of the volume with distilled water and filtrate the solution by vacuum with a 0,22 µm porous membrane filter. Store the final solution at room temperature.

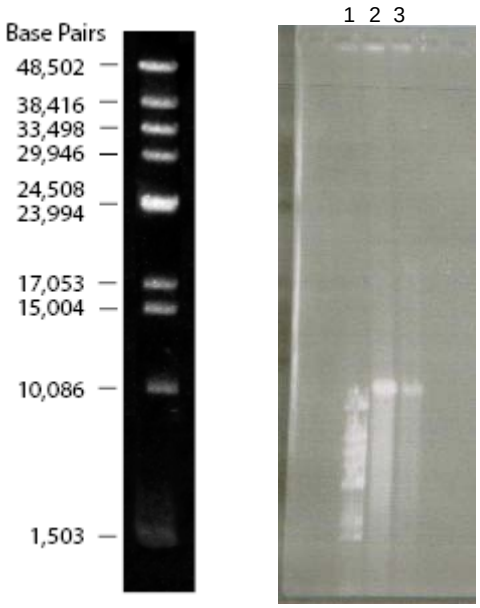

Running conditions:

Parameters	Values
Gel	1%
Initial pulse time	1 sec.
Final pulse time	2 sec.
Run time	16 hours
Voltage	6 V/cm
Angle	90º

Lanes:

1. **Ladder: λ-monocut mix**
2. **Non-digested sample**
3. **AscI digested sample**

Figure 21. **λ-DNA Mono cut mix fragments' sizes** (left) **and PFGE photo** (right). Here, the first set of parameters for PFGE was used and the samples were extracted from previously frozen pellets.

In the end of the work, after executing the protocols, the result obtained (**Figure 21.**) was not the expected. The PFGE image was supposed show a shift between the digested and non-digested samples, which was not the case. When the same protocol was performed using a Hes5 BAC the shift was visible and from that shift one could conclude that the DNA had been digested.

Protocol studies using the "PSI Ψ Clone Big BAC – DNA isolation kit"

The initial assumption was that the image resulting from the PFGE should show a shift between the digested and non-digested samples, which was not the case. The observed shift would indicate if the BAC had been successfully linearized or not. The digested sample band should appear above the non-digested because the circular DNA construct migrates faster than the linear one in the gel.

At first it was thought that this could be due to the fact that the pellets from which the DNA was extracted had been frozen for several months. However, after growing new cells and proceeding with the same protocols the image resulting from the PFGE was similar (**Figure 22.**).

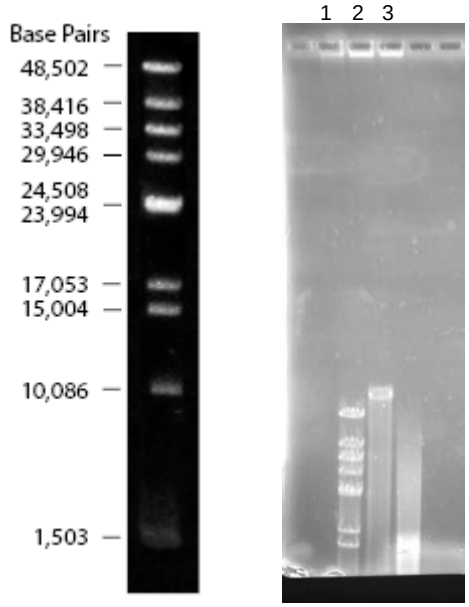

Running conditions:

Parameters	Values
Gel	1%
Initial pulse time	1 sec.
Final pulse time	2 sec.
Run time	16 hours
Voltage	6 V/cm
Angle	90º

Lanes:

1. **Ladder: λ-monocut mix**
2. **Non-digested sample**
3. **AscI digested sample**

Figure 22. **λ-DNA Mono cut mix fragments' sizes** (left) **and PFGE photo** (right). Here, the first set of parameters was used for PFGE and the samples were extracted freshly prepared pellets. In lane 3, AscI digested sample, only a smear is observed.

Moreover, regarding **Figure 22.**, the digested sample seemed to be degraded, which could indicate that the digestion step was degrading the DNA. The restriction enzyme, AscI, was the first component of the digestion mixture to be suspected of because it was the most suitable to become deregulated or inactivated (e.g. upon temperature alterations). Although, the possibility that AscI was responsible for degrading the DNA was very unlikeable because enzymes rarely cause this.

Therefore, samples of the wastes from the lysis step were taken (specifically from the pellet formed upon centrifugation, after the neutralization and before the column purification steps from the kit – these steps are detailed furtherer in this thesis, in the *extraction protocol studies* chapter). Different DNA quantities of these samples were then digested with three different enzymes (AscI, NotI and XhoI – see **Figures 18.**, and **19.** and **Table III.** for

clarification) in order to try to understand what was wrong (**Figure 23.**). This particular step, the lysis step, was chosen to start these studies because it was the most "aggressive" step for the organic compounds and if it was not producing the intended results then the rest of the steps would be affected.

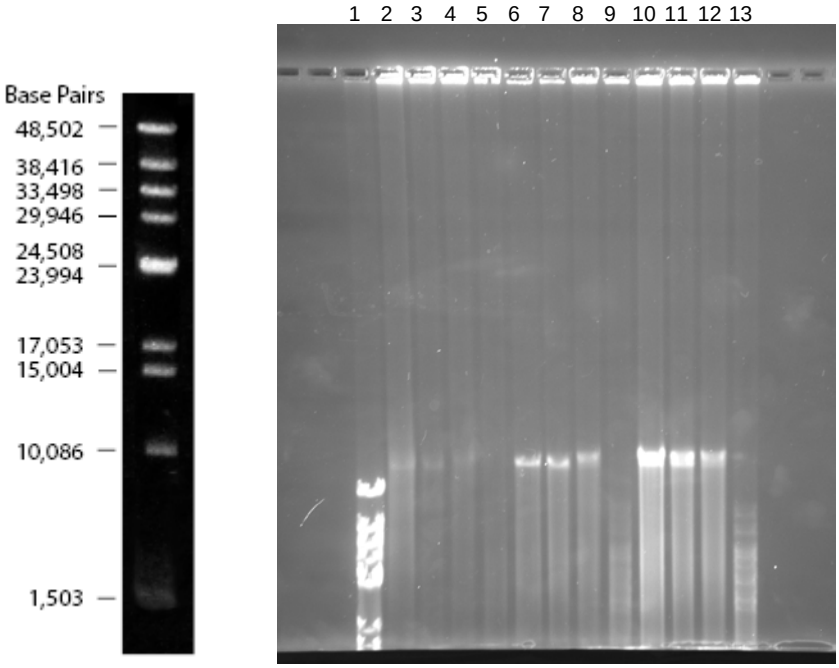

Running conditions:

Parameters	Values
Gel	1%
Initial pulse time	1 sec.
Final pulse time	2 sec.
Run time	16 hours
Voltage	6 V/cm
Angle	90º

Lanes:

1. **Ladder: λ-monocut mix**
2. **Lysis Non-digested sample**
3. **Lysis AscI digested sample**
4. **Lysis NotI digested sample**
5. **Lysis XhoI digested sample**
6. **5 µg Non-digested sample**
7. **5 µg AscI digested sample**
8. **5 µg NotI digested sample**
9. **5 µg XhoI digested sample**
10. **10 µg Non-digested sample**
11. **10 µg AscI digested sample**
12. **10 µg NotI digested sample**
13. **10 µg XhoI digested sample**

Figure 23. λ-DNA Mono cut mix fragments' sizes (left) **and PFGE photo** (right) **(First conditions).** The lysis samples (lanes 2, 3, 4 and 5) do not show any unexpected result and no significant amount of DNA is present.

Observing **Figure 23.**, NotI digestion bands (lanes 8 and 12) appeared above the non-digested bands (lane 6 and 10), i.e. a shift was observed, meaning that NotI was linearizing the *Dll1* BAC. Moreover, AscI digested DNA bands (lane 7 and 11) do not produce a shift when compared with the same non-digested samples, which could mean, once again, that the AscI

digestion step might not be working and, particularly, that the activity of the enzyme was reduced, or even completely inhibited.

Indeed, after testing the AscI that was used so far in parallel with a new AscI enzyme to digest a plasmid with a restriction site for this enzyme, we could see that the enzyme was not working well. The resulting image showed a partially digested patterning for the "old AscI" (**Figure 24.**).

Additionally, XhoI digestions (lanes 9 and 13) also produced fainted bands of different sizes corresponding to the expected (**Table III.**). The lane corresponding to the lysis sample digested with XhoI (lane 5) showed even more fainted bands when compared to the corresponding digested BAC DNA samples (lanes 9 and 13), which means that the BAC DNA amount present in the lysis wastes was very low. This result was expected because the solid phase of the lysis should only contain all genomic DNA and high molecular weight molecules. Consequently, these results meant that the BAC DNA amount lost during the lysis step was insignificant for the study.

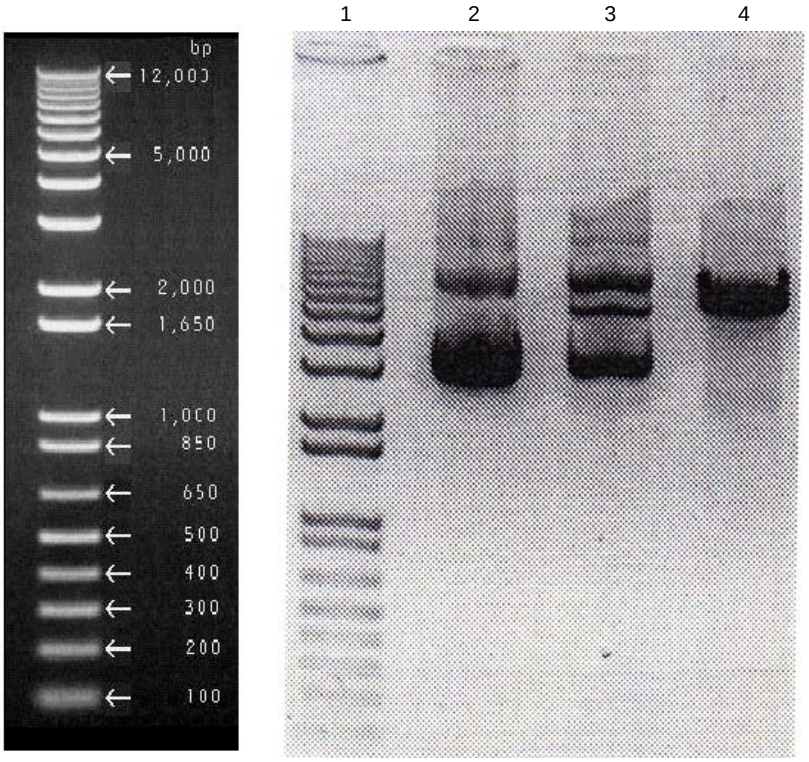

Lanes:

1. **Ladder: 1 kb plus ladder**
2. **Non-digested sample**
3. **Old AscI digested sample**
4. **New AscI digested sample**

Figure 24. 1 kb plus ladder fragments' sizes (left) **and electrophoresis gel photo for AscI testing** (right)**.** Lane 2 shows both super-coiled (lower band) and relaxed form (upper band) of the plasmid. In lane 3 the partial digestion is observed. Lane 4 shows complete digestion with new AscI enzyme.

The results obtained on **Figure 24.** confirmed that the enzyme was not working well so a new enzyme was used from that point on.

However, there is no visible DNA degradation in any of the samples, thus we could not attribute the previous observation of DNA degradation to the enzyme activity.

At that point there were some samples already stored at -20ºC from previous extractions (kept in the storage step, remaining conserved until electroporation). Based on the results obtained until then these samples were supposedly only "partially digested". After digesting one of these samples with the new AscI in PFGE and assessing it in PFGE only a smear was obtained, and additionally, the partially digested sample only showed a smear too (**Figure 25.**). The chosen sample had not showed band shift or DNA degradation in both digested and non-digested samples in the previous tests, which are implicit in this work.

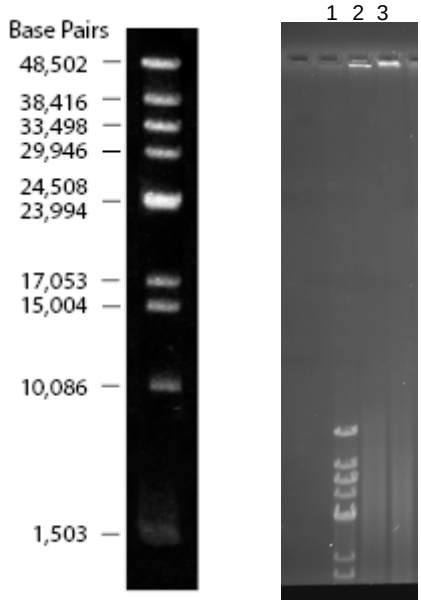

Running conditions:

Parameters	Values
Gel	1%
Initial pulse time	1 sec.
Final pulse time	2 sec.
Run time	16 hours
Voltage	6 V/cm
Angle	90º

Lanes:

1. **Ladder: λ-monocut mix**
2. **Only Old AscI digested sample**
3. **Old and New AscI digested sample**

Figure 25. λ-DNA Mono cut mix fragments' sizes (left) **and PFGE photo** (right). The DNA samples (lanes 2 and 3) only show a smear. The first set of conditions for the PFGE run was used.

Figure 25. only showed a smear in both samples partially digested and digested with the new AscI. Reviewing the protocol we noticed that, before storage, the DNA was precipitated. Never a sample of this step had been tested before. Therefore, the whole protocol was executed once more to take a sample of the final precipitated DNA to visualize it, along with the standard samples, as referred before (**Figure 26.**).

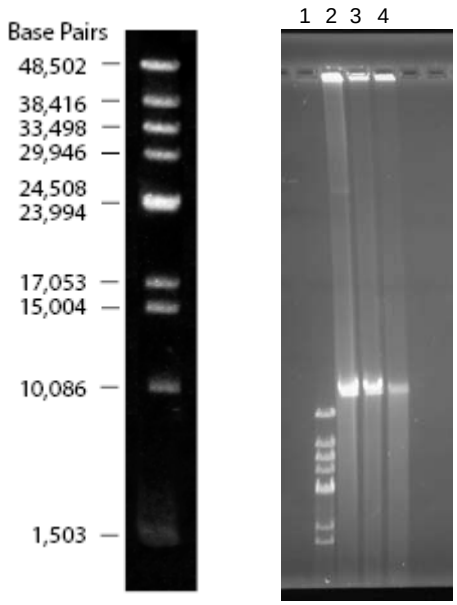

Running conditions:

Parameters	Values
Gel	1%
Initial pulse time	1 sec.
Final pulse time	2 sec.
Run time	16 hours
Voltage	6 V/cm
Angle	90º

Lanes:

1. **Ladder: λ-monocut mix**
2. **Non-digested sample**
3. **New AscI digested sample**
4. **New AscI digested and precipitated sample**

Figure 26. λ-DNA Mono cut mix fragments' sizes (left) **and PFGE photo** (right). The DNA samples (lanes 2, 3 and 4) all show a visible band. The first set of parameters for the PFGE run was used.

Surprisingly, all the DNA samples showed a bright band at the same level, although a slight background smear was also observed. The precipitated sample band in less bright than the others which means that some DNA was lost in the process (he more the DNA present in the sample the more bright the band will be). By this result, we could only conclude that the stochastic observation of smear should be attributed to excess of manipulation of the DNA and that its storage for some days also contributes for degradation.

Despite this, and as the intention was only to study the several steps of the extraction and visualization protocols, from that point on it was decided to do only analytic digestions (40-60 µL) to avoid the following precipitation step (and consequent DNA loss and/or degradation). The main importance of this step was to purify the DNA for electroporation, which is not needed for studying purposes. However, the DNA was much diluted in the digestion step and therefore this step had to be performed in each execution of the protocol to concentrate it. This alteration has no significant impact in the digestion calculations because only the final total volume is changed.

Though, after all the tests performed until that time, the non-observed shift was still unexplainable. Moreover, the observation of very evident smear in the samples was still not understood.

What if the pretended result was not a shift in the bands as previously supposed?

AscI could be linearizing the BAC effectively but we could not be visualizing it in the right way, not resolving the gel in the right way, which means that the set of parameters used in PFGE could not adequate.

Until now, when observed, the non-digested bands and the ones digested with AscI and NotI were always very bright. However, the bands resulting from XhoI digestion has much lower brightness when compared to those. Although smaller bands also show lower brightness due to the amount of base pairs present in the sample, this difference observed in the tests perfomed was not expected.

Regarding again AscI and NotI digested samples ran in the PFGE using the first set of conditions one could say that what was observed was nothing more than the piling up of high molecular weight DNA fragments.

Indeed, that was the case because when the results from the same extraction protocol were visualized using the first set of conditions for PFGE in parallel with a λ-DNA ladder sample (high molecular fragments' ladder) the piling up was observed (**Figure 27.**). Additionally, a sample of the BAC tested some months before, the Hes5 BAC, was also visualized and the piling up was observed in those samples (**Figure 27.**).

The *Hes5* BAC has a digestion profile for AscI similar to *Dll1* BAC for the same enzymes (see **Table III.**) because they were constructed the same way, using the same vector. Also, both produce many DNA bands upon XhoI digestion. The main difference is the size, since *Hes5* BAC has only 153 419 bp, which much smaller than *Dll1* BAC (256 634 bp). A major advantage in using *Hes5* BAC is the fact that it produces intermediate size bands upon NotI digestion, enhancing the significance of the PFGE images obtained (several sized fragments instead of only having very large and very small and DNA fragments as with AscI).

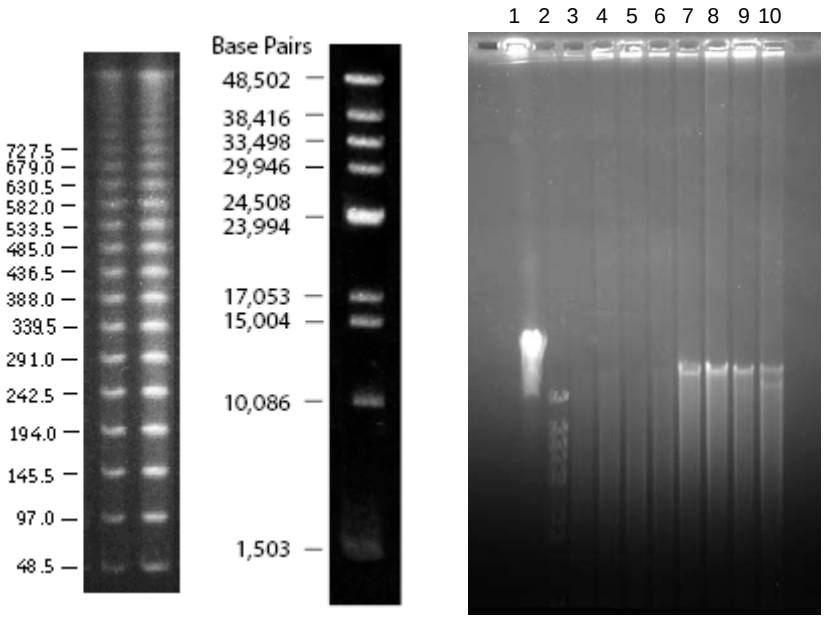

Running conditions:

Parameters	Values
Gel	1%
Initial pulse time	1 sec.
Final pulse time	2 sec.
Run time	16 hours
Voltage	6 V/cm
Angle	90º

Lanes:

1. **Ladder: λ-DNA**
2. **Ladder: λ-monocut mix**
3. **Dll1 BAC Non-digested sample**
4. **Dll1 BAC AscI digested sample**
5. **Dll1 BAC XhoI digested sample**
6. **Dll1 BAC NotI digested sample**
7. **Hes5 BAC Non-digested sample**
8. **Hes5 BAC AscI digested sample**
9. **Hes5 BAC XhoI digested sample**
10. **Hes5 BAC NotI digested sample**

Figure 27. λ-ladder fragments' sizes (left)**, λ-DNA Mono cut mix fragments' sizes** (middle) **and PFGE photo** (right). The Hes5 DNA samples (lane 7, 8, 9 and 10) all show a visible band. The λ-ladder is compacted in the middle of the gel.

As observed in **Figure 27.** the PFGE conditions were not adequate for visualizing the *Dll1* and the *Hes5* BAC due to their high molecular weight. All DNA larger than 50 kbp was piling up in the middle zone of the gel as the λ-ladder did. Moreover, the Hes5 BAC, in which the shift was visible before, is still visible now though its integrity cannot be assured.

The Pulsed Field Gel-Electrophoresis (PFGE)

The concept that DNA molecules larger than 50 kbp can be separated by using two alternating electric fields (i.e. PFGE) was introduced in 1982, by Schwartz et al.

It has been demonstrated that DNA fragments from a few kbp to over 10 Mbp can be separated using this system.

The conventional electrophoresis used for DNA separation is based on a unidirectional and continuous electric field, where only the voltage, the running time and the gel density can

be adjusted in order to fulfill the separation needs. In the PFGE, the separation method is based on a bidirectional pulsed electric field that not only pushes DNA towards the base of the gel but also along side, to enhance its separation along the gel (**Figure 28.**).

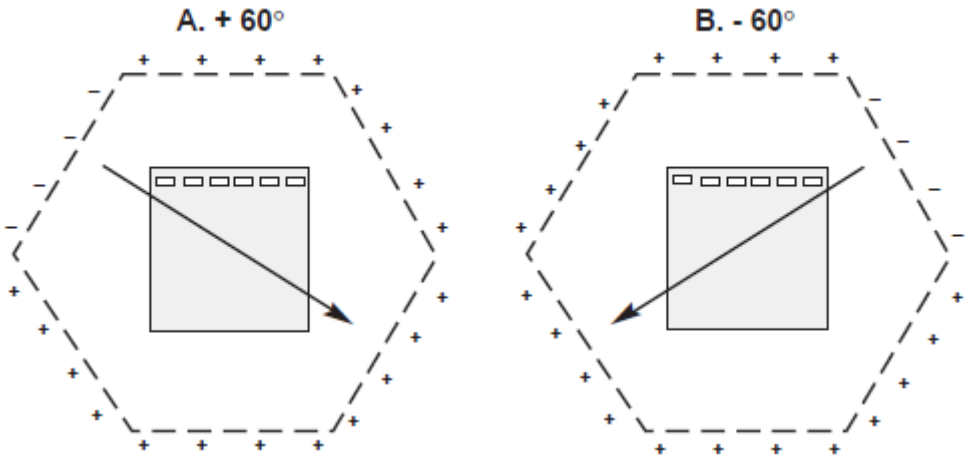

Figure 28. Voltage clamping by the *CHEF-DR III system*. A. Relative electrode potentials when the + 60° field vector is activated. B. Relative electrode potentials when the - 60° field vector is activated (*Chef-DR III instructions manual*).

In PFGE, several parameters can be manipulated to achieve the most suitable separation:

Pulse times: The pulse time parameter refers to the time during which the electric field stays ON before redirecting itself to the opposite field (e.g. –60º to +60º). The *CHEF-DR III systems* is capable of memorizing two pulse times (an initial and a final one) and create a ramp of pulse times from one to the other following a linear increment during the chosen run time. For example if we choose pulse times of 5-30 sec on 16 hours run, the increment in each hour will be of 1,56 sec./hour ((30-5)/16=1,56). The machine will start creating electric fields of 5 sec. duration, alternating the field angle, and near the 16th hour the pulses will be of 30 sec. duration.

One thing to have in mind is that the more the machine stays in the same pulse time, i.e. the lower the pulse time increment, the better will be the resolution (thinner bands). This means there has to be a balance between the pulse time interval and the run time.

Run time: The longer the run time, the further the DNA migrates (if the other parameters stay the same). This parameter is one of the most important when taking advantage of the gel's area to separate the DNA along it.

Voltage gradient, *V*: The voltage has to be set according to the size of the DNA that will be separated. The higher the size of DNA to separate the lower voltage (down to 1 V/cm) should be used not to shear it. Usually the voltage of the system is set for 6 V/cm which is the most suitable for separating DNAs up to 2 Mbp.

Reorientation angle, *θ*: This parameter specifies the absolute angle (between the horizontal and the electric field direction). For example, choosing an angle of 90º is equivalent to choose an unidirectional field where each pulse is coincident to the next. Using this value for the

alternation angle is similar to work with a conventional electrophoresis gel. This might explain, in part, why using the first set of parameters did not allowed resolution above 50 kbp. On the opposite one can choose angle of 120º which corresponds to an alternation angle of –60º/+60º, which induces greater lateral displacement and therefore increases resolution.

Temperature, *T*: The chamber's temperature must be maintained relatively cold in order to constraint DNA's mobility. The higher the temperature the more the DNA moves, creating blurred bands or, if the temperature is too high, the DNA denatures. Usually the temperature is set for 14ºC, which is suitable to restrict the mobility of the DNA and is relatively easy to maintain without significant oscillations.

Defining PFGE conditions

Defining new parameters for PFGE requires several trials, adjusting the parameters to obtain the best separation in each of them until the intended result is achieved. However, the literature can also provide major clues for the setting of parameters for PFGE (**Table VII.** – The highlighted conditions are the ones to take in account to visualize *Dll1* and *Hes5* BACs).

Table VII. Suggested parameters for several DNA size ranges. (*Chef-DR III instructions manual*).

	DNA 1-100 kb	DNA 0.1 - 2.0 mb	DNA 2 - 4 mb	DNA > 4 mb
% Agarose	1.0–1.2%	0.8–1.2 %	0.6–1 %	0.5–0.8 %
Buffer	0.5x TBE	0.5x TBE	1.0x TAE	1.0x TAE
Temperature	14 °C	14 °C	14 °C	14 °C
Voltage	6–9 V/cm	4.5–6 V/cm	2–3 V/cm	1.0–2.5 V/cm
Pulse Parameters	0.05–10 sec	10–200 sec	200–1,800 sec	10–60 min
Run Times	2–15 hr	15–30 hr	24–72 hr	72–144 hr
Angle	120°	120°	120°, 106°	106°

Some empirical calculations may also be performed to restrict the parameters to be used (**Equation 2.**).

$$\max\_resolved\_size\_(kbp) = 0{,}034 \times (T + 40) \times V^{1{,}1} \times (3 - A)^{0{,}6} \times t^{0{,}875}$$

$$\min\_resolved\_size\_(kbp) = 0{,}75 \times \max\_resolved\_size\_(kbp)$$

Equation 2. Relation between the maximum and minimum resolved DNA sizes and the chosen parameters in PFGE. *T* is the chamber's temperature (ºC), *V* is the applied voltage gradient (V/cm), *A* is the agar percentage in the gel (%) and *t* is the sought pulse time (sec.) (*Current Protocols in Molecular Biology*).

The chamber's temperature, the gel's concentration and the applied voltage gradient are the parameters with the lower visible influence in the DNA separation (for small variations). In the literature and technical supporting manuals there are also several examples of enhanced separations using previously studied combinations of parameters. Only when it comes to

separate very large DNA fragments (up to 1 Mbp) a suitable alteration of these three parameters is need. Also, the alternation angle can be adjusted in order to achieve better separation in those cases, but normally it is set for 120º.

The intent in this study is to separate DNA between around 1-300 kbp. Using the usual values (T=14ºC, V=6 V/cm and A=1% – concentration of the gel) we can calculate the final pulse time needed to establish the maximum resolution size. Because the minimum resolved size is related to the maximum resolved size (**Equation 2.**) and we want to separate fragments up to approximately 256 kbp the choice for the final pulse time has to be centered on that value:

$$t = 20\,\text{sec.}: \qquad t = 21\,\text{sec.}:$$
$$\max = 274{,}7\,kbp \qquad \max = 287{,}7\,kbp$$
$$\min = 206{,}0\,kbp \qquad \min = 215{,}0\,kbp$$

Both t=20 sec. and t=21 sec. could be chosen to delineate the "maximum resolution zone[13]". These values are not restrictive, i.e. using other values one can also separate the same DNA sizes, because different combinations of the parameters can lead to similar results.

In a PFGE gel image observe 3 different regions may be observed:

1. **The pile up zone:** which can be delineated by an horizontal line passing on the high DNA density zone in the lane containing the ladder (if the molecular size range is sufficient to pile up);
2. **The maximum resolution zone:** which can be understood as the zone where the DNA migrates according to its reorientation time[14] (this is only observed above 50 kbp, because below that size range the reorientation time has little influence in the DNA migration). DNA molecules with a reorientation time below the initial pulse time will migrate approximately the same way, creating a pile up zone in the middle of the lane, or they can migrate in the linear zone (if we use 1 sec. initial pulse times the "transition" between regions is not visible, but for 2 sec. it starts to get noticed).
3. **The linear migration zone:** This is the zone that can also be resolved using a normal gel electrophoresis (up to 50 kbp) and where the reorientation time as no significant influence. Here, the DNA migration distance can be linearly related to the logarithm of the molecular weight.

Another very important factor that weights in our final pulse time choice is the run time. The longer the run time the better the resolution (thinner bands) however that would cause the smaller DNA fragments to exit the gel, therefore, we have to attend to their migration velocity (**Equation 3.**).

[13] For some authors the maximum resolution zone is limited by the two calculated values and the other zone is called the non-linear migration zone. In our case we considered those two zones as only one, taking it only in account to center on the pretended DNA size.

[14] In order to migrate through the gel in a PFGE run the DNA must horizontally change course every time the field is inverted. The larger the DNA the longer its reorientation time before really progressing vertically through the gel.

$$10kbp\_velocity(cm/h) = \frac{0{,}0012 \times (T+25) \times V^{1,6} \times \cos\left(\frac{\theta}{2}\right)}{A}$$

Equation 3. Relation between the 10 kbp sized DNA and the chosen parameters in PFGE. (*Current Protocols in Molecular Biology*).

In the case of the BACs used (T=14ºC, V=6 V/cm, θ=120º and A=1% – concentration of the gel) the velocity of the 10 kbp DNA would be around 0,411 cm/h (**Equation 3.**). Knowing that the gel is 12 cm length we can only choose run times lower than 29,2 hours (even less because we intend to see DNA sizes even smaller than 10 kbp).

The final pulse time chosen was the lowest so that the time increment per hour was the lowest too. This way resolution was improved, because DNA migrates longer in the same reorientation time which results in thinner observed bands, as said before. The run time was chosen based on several trials and the old conditions. With the 16 hours runs the smallest bands already migrated down to bottom of the gel. Increasing the time up to 20 hours showed to be suitable for the resolution intents and the smaller bands still appear in the gel.

The final set of parameters for the PFGE run adopted for visualizing the BACs is shown in **Table VIII.**.

Table VIII. PFGE running conditions established after the study.

Parameters	Values
Gel	1%
Initial pulse time	1 sec.
Final pulse time	20 sec.
Run time	20 hours
Voltage	6 V/cm
Angle	120º

After studying the PFGE conditions one could conclude about what was being observed before. Only XhoI had showed the right digestion bands so far because its restriction activity produces many bands with sizes lower than 50 kbp (the limit that the previous conditions could resolve).

However, although the results have changed and the pile up zone was not observed anymore, the only result obtained at that moment was just a smear in the lanes containing the BAC DNA samples and sometimes some fainted, but rightly positioned, restriction fragments (**Figure 29.**).

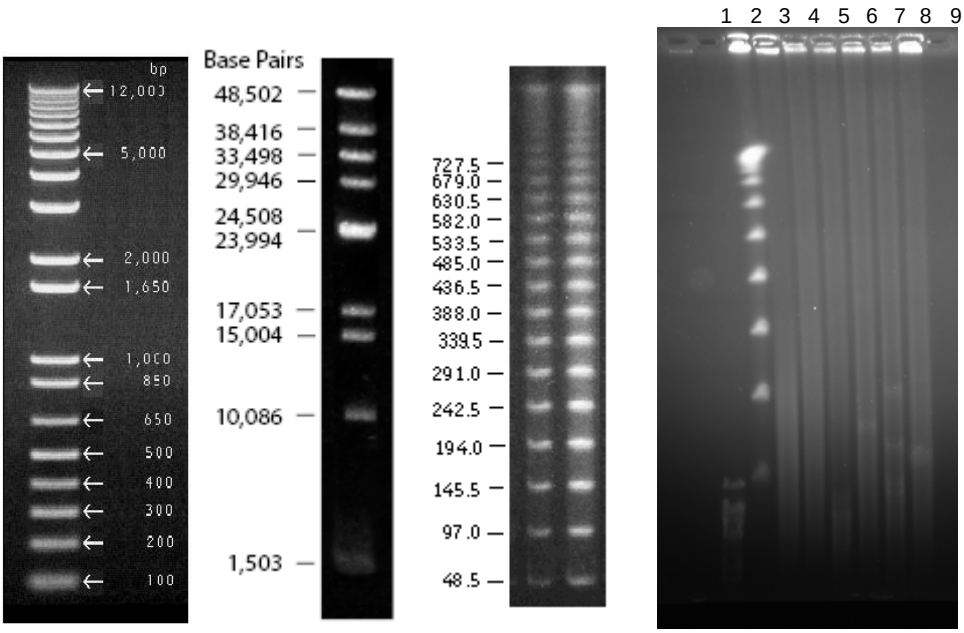

Running conditions:

Parameters	Values
Gel	1%
Initial pulse time	1 sec.
Final pulse time	20 sec.
Run time	20 hours
Voltage	6 V/cm
Angle	120º

Lanes:

1. **Ladder: 1 kb plus ladder**
2. **Ladder: λ-monocut mix**
3. **Ladder: λ-DNA**
4. **Dll1 BAC Non-digested sample**
5. **Dll1 BAC AscI digested sample**
6. **Dll1 BAC XhoI digested sample**
7. **Dll1 BAC PvuI digested sample**
8. **Dll1 BAC MluI digested sample**
9. **Dll1 BAC AscI + PmeI digested sample**

Figure 29. 1 kb plus ladder, λ-DNA Mono cut mix and λ-ladder fragments' sizes (left, in order)**, and PFGE photo** (right). Lanes 7, 8 and 9 all show slight visible bands. The 1 kb plus ladder is not visible in the gel.

So far, all theories had been only towards the post extraction phase, wondering if the BAC was degraded during digestion, or during the PFGE run. There were some reports of tris-dependent radical formation in the characterization of some *E. coli* and yeast strains, capable of degrading the DNA during the run (PFGE degradation articles). This reports called our attention but it had never been shown to happen when using only DNA extracted from the cells.

We used cut and non-cut tips throughout the post extraction steps and even tried to load the DNA samples in agar discs into the wells to prevent stress shearing of the chains, but no improvements were seen. The results kept showing the same smears and some of the small bands sometimes.

At some point, we started questioning whether the DNA was already degraded at the end of the extraction. In fact, the use of the kit had not been proved to be efficient extracting large BACs, in the lab, yet. Moreover, DNA degradation could explain why only sometimes DNA bands are visible (only low weight bands). If the BAC was degraded (stochastically) it is most probable that smaller digestion fragments remain intact inside larger fragments. This way, large

degradation fragments that are seen as smear in the non-digested sample can create a great amount of low weight digestion fragments, i.e. many intact small DNA fragments are excised.

Consequently, the search was redirected to the extraction protocol itself (the digestion and visualization steps were already defined).

To pursue the problem in the extraction protocol we abandoned the kit usage and started testing the traditional extraction methods.

Traditional extraction protocol studies

The traditional DNA extraction protocol follows some basic procedures that are modified according to the needs:

- Cells resuspension (the buffer may contain RNase or that step can be added only in the end);
- Lysis and neutralization (enough to disrupt the cells membrane without letting the genomic DNA get out or degraded, not to contaminate the final sample);
- Deposition and separation (the BAC will remain in the liquid phase as well as low weight molecules);
- Purification – Phenol:chloroform extraction;
- Precipitation (final DNA recovery);

(*BAC extraction protocols)*

Again, the first step was to assess the lysis samples, but this time trying to visualize the extracted DNA instead of the wastes. We also tested several lysis times between 0 and 5 minutes to see whether there was DNA degradation or not.

By abandoning the kit we were lacking a purification step which is needed if we want to enhance the efficiency of the transfection and avoid problems related to the introduction of impurities in the cells. For this reason a phenol:chloroform extraction step was also added, allowing the dissolution of organic molecules in the organic phase (composed mainly by chloroform), while the DNA remains in the aqueous phase. Different times of lysis were tested and the samples were digested with NotI and XhoI (to linearize the BACs). Each one of these samples was also tested with and without the phenol:chloroform step. The results were visualized in a normal gel electrophoresis (**Figure 30.**).

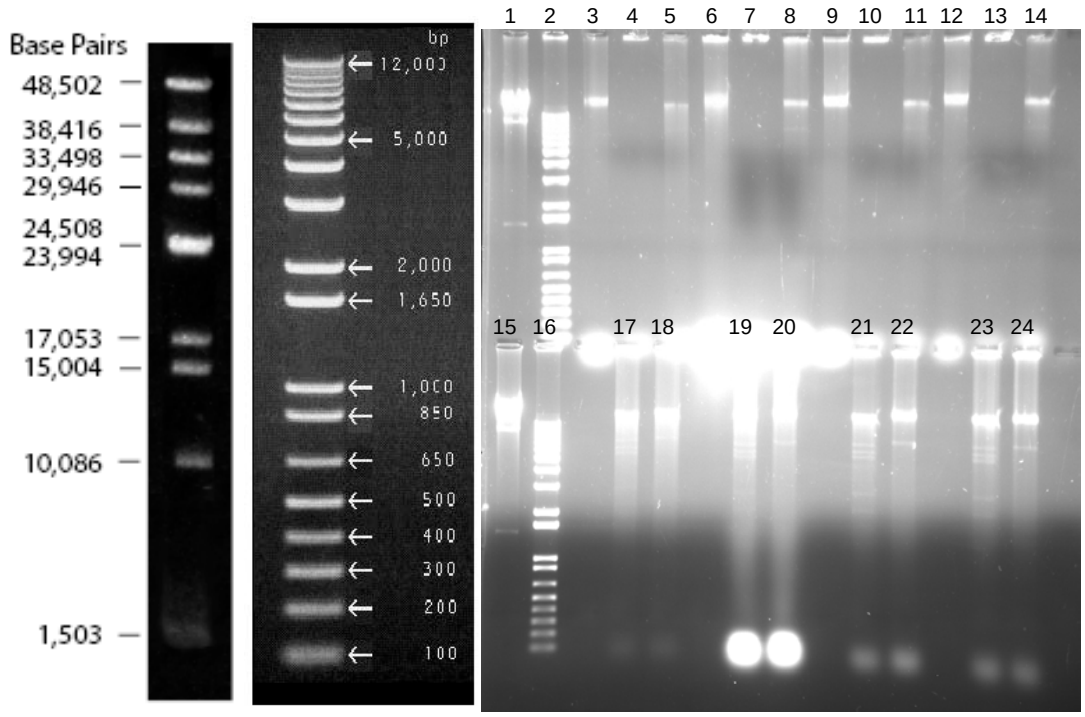

Lanes:

1. **Ladder: λ-monocut mix**
2. **Ladder: 1 kb plus ladder**
3. **Dll1 BAC Non-digested sample (0 min.)**
4. **Dll1 BAC XhoI digested sample (0 min.)**
5. **Dll1 BAC NotI digested sample (0 min.)**
6. **Dll1 BAC Non-digested sample (1 min.)**
7. **Dll1 BAC XhoI digested sample (1 min.)**
8. **Dll1 BAC NotI digested sample (1 min.)**
9. **Dll1 BAC Non-digested sample (3 min.)**
10. **Dll1 BAC XhoI digested sample (3 min.)**
11. **Dll1 BAC NotI digested sample (3 min.)**
12. **Dll1 BAC Non-digested sample (5 min.)**
13. **Dll1 BAC XhoI digested sample (5 min.)**
14. **Dll1 BAC NotI digested sample (5 min.)**
15. **Ladder: λ-monocut mix**
16. **Ladder: 1 kb plus ladder**
17. **Dll1 BAC XhoI digested + ph:chloro (0 min.)**
18. **Dll1 BAC NotI digested + ph:chloro (0 min.)**
19. **Dll1 BAC XhoI digested + ph:chloro (1 min.)**
20. **Dll1 BAC NotI digested + ph:chloro (1 min.)**
21. **Dll1 BAC XhoI digested + ph:chloro (3 min.)**
22. **Dll1 BAC NotI digested + ph:chloro (3 min.)**
23. **Dll1 BAC XhoI digested + ph:chloro (5 min.)**
24. **Dll1 BAC NotI digested + ph:chloro (5 min.)**

Figure 30. λ-DNA Mono cut mix fragments' sizes (left)**, 1 kb plus ladder fragments' sizes** (middle)**, and photo of the gel** (right). Lanes in the bottom row show bright bands. The λ-DNA Mono cut mix is compacted in the top of the lane as well as the rest of the high molecular DNA samples. ("ph:chloro" stands for phenol:chloroform step).

As observed in **Figure 30.**, there was no difference between 1 and 5 minutes lysis. Only the 0 minutes lysis showed a lower DNA amount which is due to lack of time to disrupt the cells membrane to release the BAC DNA. However, regarding the same image one could say that the best lysis time would be between 3 and 5 minutes, which is enough to release the DNA and remains inside the time interval for which the lysis was tested.

Another conclusion to take from **Figure 30.** is that the phenol:chloroform step enhances the DNA purity because the bands are more bright, which means that the sample is more concentrated.

When searching for extraction methods containing a phenol:chloroform purification step the protocol described by Bill Richardson and Nicoletta Kessaris, in 2006, was found (see *Final extraction protocol* chapter). This protocol had already been tested for high weight BACs

This protocol is based on the traditional extraction methods and has the particularity of having an extended neutralization time (1 hour in ice) that allows the DNA to recover from the lysis step and to get through the consequent steps. Also, the temperature remains approximately the same during all the extraction procedure and it is very explicit about how carefully we must handle the BAC.

As observed in **Figure 31.**, we managed to extract the BAC DNA and assess it, using this extraction protocol and the previously established PFGE conditions.

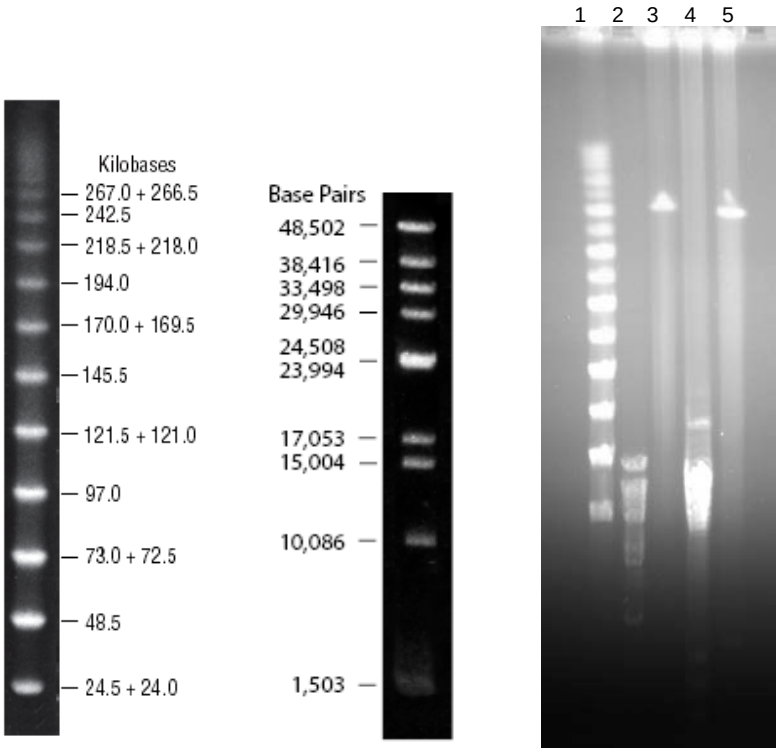

Running conditions:

Parameters	Values
Gel	1%
Initial pulse time	1 sec.
Final pulse time	20 sec.
Run time	20 hours
Voltage	6 V/cm
Angle	120º

Lanes:

1. **Ladder: MidRange II PFG Marker**
2. **Ladder: λ-monocut mix**
3. **Dll1 BAC Non-digested sample**
4. **Dll1 BAC XhoI digested sample**
5. **Dll1 BAC NotI digested sample**

Figure 31. MidRange II PFG marker fragments' sizes (left)**, λ-DNA Mono cut mix fragments' sizes** (middle)**, and PFGE photo** (right). All DNA samples are visible, although XhoI digestion is a bit blurred. The small sized bands are also visible if we adjust the brightness.

To end this study there was only one more test to do: compare extracted samples from both the kit and the new extraction protocol (**Figure 32.**).

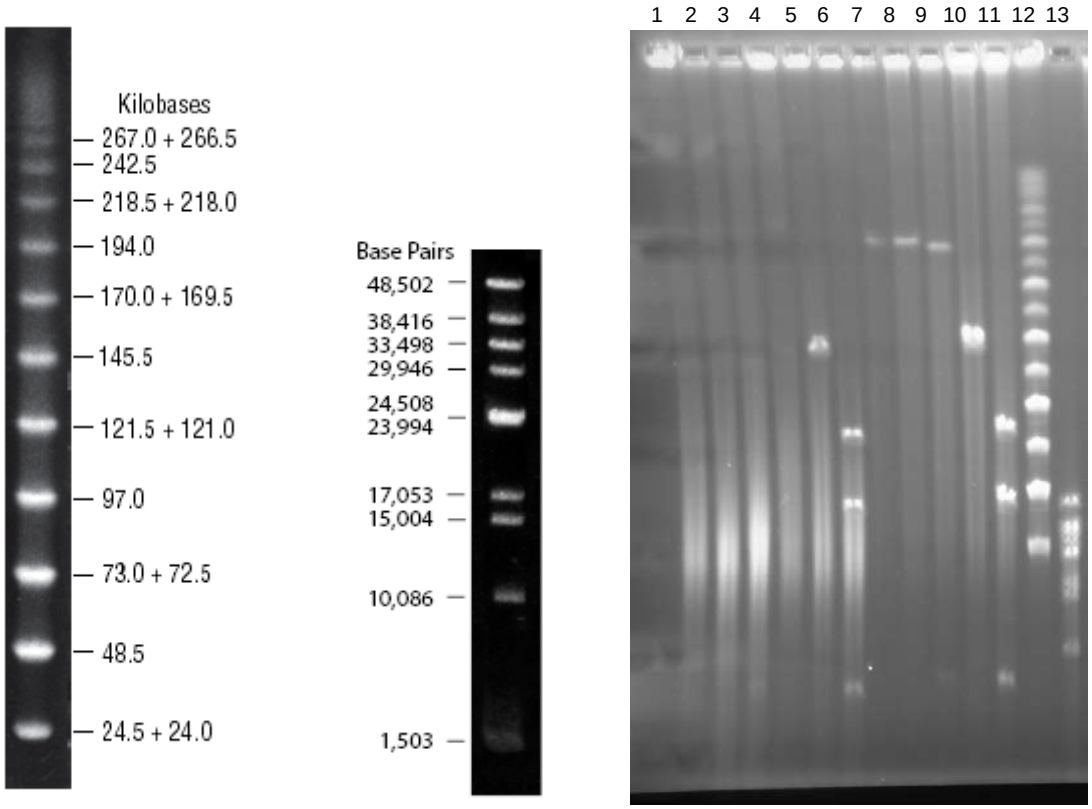

Running conditions:

Parameters	Values
Gel	1%
Initial pulse time	1 sec.
Final pulse time	20 sec.
Run time	20 hours
Voltage	6 V/cm
Angle	120º

Lanes:

1. **Dll1 BAC Non-digested sample (kit)**
2. **Dll1 BAC AscI digested sample (kit)**
3. **Dll1 BAC NotI digested sample (kit)**
4. **Hes5 BAC Non-digested sample (kit)**
5. **Hes5 BAC AscI digested sample (kit)**
6. **Hes5 BAC NotI digested sample (kit)**
7. **Dll1 BAC Non-digested sample (Nicoletta)**
8. **Dll1 BAC AscI digested sample (Nicoletta)**
9. **Dll1 BAC NotI digested sample (Nicoletta)**
10. **Hes5 BAC AscI digested sample (Nicoletta)**
11. **Hes5 BAC NotI digested sample (Nicoletta)**
12. **Ladder: MidRange II PFG Marker**
13. **Ladder: λ-monocut mix**

Figure 32. MidRange II PFG marker fragments' sizes (left)**, λ-DNA Mono cut mix fragments' sizes** (middle)**, and PFGE photo** (right). All DNA samples obtained using Nicoletta's protocol are visible. Using the kit we can only see the Hes5 BAC bands, with a visible smear though. The samples from the protocol described by Nicoletta show much less smear.

As observed in **Figure 32.**, the extraction protocol described by Nicoletta et al. not only is capable of extracting the BAC but also the purity achieved is much higher than when using the

kit. We could say that using the kit we can only extract lower weight DNA constructs (about 150 kbp – *Hes5* BAC size).

It is also deducible that the purification step using the column was the one responsible for degrading the BAC. Moreover, the fact that the temperature does not remain constant during the usage of the kit may also contribute for the degradation of the DNA.

Final extraction protocol

The protocol established in the lab in the end of the study is described below:

This method is suitable for preparing 2 Identical Maxi-Preps DNA amounts.

Inoculate 400 mL LB media supplemented the resistance drug using 500 µL of starter culture (pre-inoculum) and grow overnight (16-24 hrs) at 250 rpm and 32ºC.

Transfer culture into 8 x 50 mL Falcons and centrifuge at 4000 rpm for 10 min. at 4ºC.

Discard supernatant and resuspend each pellet in 8 mL of P1[15] + RNase solution using a 10 mL pipette.

Add 8 mL of freshly prepared P2 solution to each tube, gently invert tube up and several times to mix the contents and leave at room temperature for no longer than 5 min.

To each tube individually: add 8 mL of P3 solution and gently but immediately rock the tube back and forth several times until all P2 turns white. Place the tubes on ice for 1 hour.

Centrifuge at 4000 rpm for 15 min. at 4ºC.

Transfer each supernatant to a new Falcon tube passing it through a double sheet of autoclaved muslin being very careful because the white pellet may become dislodge and fall.

Centrifuge again at 4000 rpm for 15 min. at 4ºC.

Transfer flow through/supernatant (avoid transferring any white precipitate material) to a Falcon tube and add an equal volume (approximately 24 mL) ice-cold isopropanol and mix by inverting tube a few times, leave at room temperature for 5 min.

Centrifuge at 4000 rpm for 15 min. at 4ºC.

Remove supernatant and pulse spin at 4000 rpm.

Remove any remaining isopropanol with a tip and add 0,25 mL TE[16] (Tris/EDTA) to each tube to resuspend the pellet (let remain 10 min. at room temperature).

Using 200 µL cut tips pool the dissolved DNA into 4 x 1.5 mL tubes.

Add 500 µL of phenol:chloroform pH=7,9 to each tube and carefully invert tube 8 times.

Spin 5 min. at 13000 rpm.

[15] The solutions used to perform the established protocol were from *Genopure Plasmid Maxi Kit* by *Roche Applied Science*.

[16] TE (Tris EDTA buffer):
- 10 mM Tris·Cl pH 7.4 or 7.5 or 8.0;
- 1 mM EDTA, pH 8.0;

Remove each supernatant (top phase) to a new 1,5 mL tube using 200 µL cut tips and repeat Phenol/Chloroform step on it.

Spin 5 min. at 13000 rpm.

Remove all supernatants (top phase) to 1 new 2ml tube using 200 µL cut tip to pull the DNA and divide the DNA equally between 4 x 1.5 ml tubes.

Add 1 mL ice-cold 100% Ethanol and mix by inverting the tube 4 times.

At this stage 2 tubes should be stored in 100% Ethanol as a backup stock.

Spin 2 tubes 10 min. 13000 rpm.

Remove the supernatant and add 1 mL room temperature 70% Ethanol to each tube mix by inverting tube 4 times to wash the DNA pellets.

Spin 5 min. 13000 rpm.

Carefully remove as much of the supernatant as possible because the pellets might become dislodged from the tube. Thus it is better to aspirate off the supernatant rather than pour it off.

Air dry pellets at room temperature and when the very edge of the pellets turn from white to translucent (most of the Ethanol has evaporated) resuspend each in 100 µL *MilliQ* water. At this step, do not use narrow bore pipette tips to mechanically resuspend the BAC DNA. Instead, allow the *MilliQ* water to sit in the tube with occasional tapping of the bottom of the tube. It should only take 10 min. to dissolve completely at room temperature.

After resuspension the DNA in the 2 tubes can be pooled into 1 tube.

2nd part – Contributing to validation of the in vitro model

Mouse ES cells line

To execute this part of the work we used a transgenic *E14* ES cell line provided by Mark J. Tomishima's lab.

This cell line contains a fluorescent reporter (green fluorescent protein, GFP) under control of the *Dll1* gene promoter (*Dll1*::*GFP* from RP23-306J23 (*gensat.org*)).

The ES cell line generation is similar to what we intend to perform (*Tomisima et al.*, *2007*).

Culture of undifferentiated ES cells and monolayer differentiation

NOTE: ES cells are grown at 37ºC in a 5% (v/v) CO_2 incubator in Glasgow Modified Eagles Medium (GMEM 1×, *Invitrogen*), supplemented with 10% (v/v) fetal bovine serum (FBS) (ES-qualified, *Invitrogen*), 2 ng/mL LIF and 1 mM 2-mercaptoethanol, on gelatin-coated (0.1% (v/v)) *Nunc* dishes.

Thaw cells in GMEM:

- Heat 10 mL GMEM 1× + LIF (1:500) in a 37ºC water-bath;
- Add 0,1% (v/v) gelatin to a *Nunc* dish (coat for minimum of 10 min.);
- Remove cells from liquid N_2 (frozen cells) and place in the 37ºC water-bath for ≈1min. (Medium color changes from yellowish to pink).
- Add 4 mL of heated medium, resuspend and spin cells down (2 min. at 1000 rpm);
- Resuspend cells in 5 mL GMEM 1× + LIF and transfer to the *Nunc* dish after removing the gelatin;

Change medium within 6-12 hours (after this step cells can stay in the same medium for a maximum of 48h).

Passage cells when the cellular density requires it (if the cellular density is too high the viability starts to decrease):

- Wash cells twice with PBS;
- Add 0,1% (v/v) Trypsin (enough Trypsin solution to cover the cells) and place in the incubator for 2-3 min.;
- Knock the flask several times to dissociate cells and check under inverted microscope to ensure the cells have dissociated;
- Add serum-containing medium (GMEM 1×) to stop trypsinization, resuspend the cells by pipetting up and down and spin cells down (2 min. at 1000 rpm);
- Resuspend cells in GMEM 1× and count the cells;

- Inoculate cells at a cell density of 3×10^4 cells/cm^2 in GMEM 1× + LIF (1:500) in fresh gelatin-coated dishes;

Start **High-Density culture** 24h before Monolayer differentiation:

- Trypsinize and count cells as before;
- Inoculate cells at 1-1,5 × 10^5 cells/cm^2 in serum-free medium ESGRO Complete Clonal Grade medium (*Millipore Inc.*) + LIF (1:500) in a fresh gelatin-coated dish;

Start **Monolayer Differentiation**:

First, observe cells on the microscope to see if cells are ready to differentiate or not.

- Trypsinize as before and resuspend in RHB-A medium (*StemCell Science Inc.*) to count;
- Inoculate cells at 1×10^4 cells/cm^2 in RHB-A medium in a fresh gelatin-coated dish;
- Change medium on day 2;
- Re-plate on day 4;

NOTE: Put apart an aliquot for FACS analysis;

Re-plating:

- Trypsinize as before and resuspend in RHB-A medium to count;
- Inoculate cells at 2×10^4 cells/cm^2 in RHB-A medium + murine bFGF (*Peprotech*) (1:200) in PDL-laminin coated-plates;
- Take sample for FACS analysis.

- Change medium on day 2;

- Re-plate again on day 4;

To quantify the number of differentiating neurons at each time point, cells are plated onto laminin-coated glass cover-slips in 24-well *Nunc* plates.

Solutions required for ES cells culture and differentiation

GMEM 1×:

Mix the following components in a 250 mL bottle:

- 200 mL of sterile of GMEM 1× (GMEM, *Invitrogen*, 4ºC);
- Check if pH is close to 7 using pH test strips of appropriate range (the color of medium should be orange shade of red).
- 2 mL of 200 mM glutamine 100× (*GIBCO*, 4ºC);
- 2 mL of 100 mM sodium pyruvate 100× (*GIBCO*);
- 2 mL of non-essential amino acids 100× (*GIBCO*);
- 200 µL of 0,1 M 2-mercaptoethanol (*Sigma*);
- 2 mL of penicillin-streptomycin solution 100× (*GIBCO*, 4ºC);
- 20 mL of FBS (ES-qualified FBS inactivated for 30 min. at 55ºC, *Invitrogen*, 4ºC);

Mix well and filter through 0,2 µm filter unit into a new sterile flask and store at 4ºC for up to 1 month.

NOTE: If the medium is more than 1 month old, supplement it again with glutamine before use.

0,1 M 2-mercaptoethanol:

Add 10 µL of 2-mercaptoethanol (*Sigma*) stock solution (approximately 14 M, >98% pure) to 1,41 mL of sterile ultra pure water, mix and store at 4ºC up to 4 weeks.

0,1% Gelatin:

Use 2% bovine gelatin solution (*SIGMA*, 4ºC) to prepare working solution diluting 1:20 with PBS to obtain 0,1%.

1× trypsin solution:

Pipet one thawed 5 mL aliquot of 2.5% trypsin (*GIBCO*) into a 50 mL Falcon tube, and add:

- 0,5 mL of inactivated chicken serum;
- 0,1 mL of 0,5 M EDTA;
- and PBS up to 50 ml;

Filter sterilize, divide in aliquots, and store at -20ºC or at 4ºC up to 4 weeks.

0,1× trypsin solution:

Dilute 1× trypsin solution (1:10) in cell culture grade PBS.

Leukemia Inhibitory Factor (LIF):

To prepare working solution dilute with GMEM 1x to final concentration of 30 ng/µl, aliquot in sterile 1,5-ml eppendorfs and store at -80ºC.

NOTE: Keep the aliquot in use at 4ºC up to 1 week Do not expose it to temperature changes.

bFGF:

Briefly spin the 50 µg vial (*Peprotech*, 50 µg) and reconstitute in sterile water to 0,5 mg/mL by rolling overnight at 4ºC. Next day distribute it into 20 µl aliquots in sterile 1,5 mL eppendorfs.

To prepare working solution (1µg/µl), thaw one aliquot and complete with DMEM:F12 (*GIBCO*) to 1 mL.

Store diluted bFGF at 4ºC for no more than 2 weeks.

PDL/Laminin-coated plastics:

Distribute sterile cover-slips in the wells of 24- or 12-well plates to do immunocytochemistry.

Prepare the required amount of PDL and Laminin working solutions in PBS:

- PDL: 10 µg/ml (1:100);
- Laminin: 2,5 µg/ml (1:400);

Use 300 µl/well of a 24-well plate.

Incubate for 1 hour at room temperature with PDL.

Wash 2 times with PBS.

Coat with Laminin, and leave in the CO_2 incubator for 2-3 h or, better, overnight.

NOTE: Laminin-coated dishes/plates can be stored wrapped at -20ºC for 6 months. In this case, equilibrate at 37ºC (CO_2 incubator) for 20 min. before use.

NOTE: Aspirate Laminin solution immediately before plating cells.

Immunocytochemistry on cover-slips

Place the cover-slips into a 24-wells plate. Make sure to have the cells side up.

Fill the wells with PBS[17] (300-500 µl will do), then carefully lower down the cover-slips to the bottom of the well, cell side up.

At each wash, aspirate the liquid from the corner of a well, trying not to disturb the cell layer which otherwise will float.

When filling the well containing a cover-slip, never discard the liquid directly over the cover-slip not to wash away all the cells. Use a plastic Pasteur pipette instead of 1 mL *Gilson* tips.

Wash twice, for 5 min. each time, with PBS.

Fix with para-formaldehyde (PFA) 1-4% cooled to room temperature (depends on the antibody to use: 4% is a default, use 1% only when it is indicated for a specific antibody) for 15 min. at 4ºC, or 10 min. at room temperature.

Wash twice, for 5 min. each time, with PBS. Do one row at a time not to let the cover-slips dry.

Can store the plate with PBS at 4ºC for 1-2 weeks.

1st day:

Before starting the antibodies recognition steps, observe cells to see if they are fixated. If not, try look at other wells and choose another one that has fixated cells.

Transfer the cover-slips to use to an auxiliary 24-wells plate.

Wash the PFA residues with freshly prepared 0,1 M Glycine in PBS for 10 min. at room temperature.

Incubate with 0,1% Triton in PBS for 10 min at room temperature (to permeabilize the cells' membrane).

Wash again twice for 5 min. each time with PBS.

Block with 300 µL 10% FCS in TBST, for 30 min. at room temperature (to block all cell signaling to avoid unspecific antibody recognition).

Prepare the immuno dish (the lid from a square *Nuncatom* dish 24,5x24,5 cm) with 3 MM paper imbibed in PBS. Place *parafilm* paper (transparent side faced up) over the 3 MM paper.

Place 15 µL of the primary antibody (diluted to a working concentration with blocking solution – valid for <1 month) onto the *parafilm* and place the cover-slips over it with the cells side down.

Cover the dish and incubate for 1 hour at room temperature (not more than 30 min. in case of Tuj1 for samples with glia cells), or better, overnight at 4ºC.

[17] PBS – Phosphate buffer, pH 7,5

2nd day:

Transfer the cover-slips to the 24-well plate, cell side up, and wash three times, for 5 min. each, with TBST.

Place 15 µL of the secondary antibody dilution in blocking solution, onto the *parafilm* and place the cover-slips over it, cell side down. Incubate for 30 min at RT.

NOTE: From this step on, protect your cover-slips from light, because we are working with fluorochrome.

Transfer again the cover-slips to the 24-wells plate, cell side up, and wash three times, for 5 min. each, with TBST.

Aspirate the last wash and place a 50 µL drop of DAPI solution (blue fluorescence) in water (15:10 000 dilution of a 1 mg/mL stock) for 5 min. maximum at room temperature.

Wash three times with TBST. Add TBST to the DAPI in the wells, remove the whole mix and then do the three washes.

Carefully dry the cover-slips with a tissue and place them, cells side down, over a small drop of mounting medium (e.g. *Mowiol*, a very viscous solution), placed beforehand on a slide (only a small drop)

NOTE: Maximum: 8 cover-slips/slide; Ideal: 4-6 cover-slips/slide.

Let dry for approximately 1 hour and verify the fluorescence under the *Leica DM5000B* microscope.

Isolate each cover-slip with varnish.

Solutions

PFA 4%:

- 4 g of para-formaldehyde (*Sigma*);
- 100 mL of PBS;

0,1 M Glycine in PBS :

- 0,37 g Glycine (*Sigma*);
- 50 mL PBS;

0,1% Triton solution is prepared from a 10% stock in PBS (w/v).

TBST (20 mM Tris-HCl pH 8,0, 150 mM sodium chloride (NaCl), 0.05 % Tween-20):

- 20 mL Tris 1 M;
- 30 mL NaCl 5 M;
- 5 mL Tween-20 (10% stock in H_2O);
- Water to 1 L;

Results and Discussion

The results showed in this part of the thesis regard the immunocytochemistry assays performed on the mouse transgenic ES cells containing a fluorescent reporter for *Dll1* (*Dll1::GFP*) gift from Tomishima et al.

The GFP antibody was used to recognize the GFP protein in every assay (consequently, Dll1 expression is monitored through GFP expression).

For each set of antibodies used to perform each assay, it is stated what type of molecules and/or which cell cycle stage the antibodies recognize. Also, in each assay, a set of images that exemplifies what can be observed is shown.

Geminin / GFP / DAPI

Geminin is a dual function molecule with roles in regulating both DNA replication and neural cell fate during embryonic development. This protein prevents re-initiation of replication within a single cell cycle by inhibiting *Cdt1* activity to maintain chromosomal integrity and euploidy. Its levels rise during S-phase and it is degraded during M by the anaphase promoting complex (APC), enabling a new round of DNA replication to be initiated in the subsequent S-phase. On the other hand, this protein controls the transition from proliferating precursor to differentiated post mitotic neuron by modulating interactions between SWI/SNF chromatin-remodeling complex and bHLH transcription factors that are critical for neurogenesis or through interactions with Six3 and Hox transcription factors and Polycomb group proteins (reviewed in *Latasa, 2008*).

Regarding its expression profile, Geminin constitutes a cell cycle marker for S-phase, G2 and M (until anaphase).

For this assay, after immunocytochemistry, rosettes were photographed and the cells inside and in the periphery of the rosettes were counted. The data obtained from cell counts is shown in **Graphic 1.**.

Figure 33. depicts a rosette with cells stained for Geminin, GFP and DAPI. It shows cells inside and outside a rosette at different distances from its center. This characteristic was referred before as a feature of the *in vitro* model: mimicking the INM in the neural tube.

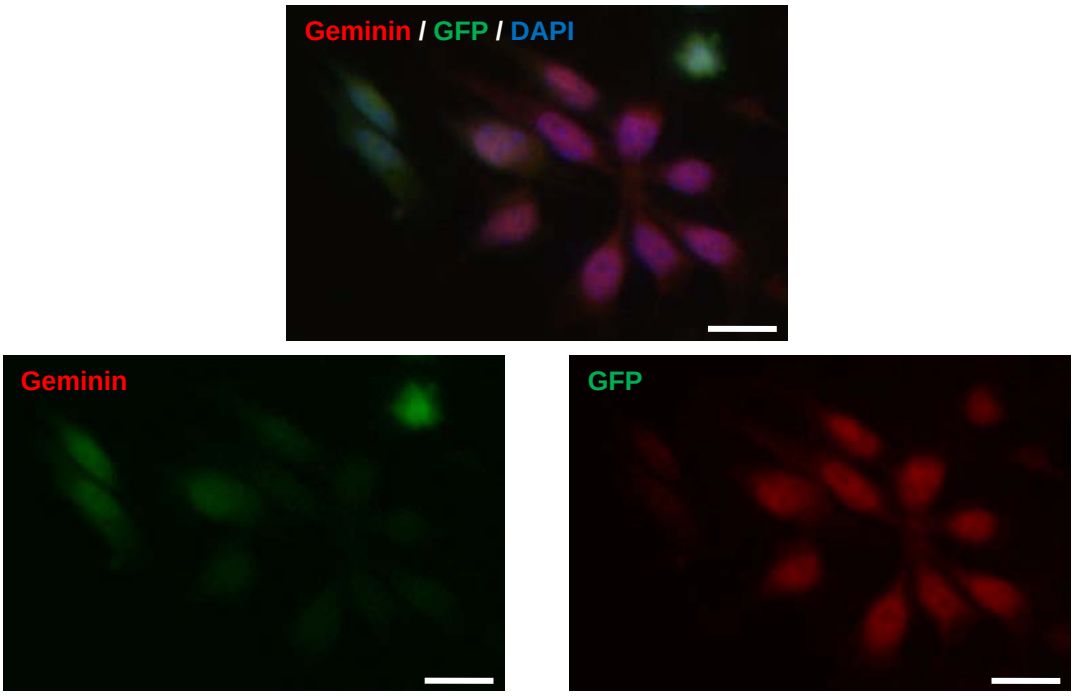

Figure 33. Immunocytochemistry: Geminin/GFP/DAPI (top)**, Geminin** (left) **and GFP** (right)**.** (Bar: 20 μm).

In **Figure 33.** it is observed the nuclei displacement along the rosette according to the cell cycle stage. By assessing the cells stained for Geminin, that recognizes cells in S-phase, G2 and M, we can see that not all cells are recognized and, most important, only cells inside the rosette are stained (cells within the cell cycle).

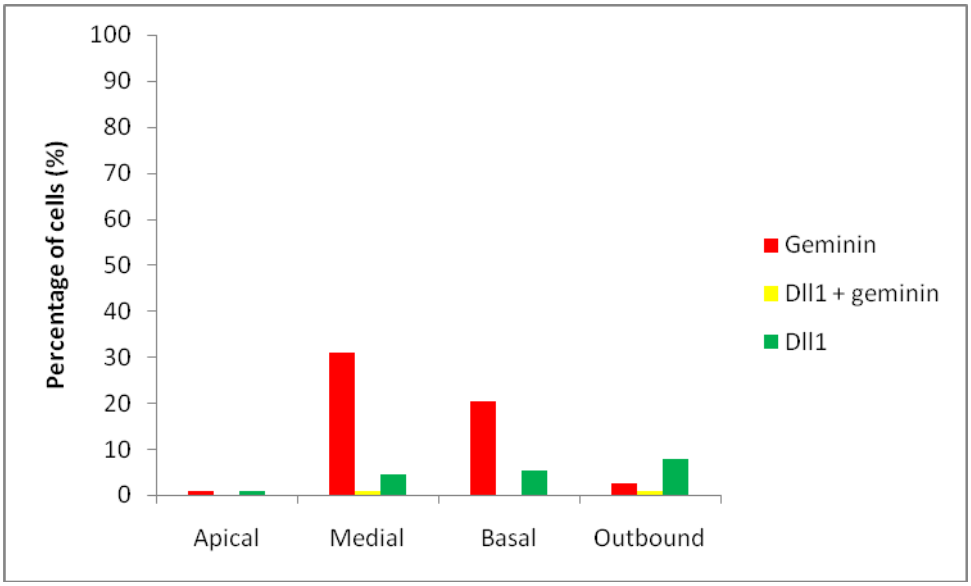

Graphic 1. Geminin (red)**, GFP** (green)**, and Geminin plus GFP** (yellow) **expression along the several levels of the apical-basal axis rosette and in the outbound**. Geminin is expressed mainly in the medial and basal zones of the rosette while GFP increases its activity towards the basal side of the rosette.

Regarding **Graphic 1.** we can see that Geminin is mostly expressed in the medial and basal zone of the rosette. These zones have been shown to contain nuclei in G1 and G2 (medial zone), and S-phases (basal layer) of the cell cycle. However, Geminin only stains cells in S-phase, G2 and M, which means that cells only expressing GFP in the medial zone are in G1 or G0 (cell cycle withdrawal). Cells in the apical zone show lower expression of Geminin or GFP. Moreover, no co-localization of the two markers was observed in M (apical zone). However, regarding the percentage of GFP cells in each zone inside the rosette we see that there is a ratio of about 1:4:5 (apical:medial:basal). Mitosis is the shortest phase of the cell cycle (about 5-10% of the cell cycle time only) and, if we look at the values, that is approximately the percentage of the total GFP cells that are found in the apical zone. This means that Dll1 might start being expressed in G2 (co-localization of Geminin and GFP in the medial zone), continue through M, G1 and G0 or through M directly to G0. These results do not contradict this hypothesis already postulated for Dll1 expression in the neural tube which means that the model might be mimicking the Dll1 expression in the neural tube.

As we can see by **Figure 36.**, the several layers from the neural tube are very difficult to limit in the rosettes obtained due the reduced number of cells. However, nuclei observation could also help us characterizing the cells cycle stage and consequently consider the image basing in knowledge introduced in the beginning of this thesis (S-phase and G2 nuclei are bigger than G1 while M nuclei are more dense and very characteristic). Though, even nuclei observation should not be relied in this case.

In the medial and basal layers of the rosette the expression of GFP is almost the same. This agrees with the fact that once a cell expresses Dll1 strongly (commitment to neuronal fate) it does not reenter the cell cycle, and migrates to the outbound of the rosette. The outbound of the neural tube (mantle layer) is where committed neurons accumulate and maturate before migrating. Regarding our data we can see that GFP levels are higher outside the rosettes, as expected too.

$p57^{Kip2}$ / GFP / DAPI

Two families of proteins have been reported to inhibit the activity of cyclin-CDK complexes: Kip/Cip family and Ink4 family. These complexes are major cell cycle regulators as explained before.

Members of the Kip/Cip family of proteins ($p21^{Cip1}$, $p27^{Kip1}$, and $p57^{Kip2}$) regulate the activity of all the G1 cyclin/CDK complexes and, to a lesser extent, cyclin B/CDK1, while members of the Ink4 family ($p16^{Ink4}$, $p15^{Ink4}$, $p19^{Ink4}$ and $p18^{Ink4}$) specifically inhibit CDK4 and CDK6.

The pituitary adenylate cyclase-activating polypeptide (PACAP) is a neuro-peptide expressed in growth zones of the brain. Particularly, PACAP38 inhibits the cyclin E-CDK2 complex via the Shh glycoprotein, the small GTPase Rho or the CDK inhibitor $p57^{Kip2}$. This

signaling may elicit cortical precursor withdrawal from the cell cycle, antagonizing mitogenic stimulators, and promote neuronal differentiation (reviewed in *Latasa, 2008*).

There are studies showing that induction of $p57^{Kip2}$ is essential for E47-mediated inhibition of cell cycle in neuroblastoma cells, strongly suggesting that *$p57^{Kip2}$* is a direct target gene recruited by bHLH transcription factors to induce quiescence of differentiated neurons. This conclusion is consistent with the general ability of $p57^{Kip2}$ to arrest cell cycle progression and proliferation when ectopically expressed at moderate levels and on its own in various cell types, including those of neuroectodermal origin.

All these results suggest that $p57^{Kip2}$ can be used as a cell cycle exit and neuronal maturation marker.

Figure 34. depicts an immunocytochemistry assay performed for recognition of $p57^{Kip2}$ and GFP. Once again, it is possible to see the rosette structures. However, when regarding only one of the colors rosettes are not so evident because none of these markers is expressed abundantly inside the rosette.

After assessing all the photos from the assays performed and the number of cells expressing $p57^{Kip1}$ and/or GFP was counted and the data was translated into **Graphic 2.**.

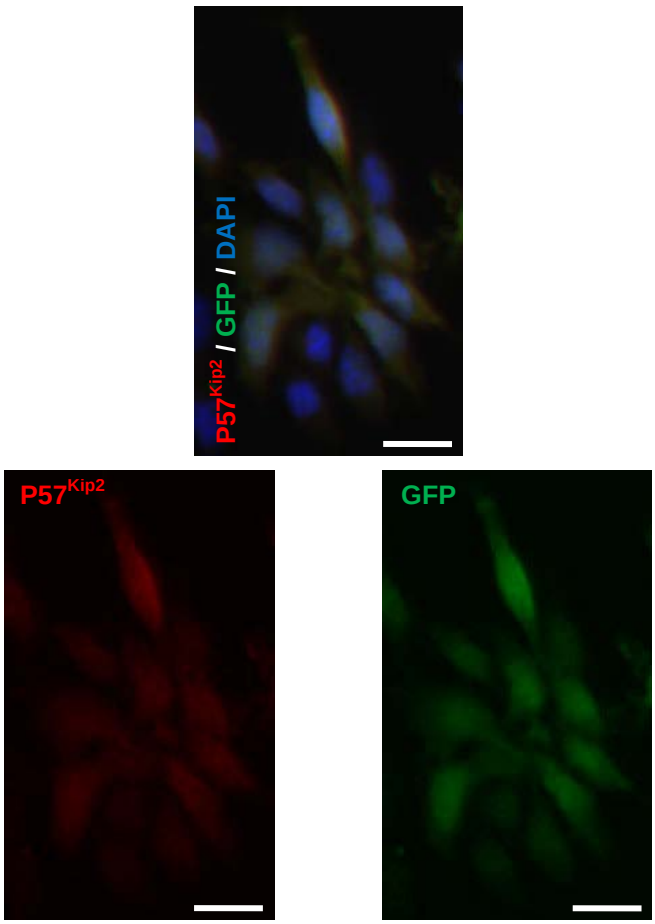

Figure 34. Immunocytochemistry: $P57^{Kip2}$/GFP/DAPI (top)**, $P57^{Kip2}$** (left) **and GFP** (right)**.** All cells expressing $P57^{Kip2}$ also express GFP. (Bar: 20 µm).

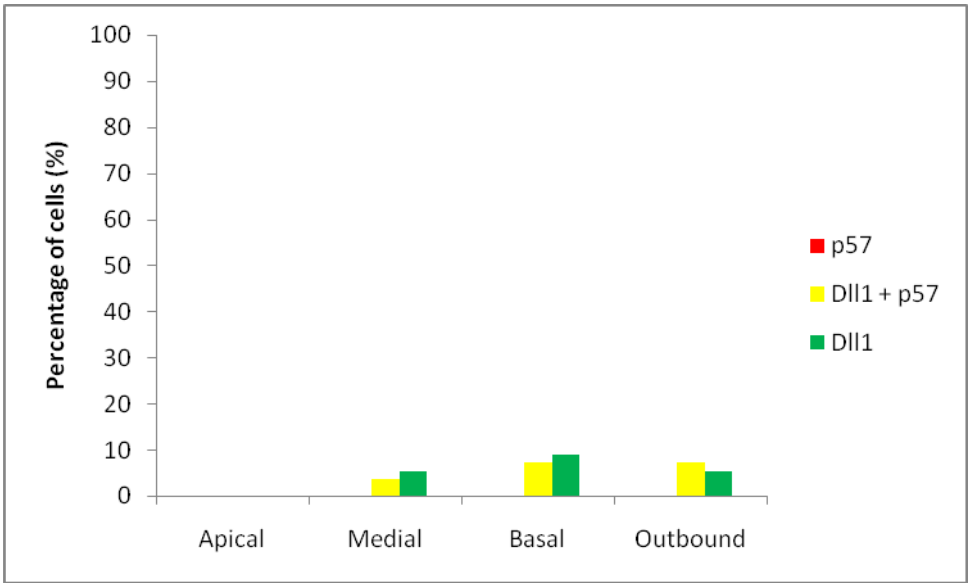

Graphic 2. P57^{Kip2} (red)**, GFP** (green)**, and P57^{Kip2} plus GFP** (yellow) **expression along the several levels of the apical-basal axis rosette and in the outbound**. P57^{Kip2} is expressed only in cells expressing GFP. Inside the rosettes, as the levels of P57^{Kip2} increase the expression of both P57^{Kip2} and GFP increases too. Outside the rosettes, the majority of cells express both markers and not only GFP.

Regarding **Graphic 2.** The most striking result is that no cell in the rosettes starts to express p57 ^{Kip2} without expressing GFP, which means that upon cell cycle exit the cells express Dll1 and p57^{Kip2} simultaneously or Dll1 was already being expressed before.

The expression of P57^{Kip2} and GFP in the neural tube is according to expected. The marker p57^{Kip2} is only expressed upon cell cycle withdrawal and during the first neuronal differentiation term, which explains why cells expressing this marker are only found in the medial and basal layers or in the outbound, outside the rosette. Cell cycle exit may happen after M or during G1, but in both cases this would happen in the medial zone predominantly. Therefore, the model is expressing p57^{Kip2} marker in the same way as the neural tube cells.

The cells expressing GFP are also distributed along the cells as expected and as depicted in **Graphic 1.**, i.e. cells in M are not visible, due to reasons stated before, and along the rest of the rosette the number of cells expressing GFP is similar (there are no evident oscillations occurring in the cells count).

The majority of cells expressing both markers are located in the medial and basal zones or in the outbound of the rosettes, which correlates with the cells cycle exit and the migration stages towards the outside of the rosette, as part of the neuronal differentiation process. We also observe that GFP-single cells in the outbound are as much as the cells expressing P57^{Kip2} and GFP in the same region. This reinforces the fact that p57^{Kip2} is not the only effector of the cell cycle withdrawal mechanism (p21 might be recruited instead).

HuC/D / GFP / DAPI and Tuj1 / GFP / DAPI

HuC and HuD proteins belong to the Embryonic Lethal Abnormal Vision (ELAV)-like family of RNA-binding proteins, and that can enhance cyclins A, B1 and D1 mRNA stability, as well as the mRNAs for MyoD and myogenin transcription factors. In neurogenesis, their expression is restricted to young and mature neurons, which are confined to the external zone of the rosettes.

Tuj-1 stains neuron-specific class III β-tubulin in differentiated neural progenitor cells.

β-III Tubulin, also known as tubulin β-4, is regarded as a neuron-specific marker. Its expression has been suggested to be one of the earliest markers to signal neuronal commitment in primitive neuroepithelium. Tubulin is the major component of microtubules, consequently, antibody Tuj1 labels neuronal cell bodies, dendrites, axons, and axonal terminations (structures that require microtubules) and is therefore commonly used for the identification of newly committed neurons.

Both **Figures 35. and 36.** depict early neuronal committed cells as referred in the introduction made regarding the kind of molecules/cells that HuC/D and Tuj1 antibodies recognize.

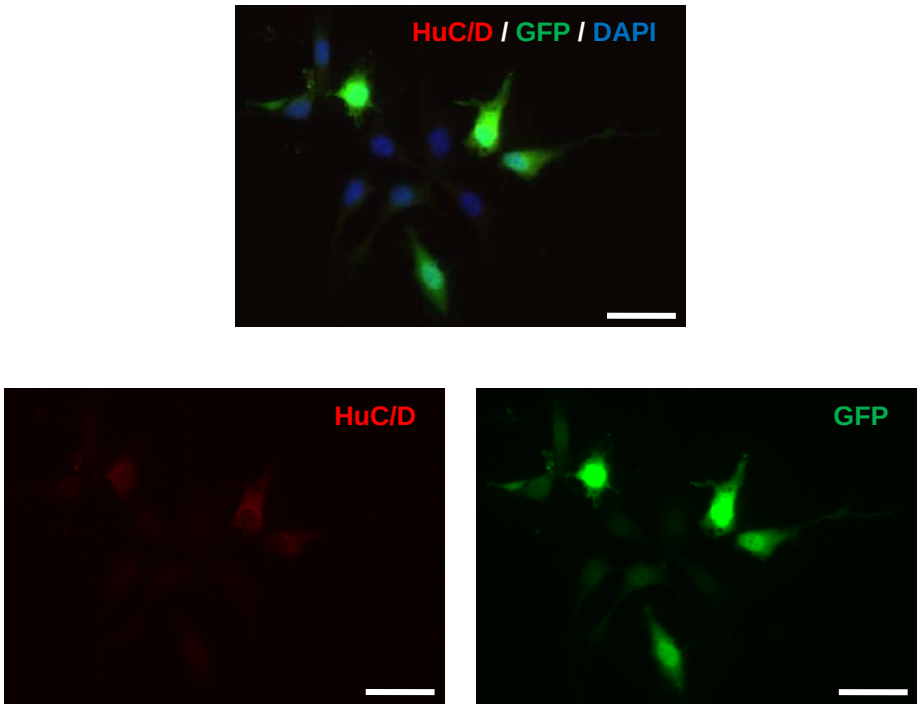

Figure 35. Immunocytochemistry: HuC/D/GFP/DAPI (top)**, HuC/D** (left) **and GFP** (right)**.** (Bar: 20 μm).

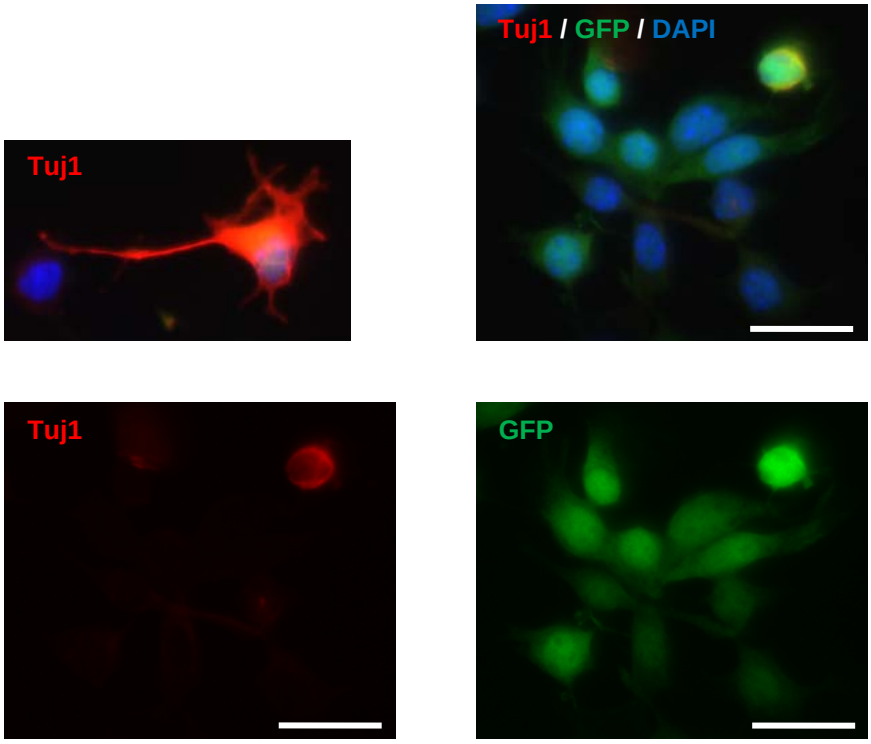

Figure 36. Immunocytochemistry: Tuj1/GFP/DAPI (top right)**, Tuj1** (bottom left) **and GFP** (bottom right)**. Neuron stained with Tuj1** (top left)**.** (Bar: 20 µm).

For this two assays no cell count was needed because upon observation of the cells one could see that all cells expressing one of the markers was also inevitably expressing GFP. Once again, this confirms the fact that the expression of Dll1 constitutes an important method for monitoring Notch activity, namely concerning neuronal commitment.

Conclusion

Although the data obtained for all the assays in the rosettes agrees with the expected behavior if cells were mimicking the neural tube environment, this data is affected by the low amount of results. The cells did not grow sufficiently to form dense rosettes as usually are obtained using the model, as seen in **Figure 12.**. To have a better and more trustable view and validation of the results one should repeat them and hopefully produce a lot more data to treat.

Also, The live imaging of the cells would be an outstanding advance in the study and reliable validation of the model of the rosette structures.

By the global results obtained regarding the model validation we can conclude that the model might be mimicking the neural tube in what concerns the Dll1 ligand expression, because the data did not contradict the several features that have been associated to its expression in the neural tube (accounting on a treatment of the data for the rosettes analogous to the neural tube analysis, i.e. several specific regions according to the cell cycle stage, etc.).

Regarding the results obtained we can say that the model might fit the one proposed by Murciano et al. (**Figure 37.**) to describe the dynamic of the neurogenesis inside the neural tube, with Dll1 being expressed in the called “neurogenic zone” and being in down-regulated in the “pre-neurogenic zone” until the cell gets definitely committed to neuronal fate. This Dll1 oscillations might explain the green “ground-coloring” obtained for cells inside the rosettes, because the GFP molecules produced inside the cells might not be following the same degradation pattern as the Dll1 molecule.

By gathering the data obtained for the assays with $p57^{Kip2}$ and Geminin one can say that cells start expressing Dll1 (neural commitment signalization) before exiting the cell cycle. Co-localization between Geminin and GFP indicates that Dll1 might be expressed even before M. Moreover, it is known that the neural tube has several domains along the anterior-posterior axis and some of them show different expression patterns for several markers. One example is the set of molecules: $p57^{Kip2}$, p21 and Dll1; that show different combinations of expression patterns according to the domain. It has been questioned whether the rosettes model could mimic that capacity to express different patterns according to determined regions and this work could provide the answer for that. Although the observation of static cultured rosettes did not revealed the answer, the dynamic study, once again, would be the most reliable way to assess it.

Restricting the neurogenic capacity to a window prior to cell-cycle exit (G0) probably prevents the execution of the differentiation program during cell-cycle phases prior to M. This prevention mechanism might be happening. As referred before, there was co-localization between Geminin and GFP, though it is still a mystery.

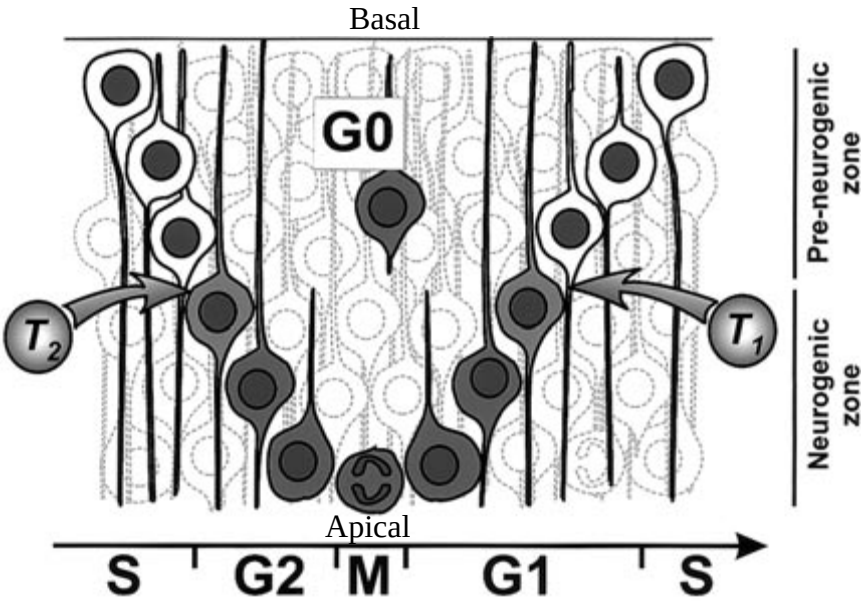

Figure 37. Scheme of the model proposed to represent the functional organization of the neuroepithelium in terms of neurogenesis. The orthogonal arrangement of the cells moving their nuclei up and down as they progress through the cell cycle is translated into the segregation of the neuroepithelium into two zones, each made up of precursors that are transiently involved in distinct functions. In the apical (or ventricular) region (neurogenic zone), proliferating cells are able to express Notch1, Delta1, and the proneural determination gene Ngn2 (dark gray), thus being subjected to lateral inhibition. In the basal epithelium (pre-neurogenic zone), precursors either cannot express these genes or express them at low levels. Postmitotic neurons in G0 still expressing Delta1, Ngn1, and Ngn2 pass through the pre-neurogenic zone as they migrate out from the neuroepithelium. T1 and T2 represent the time points corresponding to the moment in G1 at which the cells lose their neurogenic capacity and the beginning of G2, respectively (image adapted from *Murciano et al, 2002*).

Future work

As said in the beginning, this work is part of a major project which aims for the generation of a transgenic mouse ES cell line. The next steps to take in this project consist in:

a. Transfect of the engineered BAC into mouse ES cells (*E14tg2a* line) and select clones with BAC transgene integration through drug resistance[18];

b. Characterize the transgenic ES clone(s) (transgene integrity, copy number);

c. Verify that the selected clones express the reporter (*Dll1*:*mCherry*:*NLS*) during ES cells self-renewal and differentiation;

d. Excision of the drug-selectable marker with Flp recombinase;

3. *In vitro* differentiation and real-time imaging of single cells of the generated reporter ES cell lines using time-lapse microscopy. Imaging of the *Dll1* reporter within neural progenitors will allow the identification of all cells that are progenitors (dividing) and cells that are differentiating (red). This will help to understand whether the cells are instructed for differentiation before the last mitosis (in the mother cell) or if this decision occurs after division (in the daughter cells). As seen in this work this question cannot be answered using "static studies";

4. Analysis of the generated real-time imaging data. The analysis of the generated real-time imaging data shall be done with the *Omero* software, with manual cell tracking and fluorescent intensities measurements;

After this, we hope that these cells will provide a considerable amount of knowledge mainly concerning the crucial steps for neuronal commitment of the cells. Ideally, it would even provide information about when and how to manipulate ES cells in order to totally control the neural cells fate.

[18] The genome insertion will be done using BAC transgenesis instead of gene targeting ("knock-in"), in order to maintain the activity of the two endogenous alleles in ES cells and, thereby, preventing haploinsufficiency phenotypes.

Future perspectives for stem cells therapies

The great dream for stem cells is to provide regenerative therapies.

A great variety of human diseases, spanning neurodegeneration, diabetes and myocardial infarction can, in theory, be overcome using cell transplantation to restore tissue function after disease or injury. ES cell-derived neural cells have been demonstrated to survive and to exhibit at least some aspects of appropriate region specific neuronal differentiation when introduced into the developing mouse brain.

However, one problem that has arisen in such studies is the probability for development of teratomas from undifferentiated ES cells present in the grafted population. This can be now reduces drastically as the purification methods improve more and more, like FACS. For any clinical application, it would be essential to ensure that such cells were eliminated by rigorous purification and/or genetic selection.

An important variable to consider in cell transplantation is the developmental stage of the donor cells. For therapies aimed at long-term reconstitution of a continuously renewing tissue such as the hematopoietic system, only stem cell transplantation will suffice. This is not the case for treatment of tissues or organs in which there is little or no cell turnover. In addition, it is possible that the plasticity of naive neural precursor cells may be advantageous for integration, and that the adult environment retains the appropriate cues to direct them efficiently into the desired cells fates.

Another concern about cell based therapy is the nonidentity between introduced cells and recipient, which will provoke immunological rejection. The advances in genetic engineering and cloning thus provide a major revolution by creating pluripotent stem cells containing the genetic material of the patient. This so-called therapeutic cloning procedure would involve the transfer of a nucleus from a somatic cell of the patient into an enucleated oocyte, development of the reconstituted embryo to the blastocyst stage, and then isolation and expansion of human pluripotent stem cells (hPSCs) (**Figure 10.**).

Even more astonishing, and contributing for this scenario of revolution in medicine and genetic engineering, is the reprogramming possibility of fully differentiated adult somatic cells into ES cells, as Yamanaka demonstrated to be possible, discarding therefore the need for nuclei transfer and all the adjacent disadvantages.

"The faculty for propagating pluripotent stem cells from mouse and human embryos is essentially fortuitous in biological origin. This gift from nature has provided unparalleled research tools for investigating mammalian development, genetics, and physiology. Now these cells offer the foundations for an entirely new form of human medicine." (*Austin Smith, 2001*)

References

Abranches, E., Silva, M., Pradier, L., Schulz, H., Hummel, O., Henrique, D., Bekman, E. (2009). *Neural Differentiation of Embryonic Stem Cells In Vitro: A Road Map to Neurogenesis in the Embryo*. PLoS ONE, Volume 4, Issue 7, 1-14.

BioRad, *CHEF-DR® III Pulsed Field Electrophoresis Systems Instruction Manual and Applications Guide.*

Copeland, N., Jenkins, N., Court, D. (2001). *Recombineering: A POWERFUL NEW TOOL FOR MOUSE FUNCTIONAL GENOMICS*. Nature, Volume 2, 769-779.

C. Wilcock, A., R. Swedlow, J., G. Storey, K. (2007). *Mitotic spindle orientation distinguishes stem cell and terminal modes of neuron production in the early spinal cord.* Development 134, 1943-1954.

Del Bene, F., M. Wehman, A., A. Link, B., Baier, H. (2008). *Regulation of Neurogenesis by Interkinetic Nuclear Migration through an Apical-Basal Notch Gradient.* Cell 134, 1055–1065.

Fior, R., Henrique, D. (2005). *A novel hes5/hes6 circuitry of negative regulation controls Notch activity during neurogenesis*. Developmental biology 281, 318-333.

Fischer, A., Gessler, M. (2007). *Delta–Notch—and then? Protein interactions and proposed modes of repression by Hes and Hey bHLH factors*. Nucleic Acids Research, Volume 35, No. 14.

J. Tomishima, M., Hadjantonakis, A., Gong, S., Studer, L. (2006). *Production of Green Fluorescent Protein Transgenic Embryonic Stem Cells Using the GENSAT Bacterial Artificial Chromosome Library.* Stem cells.

Kageyama, R., Ohtsuka, T., Shimojo, H., Imayoshi, I. (2008). *Dynamic Notch signaling in neural progenitor cells and a revised view of lateral inhibition*. Nature, Volume 11, 1247-1351.

Kessaris, N., Richardson, B. (2006). *DNA Isolation from PAC or BAC Clones*.

Kopan, R., Ilagan, M. (2009). *The Canonical Notch Signaling Pathway: Unfolding the Activation Mechanism*. Cell 137, 216-233.

Latasa, M., Cisneros, E., Frade, J. (2008). *Interkinetic nuclear migration and the coordination between cell cycle and neurogenesis in the vertebrate central nervous system*.

L. Frank, C., Tsai, L. (2009) *Alternative Functions of Core Cell Cycle Regulators in Neuronal Migration, Neuronal Maturation, and Synaptic Plasticity*. Neuron review 62.

Louvi, A., Spyros Artavanis-Tsakonas, S. (2006). *Notch signaling in vertebrate neural development*. Nature, Volume 7, 93-102.

Murciano, A., Zamora, J., López-Sánchez, J., Frade, J. (2002). *Interkinetic Nuclear Movement May Provide Spatial Clues to the Regulation of Neurogenesis*. Molecular and Cellular Neuroscience 21, 285-300.

Nature, *Neurosciences reviews*.

Rodrigues.C. (2007). *Novel Strategies For Gene Manipulation in Mammalian Cells*. Dissertação para obtenção do Grau de Mestre em Engenharia Biológica.

Shimojo, H., Ohtsuka, T., Kageyama, R. (2008). *Oscillations in Notch Signaling Regulate Maintenance of Neural Progenitors.* Neuron 58, 52–64.

Silva, J., Smith, A. (2008). *Capturing Pluripotency.* Cell 132(4): 532-536.

Smith, A. (2001). *EMBRYO-DERIVED STEM CELLS: Of Mice and Men*. Annu. Rev. Cell Developmental Biology, 17:435-62

Wiley, J. and Sons (2007). *Current Protocols in Molecular Biology.* Current protocols.

Ying, Q., G. Smith, A. (2003). *Defined Conditions for Neural Commitment and Differentiation.* Methods in enzymology, VOL. 365

Ying, Q., Nichols, J., Chambers, I., Smith, A. (2003). *BMP Induction of Id Proteins Suppresses Differentiation and Sustains Embryonic Stem Cell Self-Renewal in Collaboration with STAT3*. Cell, Volume 115, 281-292.

Ying, Q., Stavridis, M., Griffiths, D., Li, M., Smith, A. (2003). *Conversion of embryonic stem cells into neuroectodermalprecursors in adherent monoculture*. Nature.

Ying, Q., Wray, J., Nichols, J., Batlle-Morera, L., Doble, B., Woodgett, J., Cohen, P., Smith, A. (2008). *The ground state of embryonic stem cell self-renewal.* Nature, Volume 453.